TABLE OF CONTENTS

ABBREVIATIONS

(Abbreviations of the enzymes indicated under each figure of the constructions.)

A_0^-	Chlorophyll of PSI, reduced in the primary electron transfer
ATP	Adenosine 5'-triphosphate
Ap^r	Ampiciline resistant
APC	Allophycocyanin
α^{PB}	α subunit of an phycobiliprotein, PB indicates the protein
α^{APCB}	α-Allophycocyanin-B
b6f	Cytochrome *b6f* complex
bp	Base pair(s)
BChl	Bacteriochlorphyll
β^{PB}	β subunit of a phycobiliprotein, PB indicates the protein
β^{18}	Allophycocyanin β^{18} subunit
CCD	Charge-coupled device
cDNA	Complementary deoxyribonucleic acid
Chl	Chlorophyll
Cm^r	Chloramphenicol resistant
CP43	Core antenna complex with apparent mass of 43 kDa
CP47	Core antenna complex with apparent mass of 47 kDa
Cys	Cysteine
Da	Dalton
dCTP	Deoxycytidine 5'-triphosphate
DEPC	Diethyl pyrocarbonate
DMSO	Dimethyl sulfoxide
EDTA	Ethylene diaminetetraacetic acid
Fd	Ferredoxin
FeS	Iron sulfur cluster
FMO	Fenna-Matthews-Olson protein
FNR	Ferredoxin-NADP(H)-oxidoreductase
Km cassette	Kanamycin resistance cassette
LC	Core-linker polypeptide
LCM	Core-membrane-linker polypeptide

LH	Light-harvesting antenna of purple bacteria
LHC	Light-harvesting complex of chloroplasts
LRC	Rod-core-linker polypeptide
LR (LRM)	Rod-linkre polypeptide, M indicates its molecular mass
MES	2-Morpholinoethanesulfonic acid
$NADP^+$ (NADPH)	Nicotinamide adenine dinucleotide phosphate (reduced form)
OD	Optical density
P680	Primary donor of photosytem II
P700	Primary donor of photosytem I
PB	Phycobiliprotein
PBS	Phycobilisome
PC	Phycocyanin
PCB	Phycocyanobilin
PCC	Pasteur Culture Collection
PCR	Polymerase chain reaction
PE	Phycoerythrin
PEB	Phycoerythrobilin
PEC	Phycoerythrocyanin
PSI	Photosystem I
PSII	Photosystem II
PUB	Phycourobilin
PXB	Phycobiliviolin
Q_A	Primary electron acceptor quinone of photosystem II
Q_B	Secondary electron acceptor quinone of photosystem II
RT-PCR	Reverse-transcription polymerase chain reaction
SDS	Sodium dodecyl sulphate
SDS-PAGE	Polyacrylamide gel electrophoresis in the presence of SDS
Sm^r	Spectinomycin resistant
Sp^r	Streptinomycin resistant
TAE	Tris-Acetate-EDTA
TCA	Trichloroacetic acid
Tris	Tris hydroxymethyl methylamine
Y_Z	Tyrosine residue of photosystem II
WH	Woods Hole Oceanographic Institute Culture Collection

WT   Wild type

Ω casette   Spectinomycin and Streptinomycin resistance cassette

Cyanobacterial strains are identified by a generic name and a PCC or WH number.

PREFACE

Revealing the origin of life on Earth has always been studied extensively and is still unknown in all details. Fossil records prove that photosynthetic organism, which created the conditions for life as we observe it today, were present on the Earth already thousands of years ago. There are diverse evidences for the existence of oxygenic photosynthesis on the Earth as early as two billion years ago, and it is widely believed that the metabolic capabilities of these ancient organisms were similar to that of contemporary cyanobacteria. Cyanobacteria are oxygenic photosynthetic prokaryotes and their existence more than two billion years ago can be inferred from the stromatolite evidence and some microfossils. It is generally accepted that the cyanobacteria are the ancestors of eukaryotic chloroplast. The advent of oxygen-evolving photosynthesis permitted the development of advanced life, by making the development of the ozone layer possible and thus shielding the Earth from UV irradiation. Cyanobacteria also provided a ubiquitous terminal oxidant, oxygen, for respiration making the existence of heterotrophs, such as animals possible. This way the appearance of cyanobacterial photosynthesis was a key event of evolution and its understanding is of special importance. In cyanobacteria, photosynthesis begins with the collection of photon energy in specialized macromolecular complexes (antennae), which are highly organized called supramolecular chromophore-containing complexes. Antennae capture light energy and guide it to the photosynthetic reaction centers, to be transformed into chemical energy.

Light conditions are very important for all photosynthetic organisms. Adaptation to the general light conditions of the habitat as well as to short term changes in it is crucial in order to maintain optimal photosynthetic activity. Light-harvesting antenna complexes increase the rate of photosynthesis by adapting to the quality and quantity of incident radiation and by absorbing and transferring the light energy to the reaction centers. The primary light-harvesting antenna of cyanobacteria is a large pigment-protein assembly, called phycobilisome. The size of the phycobilisome is 5-10 x 10^6 Da, about twice as large as ribosomes. Phycobilisomes consist of the chromophore-containing phycobiliproteins, which are connected by smaller linker polypeptides, which do not contain pigments. Phycobiliprotein-containing organisms feature a great range of spectral variation in their antenna pigments consequently excellent adaptation to the various light conditions. Energy transfer in the phycobilisome is unidirectional and its efficiency approaches 95%.

The initial assembly of this huge complexes as well as its structural adaptation allowing fast and efficient energy transfer under a variety of conditions are still being studied extensively. Relatively little is known about the linker polypeptides, which may have an

important role in these processes. Thus revealing their exact roles is important for the understanding of the structure formation and the efficient energy transfer in the phycobilisomes.

Apart from examining the above role of linker polypeptides, this study also treats an other yet unresolved aspect of cyanobacterial photosynthesis, the last step in the light-dependent reactions of photosynthesis. It is the electron transfer between ferredoxin and $NADP^+$ catalyzed by the ferredoxin-NADP(H)-oxidoreductase. In the process of phycobilisome preparation this enzyme frequently co-purifies with the phycobilisome. Beside NADPH production in photosynthesis the ferredoxin-NADP(H)-oxidoreductase participates in other important physiological processes, such as respiration. Two ferredoxin-NADP(H)-oxidoreductase isoforms have been detected in various cyanobacterial strains, but the exact role of these two isoforms is not known yet.

Our aim was to study the role of the linker polypeptides in the phycobilisome assembly and to examine how the two isoforms of the ferredoxin-NADP(H)-oxidoreductase is produced in *Synechocystis* sp. strain PCC6803 cyanobacterium. We also studied the localization of the ferredoxin-NADP(H)-oxidoreductase in relation to the phycobilisome, using molecular genetic and biochemical approaches.

Before presenting results a short description of the cyanobacteria will be given with especial emphasis on the diversity of their chromophores, and our model organism the, *Synechocystis* sp. strain PCC6803 will also be introduced. A brief description of the photosynthetic process and the role of the major photosynthetic complexes photosystem II, the cytochrome b_6f, photosystem I and the ATP-synthase will be followed by a chapter on the fifth main complex the light-harvesting antennae. The last part of the introduction is a more detailed discussion of the structure and the function of the phycobilisome.

I. INTRODUCTION

I. 1. Cyanobacteria

Cyanobacteria (oxyphotobacteria) are defined by their ability to carry out oxygenic photosynthesis based on the coordinated work of two photosystems. The term cyanobacteria includes large number of strains isolated and described. These are all gram-negative prokaryotes exists as unicellular or as multicellular forms. Cyanobacteria occupy a rather wide range of illuminated niches in terrestial, freshwater, marine and hypersaline environments [6]. All cyanobacteria are able to grow using CO_2 as the sole source of carbon. Their chemoheterotrophic potential is typically restricted to the mobilization of reserve polymers (mainly glycogen but also polyhydroxyalkanoates) during dark periods, although some strains are known to grow chemoheterotrophically in the dark at the expense of external sugars. Some cyanobacteria are able to perform N_2 fixation. Many cyanobacterial strains were isolated, purified and collected in culture collections such as the Pasteur Culture Collection (PCC) and the Woods Hole Oceanographic Institute Culture Collection (WH). Such strains are identified by a generic name and a PCC or WH number. The cyanobacterium is a good model organism for photosynthetic studies because many strains are genetically accessible and several species have been fully sequenced (http://www.kazusa.or.jp/cyano/). The introduction of foreign DNA into cyanobacterial cells can be achieved by various methods such as electroporation, conjugation and also by natural transformation [7]. Integration of the introduced DNA, via homologous recombination is very efficient, allowing stable insertions into the chromosome [8]. Standard bacterial antibiotic resistance genes, like *aphI*, the gene of kanamycin resistance and the Ω cassette with *aadA*, the gene of resistance to streptomycin and spectinomycin, can be expressed in cyanobacteria, making the selection of the mutants possible. Most, if not all, cyanobacteria possess multiple copies of the genome, therefore cells with a newly introduced mutation will be heterozygous until replication and subsequent segregation of these genomes produce a cell that is homozygous for the mutation [8].

All cyanobacteria synthesize chlorophyll *a* as photosynthetic pigment, and most strains contain phycobiliproteins as light-harvesting pigments. The epithets "blue-green algae", "Cyanophyceae", "Cyanophyta" and "Myxophyceae" have all been used to cyanobacteria. Previously, a separate group of organisms with equal rank to the cyanobacteria, the so-called Prochlorophytes (with two genera, *Prochloron*, a unicellular symbiont of marine invertebrates, and *Prochlorothrix*, a free-living filamentous form) had been recognized [9].

11

They were distinguished from cyanobacteria on the basis of their lack of phycobiliproteins and the presence of chlorophyll *b*. The recently recognized genus of marine picoplankton *Prochlorococcus* could be included here, even though the major chlorophylls (Chl) in this genus are divinyl-Chl *a* and divinyl-Chl *b*. The original distinctions leading to the separation of the Chl *b*-containing oxyphotobacteria from the cyanobacteria are questionable, since in *Prochloroccoccus marinus*, functional phycoerythrin and genes encoding for phycobiliproteins have been detected [10]. Additionally, phylogenetic analysis of 16S rRNA genes indicate that the three genera of prochlorophytes evolved independently from each other as well as from the main plastid line, this result is supported by the comparative sequence analysis of the respective Chl *a/b* binding proteins also [11]. Thus prochlorophytes are regarded as greenish cyanobacteria, and are not treated separately. The recent discovery of Chl *d*-containing *Acaryochloris marina* [12] confirms the evolutionary diversification of light-harvesting capabilities among oxyphotobacteria.

According to phylogenetic analysis of 16S rRNA sequences, the cyanobacteria are a diverse phylum of organisms within the bacterial radiation, separated from their closest relatives. This analysis supports the theory of the endosymbiotic origin of plant chloroplasts, by placing plastids from all investigated eukaryotic algae and higher plants in a diverse, but monophyletic, deep-branching cluster. More information: http://141.150.157.117:808/ prokPUB/chaphtm/239/01_00.htm

I. 1. A. *Synechocystis* sp. strain PCC6803

Synechocystis PCC6803 is a non-nitrogen-fixing, unicellular cyanobacterium with spherical cells. This cyanobacteria is a fresh water habitant, it is photoheterotroph, relaying on glucose as a carbon source. The whole genome of *Synechocystis* PCC6803 has been sequenced, and deposited in the CyanoBase database (http://www.kazusa.or.jp/cyano/Synechocystis/). The genome size of the *Synechocystis* PCC6803 is 3.3 Mbp. *Synechocystis* PCC6803 has multiple copies of the genome and has proven to be naturally transformable by exogenous DNA [13]. The presence of two photosystems makes *Synechocystis* PCC6803 a good and commonly used model organism for photosynthesis studies.
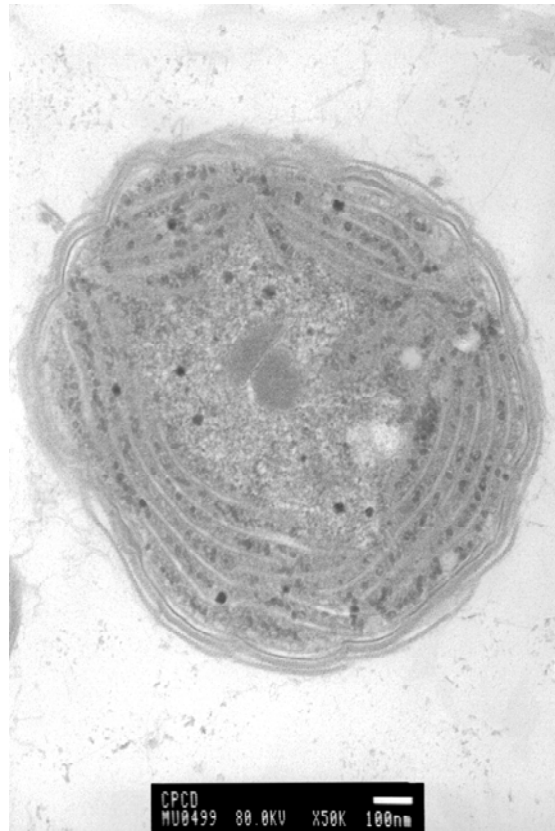
Figure 1. A *Synechocystis* PCC6803 cyanobacterium cell.

Electron microscope image of a *Synechocystis* PCC6803 cyanobacterium cell. Kindly provided by László Mustárdy. Bar = 100 nm

I. 2. Oxygenic photosynthesis

It is generally accepted that the Earth was formed about 4.6 billion years ago and life began about 3.5 billion years ago, when the first photosynthetic bacteria appeared. Photosynthesis is the process by which electromagnetic energy (light) is converted into biochemical energy. This process is either oxygenic as in cyanobacteria, algae and higher plants or anoxygenic as in purple bacteria, green filamentous bacteria, green sulfur bacteria and heliobacteria. Fossil records indicate that cyanobacteria evolved more than 2 billion years ago leading to the accumulation of oxygen in the atmosphere [14]. Oxygenic photosynthesis requires two substrates: water and carbon dioxide from which oxygen, carbohydrates are produced as well as other organic components, used by heterotrophs. Organisms performing oxygenic photosynthesis are called photoautotrophs because they use light energy to synthesize their own organic components. It is the presence of oxygen and the production of organic materials what made the existence of heterotrophs such as animals possible. Heterotrophs, including humans, consume the products of photosynthesis as foodstuff and derive energy from them by respiration, a process by which the organic compounds are oxidized back to carbon dioxide and water. Photosynthesis therefore serves as a vital link between the energy of light and heterotrophs [15].

The photophysical and photochemical processes of oxygenic photosynthesis take place in the chlorophyll-containing thylakoid membrane. This is an extensive membrane system inside the chloroplasts' stroma or in the cytoplasm of cyanobacteria, called thylakoid (from the Greek word meaning sac-like. The thylakoid membranes are independent from the outer membranes. The intra-thylakoidal space forms a compartment called lumen [16]. The essential photochemical process includes the decomposition of water into oxygen, which is released to the atmosphere, and the generation of reducing power in the form of NADPH, and of ATP, a principal energy source formed by the aid of photosynthetically generated proton gradient. Both NADPH and ATP contribute to the synthesis of carbohydrates. Biosynthesis of carbohydrates from carbon dioxide, *via* the Calvin cycle, occurs in the cytoplasm of cyanobacteria or in the stroma of the chloroplasts of algae and higher plants [17, 18].

I. 2. A. Light induced charge transfer

The major photosynthetic complexes embedded in the thylakoid membrane are: photosystem II (PSII), the cytochrome b_6f (b_6f), photosystem I (PSI) and the ATP-synthase.

Referring to its function the **PSII** complex is also called "water-plastoquinone oxidoreductase". Excitation of the reaction center chlorophyll initiates the primary charge separation to form oxidized chlorophyll (P680$^+$) and reduced pheophytin (Pheo$^-$). P680$^+$ successively extracts four electrons from two water molecules, through the manganese cluster and tyrosine Y_Z, to release one molecule of oxygen and four protons into the lumen [19, 20]. The electron on Pheo$^-$ is rapidly transferred to a tightly bound quinone (Q_A), which, in turn, passes this electron to a loosely bound plastoquinone (Q_B). For every pair of water molecules, two fully reduced and protonated plastoquinols are formed. When Q_B acquired two electrons from Q_A in two successive photoacts and extracted two protons from the stroma (or the cytoplasm), it is replaced by a plastoquinone at the binding site, and the plastoquinol transfers electrons to the b_6f complex. [21-24].

At the cytochrome b_6f complex, or "plastoquinol-plastocyanin oxidoreductase", plastoquinol is oxidized at the lumenal side of the membrane. In this process, it loses two electrons and releases two protons to the lumen. The plastoquinol is first oxidized to a semiquinone by the Rieske iron-sulphur cluster, which is subsequently oxidized by the cytochrome f that releases the electron to a soluble electron carrier (plastocyanin or cytochrome c_6). The semiquinone is reduced by two b-haems and the recently discovered c-haem of the b_6 [25, 26]. The haems operate in the so-called "Q-cycle", similar to that in the cytochrome bc_1 complex, and provide additional proton translocation into the lumen.

The **PSI** complex is also called "plastocyanin-ferredoxin oxidoreductase". Excitation energy absorption of P700*, the reaction center chlorophyll, results in a charge separation to form an oxidized chlorophyll (P700$^+$) and a reduced one called A_0^-. An electron from plastocyanin (or cytochrome c_6) reduces P700$^+$. The electron on A_0^- is rapidly transferred to a phylloquinone, and then in a series of redox reactions to three iron-sulphur clusters, FeS-X FeS-A and FeS-B and finally to the soluble ferredoxin (Fd) [19, 27, 28]. Fd reduces NADP$^+$ to NADPH in a reaction catalyzed by a soluble enzyme the ferredoxin-NADP$^+$-reductase. [29-31].

The consequence of this electron transport is the generation of an electrochemical potential across the membrane, with positive charges in the lumen. A proton gradient is

also developed across the membrane, which provides energy to drive ATP synthesis, by the fourth complex, the **ATP-synthase**. In this process, protons flow from the lumen through the integral membrane part CF_0 of the ATP-synthase to CF_1, which is located in the stroma, to achieve ATP synthesis. [32-35].
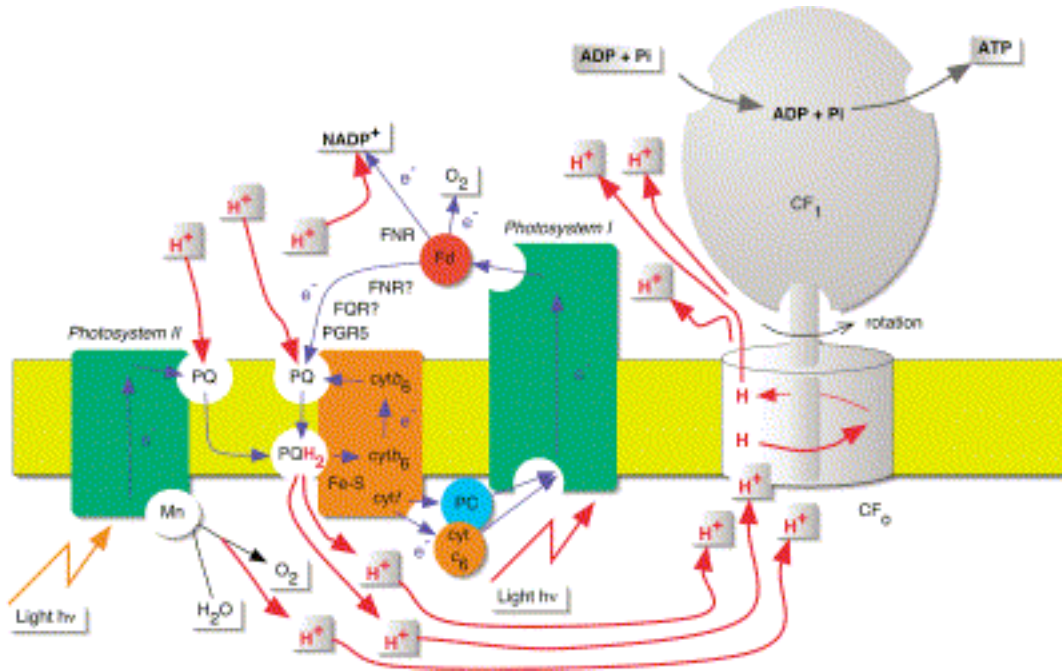
Figure 2. Photosynthetic electron transport.

Electron transport (e⁻) (blue) is arranged vectorially in the thylakoid membrane (yellow). Proton (H⁺) translocation (red) from the stroma (above the membrane) into the lumen (below the membrane) establishes a proton motive force that couples electron transport to ATP synthesis. From a minireview by J. F. Allen [36].

I. 2. B. Light-harvesting antenna

Energy for the above discussed electron transport and protein gradient is provided by excited reaction center chlorophylls. The excitation energy is transferred to them from the light harvesting antenna complexes. These are special protein complexes, which bind the light-absorbing chromophores. The structural variability of light-harvesting antennae of different organisms reflects a variety of solutions to the same problem: how to collect most efficiently light utilizing various wavelengths and a wide range of intensities. Light-harvesting antenna complexes increase the rate of photosynthesis by absorbing light and transferring the excitation energy to the reaction center chlorophylls [1].

Antennae can be regarded as **energetic funnels**, in which pigments that are on the periphery of a complex absorb at shorter wavelengths and therefore higher excitation

energy than those close to the trap. For the funnel arrangement to work, there must be both a spatial and an energetic hierarchy of the antenna pigments, so that the shorter-wavelength-absorbing ones are farther from, and the longer-wavelength-absorbing ones are closer to the trap. During energy transfer excitation moves from higher- to lower-energy pigments, at the same time heading towards the reaction center. With each transfer, a small amount of energy is lost as heat. The energy lost in each step provides a degree of irreversibility to the process, so the net result is that the excitation is funneled to the reaction center, where the energy is converted into chemical energy [1].

Energy

| Blue-absorbing Pigments |
| Orange-absorbing Pigments |
| Red-absorbing Pigments |
| Reaction Centers |
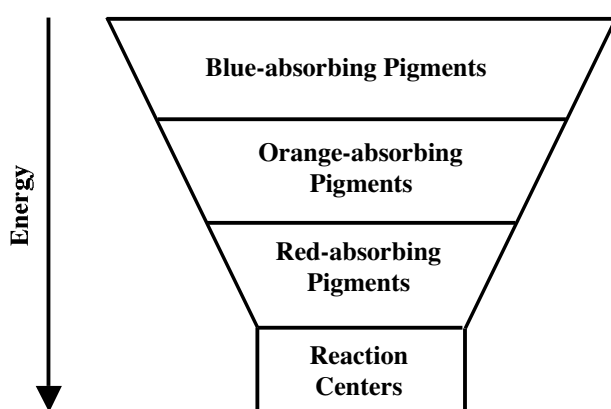
Figure 3. The funnel concept in photosynthetic antennae.

Sequential excitation transfer from the higher-energy (blue-absorbing) pigments to lower-energy (red-absorbing) pigments deliver excitations to the proximity of the reaction center. (from [1]).

The photosynthetic reaction centers of cyanobacteria, algae and the higher plants are very similar in structure and function. The predominant differences among the photosynthetic apparatus of different photosynthetic organisms derive from the diversity of their light harvesting antenna systems. The diversity of the photosynthetic antenna derives from their associated chromophores as well as from their protein structures.

The chromophores used by photosynthetic organisms belong to three families: 1. **chlorophylls** (Chl) and **bacteriochlorophylls** (BChl), 2. **phycobilins**, and 3. **carotenoids** [37]. Chls are cyclic tetrapyrroles, called porphyrin ring, carrying a characteristic isocyclic five-membered ring, they generally contain a central magnesium ion. (BChl has a partly saturated ring B in addition to ring D). Chls function as light-harvesting pigments in the antennae as well as electron donors in the reaction centers. Phycobilins are open-chained tetrapyrroles with no metal ligand. Carotenoids are the structurally and functionally most diverse group of photosynthetic pigments. They are classically defined as diterpenes: two C_{20}-units are joined tail-to-tail to a chain of 32 carbon atoms bearing eight methyl side-chains. In some carotenoids the basic carbon skeleton is slightly modified, for example by

cyclization at one or both ends. Other pigments absorbing in the same spectral range can largely substitute light harvesting by carotenoids, but carotenoids are also crucial as protective pigments against direct and indirect photo oxidative damage.

The light-harvesting protein complexes can be divided into **integral membrane complexes** and **external membrane complexes** [1] (Table 1).

Peripheral membrane antennae	Integral membrane antennae		
	Fused	**Core**	**Accessory**
Phycobilisome of cyanobacteria and red algae	**Photosystem I reaction center**	**CP43 and CP47 complexes of photosystem II**	**LHCII complexes of photosystem II**
Chlorosomes and FMO protein of green bacteria	**Green sulfur bacteria reaction center**	**LH1 complex of anoxygenic bacteria**	**LHCI complexes of photosystem I**
Peridinin-chlorophyll proteins of dinoflagellates	**Heliobacterial reaction center**		**LH2 complex of purple bacteria**

Table 1. Classes of photosynthetic antennae. See text for further explanation. (from [1]).

Integral membrane antenna proteins cross the lipid bilayer and are quite diverse in terms of structure and relative position in the energy transfer chain. **Fused antenna/reaction center complexes** cannot be separated biochemically from the electron transfer components, because they are bound to the same proteins. The class of integral membrane antennae known as **core antenna complexes** are closely associated with the reaction center, but can be separated from it. Another group of integral membrane antenna complexes is called **accessory antennae**, because they are found in addition to the core (or to the fused) antennae. They are often present at variable amounts, depending on growth conditions.

External membrane antennae are associated with components embedded in the membrane, but they do not span the membrane. They are attached to one side of the photosynthetic membrane and constitute accessory antennae.

Major of antenna complexes were classified in seven families [38]:

Before focusing on the structure and function on one of them, the basic characteristic of all seven are discussed briefly.

1. **Core antenna complexes**: Fused core antennae are found in the PSI reaction center of cyanobacteria, algae and higher plants (containing Chl *a*), in the reaction centers of green sulfur bacteria (containing BChl *a*) and of heliobacteria (containing BChl *g*) [38, 39]. The core antenna of PSII, called CP47 and CP43, are structurally and evolutionarily related to the fused antenna/reaction center complexes of the PSI reaction center proteins.

2. **Proteobacterial antenna complexes** (LH1, LH2, and LH3): The basic unit of the LH1 core antenna of purple bacteria is a dimer of two small polypeptides, α and β, each having one membrane-spanning helix and binding one BChl *a* or BChl *b*. The distal accessory antennae LH2 and LH3 are composed of rings of α and β polypeptides that are related to the LH1 α and β polypeptides, but their α/β dimer binds a third BChl [40].

3. **Eucaryotic LHC superfamily**: The light-harvesting complex (LHC) found in plants and algae is an accessory type integral membrane antenna. A large number of similar proteins are found in the membrane of green algae and plants, and these proteins are called LHCI or LHCII, associated with photosystem I or photosystem II, respectively. Interestingly, cyanobacteria do not have LHC, and red algae have only LHCI. In plants LHCs contain Chl *a* and Chl *b*, but in some organisms, like red algae, it contains only Chl *a*, while in other organisms (LHC of diatome, dinoflagellate and brown algae) it contains both Chl *a* and Chl *c* [41].

4. **Peridinin-Chl *a* protein**. Dinoflagellate algae contain a soluble peridinin-Chl *a* antennae located in the thylakoid lumen [42]. Peridinin is a highly-oxygenated carotenoid. The peridinin-Chl *a* protein transfers energy to a Chl *a*/*c* LHC.

5. **Chlorosome**: Green sulfur bacteria and green filamentous bacteria have cigar-shape antenna complexes, the chlorosomes, appressed to the cytoplasmic side of the inner cell membrane. It is largely made up of BChl, with a relatively small amount of protein. The BChls (BChls *c*, *d* or *e*) are organized in rod-shaped aggregates surrounded by a lipid monolayer that forms the chlorosome envelope. An integral part of the chlorosome containing small amount of BChl *a* is known as the blaseplate [43].

6. **Fenna-Matthews-Olson (FMO) protein**: The localization of the BChl a-containing FMO protein within the green bacteria is still uncertain. Trimers of the FMO proteins are often modeled as forming a layer between the chlorosome baseplate and the reaction center, or partly embedded in the lipid bilayer beside the RC [43].

7. P**hycobilisome**: The primary light-harvesting antenna of cyanobacteria and red algae is a large bilin-protein complex called the phycobilisome. The phycobilisome is the only light-harvesting antenna to utilize linear tetrapyrroles, bilins, as chromophores [44].

I. 3. The phycobilisome

I. 3. A. Structure

The phycobilisome (PBS) is a high-molecular weight, $5\text{-}10\text{x}10^6$ Da protein complex located on the thylakoid membrane. It absorbs visible light between 450-665 nm extending the spectral range for photosynthetic light harvesting to the region between the red and blue absorption bands of Chl. Phycobiliprotein-containing organisms show the largest variation in the spectral range of their antenna pigments and thus the greatest adaptability to the quality and quantity of incident radiation [45]. Various environmental conditions such as nutrient availability, temperature, salinity or pH may also influence this antenna complex [46].

The PBS is primarily composed of chromophore-containing phycobiliproteins (~ 80 %) and smaller amounts of colorless linker polypeptides (~ 20 %) [47]. Energy transfer in the PBS is unidirectional, approaching 95 % efficiency. Four types of PBS morphology exist: hemidiscoidal, hemiellipsoidal, bundle-shape and block-shape [44]. The hemidiscoidal PBS - like the PBS of *Synechocystis* sp. strain PCC6803 (*Synechocystis* PCC6803) - is the most common one, it contains two main structural elements: a core substructure from which six pheripherical rods radiate (Figure 4) [48].
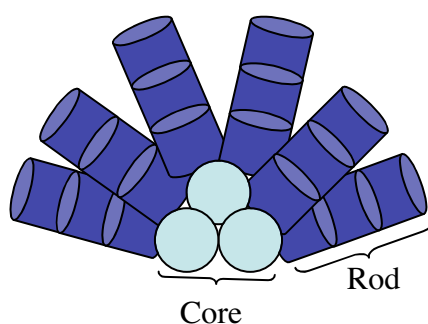
Figure 4. Schematic representation of a hemidiscoidal PBS.

The PBS has two main structural elements: the core and the peripherical rods.

Phycobiliprotein monomers are heterodimers consisting of two different subunits called α and β. The α and β subunits have very similar tertiary structure. They have a globin-like fold, which reminds the myoglobin fold. Based on the nomenclature of the myoglobin six helices the phycobiliprotein subunits were denoted as A, B, E, F, G, H, and two additional helixes of the phycobiliprotein, which are responsable for the dimerization of the αβ subunits, X and Y. [49]. The comparison of the globin and the phycobiliprotein supports the idea that oxygen-binding proteins and phycobiliproteins are related members of the same protein family. The different functions of these proteins may be the result of

divergent evolution from a common ancestor [50]. Phycobiliprotein monomers are assembled into disc-like trimers $(\alpha\beta)_3$ with a diameter of 12 nm and a thickness of 3 nm, the disc possessing a central hole of 3 nm in diameter (Figure 5. A) [51]. The fundamental assembly units of PBS are trimeric or hexameric aggregates [52]. Phycocyanin hexamers are formed by face-to-face aggregation of trimeric disks (Figure 5. B) [4].

A.

Phycocyanin trimer   **Allophycocyanin trimer**

B.   **Phycocyanin hexamer**

Face view   Side view

6 x 12 nm
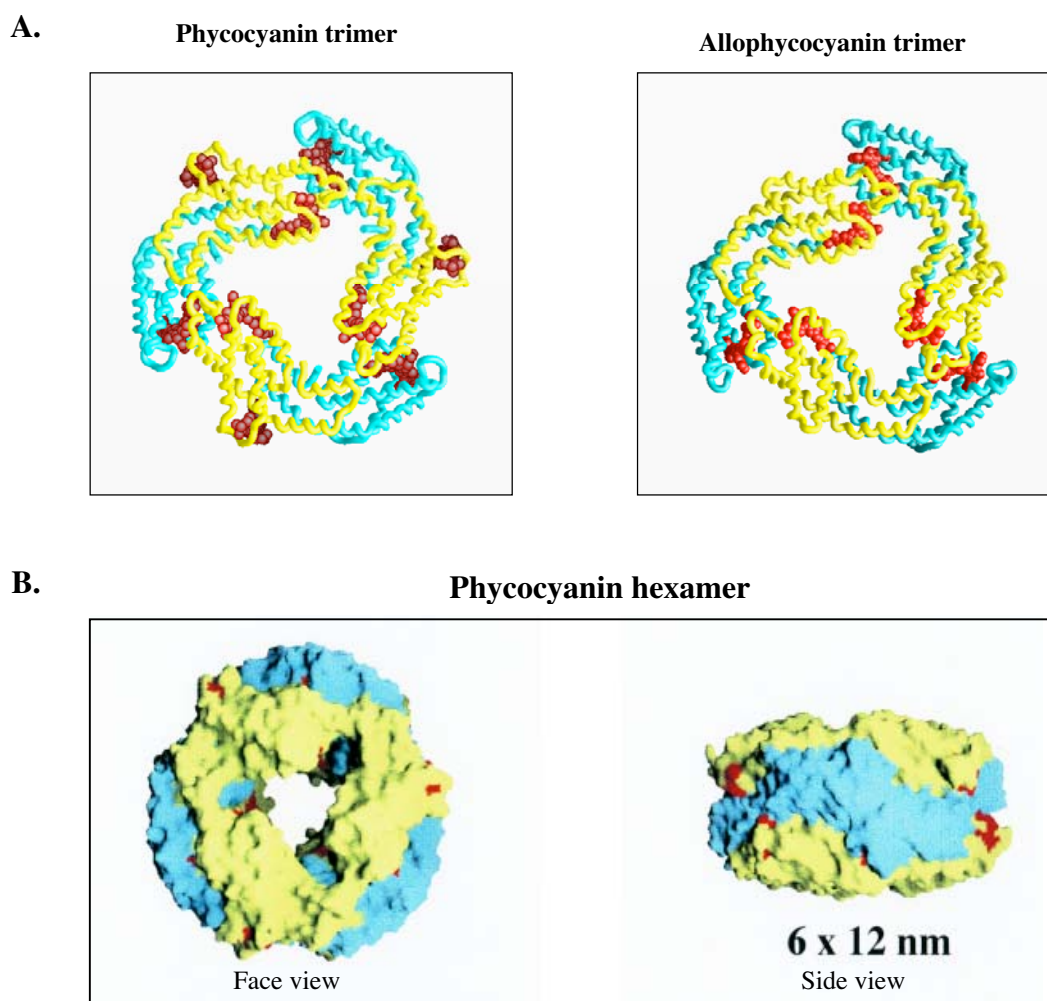
Figure 5. Crystallographic structural models of phycocyanin and allophycocyanin trimers.

A. Cα backbone (α-subunit: blue; β-subunit: yellow) and PCB chromophores (red).
B. Molecular surface of a phycocyanin hexamer
Kindly provided by Daniel Picot. [4, 5]

I. 3. A. 1. Phycobiliproteins

Phycobiliproteins are water-soluble proteins containing open-chain tetrapyrroles, known as phycobilins. All phycobilins are related to biliverdin, their biosynthetic precursor. Biological tetrapyrroles, like phycobilins and chlorophylls, could be arranged as branches of a single biosynthetic pathway (Figure 6).
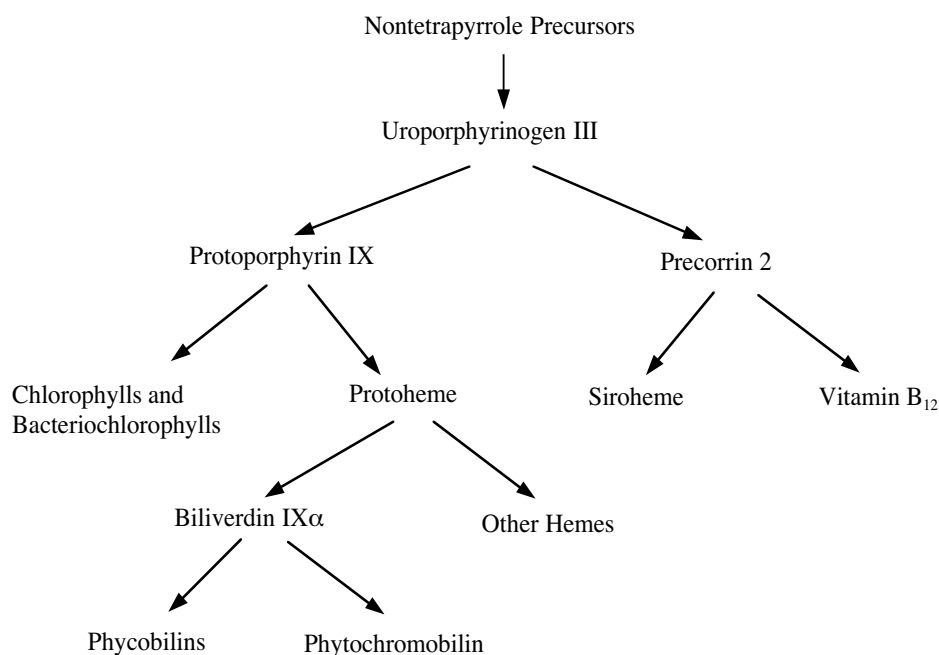
Figure 6. Biosynthetic pathway of tetrapyrroles.

Four main types of the phycobilins are present in cyanobacteria and red algae: the blue-colored **phycocyanobilin** (PCB); the red-colored **phycoerythrobilin** (PEB); the yellow-colored **phycourobilin** (PUB); and the purple-colored **phycobiliviolin** (PXB) (also named cryptoviolin) (Figure 7).
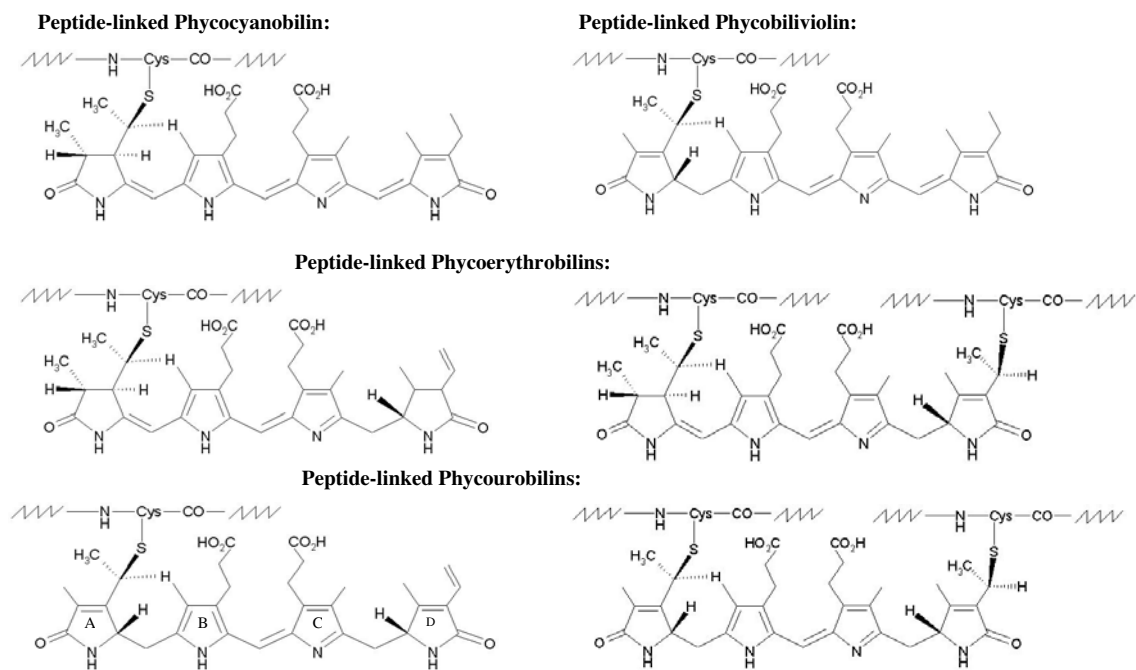
Figure 7. Phycobilin structures and bilin-peptide linkages in phycobiliproteins.

Phycobilins are bound at conserved positions of phycobiliproteins either by one cysteinyl-thioether linkage through the vinyl substituent on the pyrrole ring A of the tetrapyrrole, or occasionally by two cysteinyl-thioether linkages through the vinyl substituents of ring A and D respectively. Phycobiliproteins are divided into four classes on the basis of their visible absorption properties (Table 2): allophycocyanin (APC, λ_{Amax} = 650 nm), phycocyanin (PC, λ_{Amax} = 620 nm), phycoerythrocyanin (PEC, λ_{Amax} = 575 nm) and phycoerythrins (PE, λ_{Amax} = 565 nm) [44].

Phycobiliproteins of the PBS core

PBS core forms a physical connection with the surface of the photosynthetic membrane. It is composed of trimeric discs of turquoise-colored allophycocyanins arranged into cylinders. Among phycobiliproteins **allophycocyanins** absorb light and emit fluorescence at the longest wavelength [44]. Allophycocyanin contains one PCB chromophore per subunit (Figure1. A). The PCB chromophores on the α and β subunits are attached to cysteins, Cys α-84 and Cys β-84, respectively [5]. The core contains various allophycocyanin subunits the allophycocyanin (APC) subunits α^{APC} and β^{APC}, the α-allophycocyanin-B (α^{APCB}) (a specific type of α subunit), the β^{18} subunit (a specific type of β subunit) or the phycobiliprotein domain of the core-membrane-linker polypeptide [53] (Table 2. A and B). The *apcBA* genes encode the β^{APC} and the α^{APC}, respectively. The *apcE*, *apcD* and *apcF* genes encode the LCM, the α^{APCB}, and the β^{18} subunits, respectively. The two terminal energy acceptors are the α^{APCB} (λ_{Amax} = 671 nm) [54, 55] and the phycobiliprotein domain of the LCM (λ_{Amax} = 665 nm) [56, 57].

Phycobiliproteins of the PBS rods

Stacked hexameric discs, called rods, radiate from the core. A phycocyanin hexamer is always located at the rod-core linkage position, while the more distal complexes might be either **phycocyanin** (PC), **phycoerythrocyanin** (PEC) or **phycoerythrin** (PE) hexamers depending on the organism and the growth condition (Table 2. A,).

The *cpcBA* genes encode the β and the α subunits of PC. Two PCBs are attached to the β^{PC} subunit at Cys β-84 and β-155, and one to the α^{PC} subunit at Cys α-84 (Figure 1. A.) [49]. PC of some marine cyanobacteria contains PEB or PUB beside PCB [44, 58]. The blue-colored PCs involved in the rod-core junction are constitutively expressed under all

growth conditions. Some cyanobacteria, which are able to adapt to various wavelength ranges, contain PC which is only induced under specific conditions [59, 60].

The shortest wavelength-absorbing rod elements are PEC or PE, when present. These elements are located at the periphery of the rods. PBS rods might contain either PEC or PE but never both. The PBS of *Anabaena variabilis* and *Mastigocladus laminosus* contains PEC, while the PBS of *Calothrix* PCC7601 (also known as *Fremyella diplosiphon*) and *Synechococcus* WH8102 contains PE. The *pecBA* genes encode the β and α subunits of the PEC, and the *cpeBA* genes encode the β and α subunits of PE [61].

In PEC the α subunit bears a PXB chromophore instead of a PCB chromophore [44]. Under medium or low light the purple-colored PEC extends the light-harvesting capacity of PBS into the green portion of the spectrum.

The red-colored PE family exhibits large diversity in chromophores and in subunit compositions. Two types of PE were described in cyanobacteria. PE-I generally contains PEB chromophores, but PE-I with PUBs have been reported [62, 63]. The α subunit of PE-I bears PEB or PUB attached to Cys α-84 and α-143; while those of the β subunit located at Cys β-84, β-155, with a third one being doubly bound to Cys β-50 and β-61 [44]. PE-II carries an additional PUB attached to Cys α-75 [44]. While PC, PEC and PE-I hexamers are assembled with non-chromophorylated linker polypeptides; PE-II hexamers are assembled with either non-chromophorylated linkers or the chromophore-bearing γ–subunits. The γ–subunit functions as a short wavelength-absorbing biliprotein as well as a linker polypeptide (see also I. 3. A. 2) [64, 65].

Table 2. Tables of phycobiliproteins.

A, Phycobiliproteins of the phycobilisome. **B,** Specific allophycocyanins, which are involved in the energy transfer to the reaction centers.

A,

Name	Abbreviation	Gene	Phycobilins of β subunit & α subunit		λ_{Amax} (nm)	Color	Location
Allophycocyanin	APC	*apcBA*	1 PCB	1 PCB	650	turquoise	core
Phycocyanin	PC	*cpcBA*	2 PCB	1 PCB	620	blue	rods
Phycoerythrocyanin	PEC	*pecBA*	2 PCB	1 PXB	575	purple	core-distal end of the rods
Phycoerythrin	PE	*cpeBA*	3 PEB or PUB (PE-II: + 1 PUB)	2 PEB or PUB	565	red	rods

B,

Name	Abbreviation	Gene
α-Allophycocyanin-B	α^{APCB}	*apcD*
Allophycocyanin β^{18} subunit	β^{18}	*apcF*
Core-membrane linker	LCM	*apcE*

I. 3. A. 2. Linker polypeptides

Different linkers are specifically associated with each type of phycobiliprotein and they stabilize the PBS and optimize its absorbance and energy transfer characteristics [47] (Table 3.). Biochemical and structural analysis suggest that linker polypeptides bind to the central cavity of phycobiliprotein discs (Figure 8) [2, 4, 66].
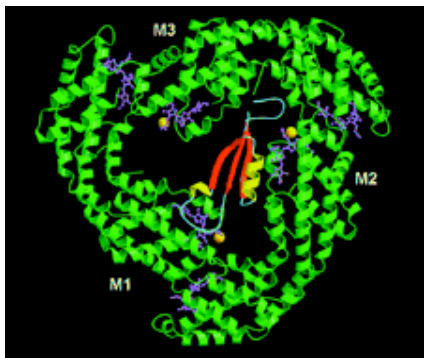
Figure 8. Crystallographic model of the entire APC•LC complex.

The $\alpha\beta$ subunits are represented in green and the chromophores in pink. The secondary structural elements of the linker polypeptide are represented in red, yellow and blue. (from: [2]).

Linker polypeptides modulate the spectral properties of different phycobiliprotein trimers and hexamers, mainly by causing a red-shift in their absorption and fluorescence maxima [67, 68]. These small spectroscopic changes are believed to facilitate unidirectional transfer of excitation energy from the rod periphery to the core of the PBS.

Linker polypeptides (Table 3) may divided into four groups according to their function:

1. The core-membrane linker (LCM): a multifunctional polypeptide;
2. The core linker (LC): participates in the assembly of the core;
3. The rod-core linker (LRC): mediates the attachment of the rods to the core;
4. The rod linkers (LR): involved in the rod assembly.

The **core-membrane-linker phycobiliprotein** (LCM), encoded by the *apcE* gene, is the largest chromophore-containing protein in the PBS and has a molecular mass that varies from 75 to 128 kDa depending on the organism. In *Synechocystis* PCC6803 the LCM is about 100 kDa. Two copies of this multifunctional polypeptide are present per PBS. The LCM funnels light energy to the photosynthetic reaction centers, and plays a key role in the core architecture and the anchoring of the PBS to the photosynthetic membrane [44]. Different domains have been identified within the LCM polypeptide (Figure 9). The amino-terminal portion contains the phycobiliprotein domain, which is homologous to the α^{APC} subunit [53]. This domain contains a small insertion of approximately 50 residues forming a loop domain. The Loop domain was involved in the attachment of the PBS to

26

the thylakoid membrane [69], but a *Synechocystis* PCC6714 mutant in which the loop encoding domain was deleted contained PBSs that were functionally equivalent to those of the wild type [70].
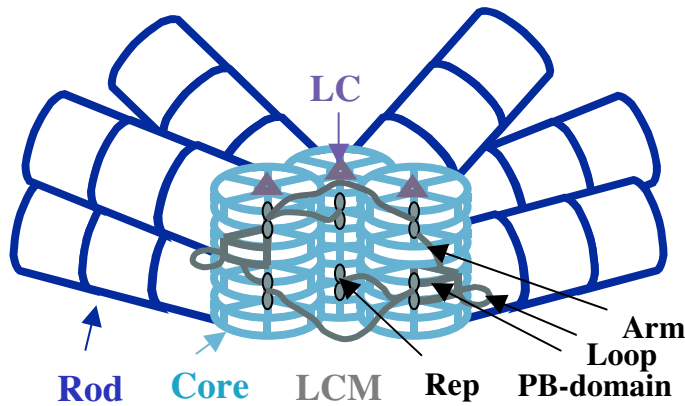
Figure 9. Schematic representation of the PBS with LCMs and LCs.

The APC containing core is in turquoise and the PC hexamer containing rods are in dark blue. LC is represented in purple. Black arrows point to the domains of the LCM (grey): Reps, phycobiliprotein domain (PB-domain), Loop and Arms.

The carboxy-terminal portion of the LCM contains repeated domains (Reps) of about 120 residues. These Reps are about 60 % similar to the conserved domains of the rod linkers and are likely to play the same role, i.e. interaction with phycobiliprotein discs. The number of Rep domains of the LCM determines the number of the cylinders in the PBS core [71]. The domains that form the connection between the phycobiliprotein and the Rep domains are called ARMs and they do not share sequence homology among themselves [72, 73].

The **small core-linker polypeptide** (LC), encoded by the *apcC* gene, is associated with trimeric APC discs at the peripheries of the core (Figure 4) [53, 74]. This linker polypeptide is not required for PBS assembly, but improves the stability and energy transfer properties of the PBS [75].

The **rod-core-linker polypeptide** (LRC)**,** encoded by the *cpcG* gene, mediates the attachment of the first PC-hexamer of the rods to the core [66-68, 76]. The LRC has two distinct functional domains: the N-terminal domain (~ 21 kDa) attached to a PC-hexamer and the C-terminal domain (~ 6 kDa) linking the rod to the core [66]. The LRC attachment causes a strong red-shift in the absorbance and fluorescence emission of the PC-hexamers to assure optimal rod-to-core energy transfer [67, 68]. Some cyanobacteria have more than one *cpcG* genes in their genome. *Anabaena* PCC7120 has four *cpcG* genes, but only three LRCs were detected in the PBS [77]. *Synechococcus* WH8102 has two rod-core linker encoding genes, *cpcG1* and *cpcG2*, and both gene products were detected in the PBS [65].

The genome of the *Synechocystis* PCC6803 contains two *cpcG* genes (see Results and Discussions IV. 1. E).

In PBS containing only PC, **rod-linker polypeptides** (LR) are divided in two groups according to their molecular masses. The first group consists of an approximately 10 kDa polypeptide (LR10), coded by the *cpcD* gene. This small linker is believed to be bound at the core-distal end of the rods, thus minimizing the heterogeneity of rod lengths [78, 79]. The second group consists of polypeptides of about 30 kDa. *Synechococcus* PCC7002 and *Thermosynechococcus elongatus* have only one 33 kDa rod-linker polypeptide, while two rod-linker polypeptides were identified in *Synechococcus* PCC7942 (also called *Anacystis nidulans*) and in *Synechocystis* PCC6803: LR33, coded by the *cpcC1* gene, and LR30, coded by *cpcC2* gene. The *cpcC* and *cpcD* genes are located in the *cpc* operon. LR30 and LR33 incorporate subsequent PC-hexamers into the rods, following the attachment of the first PC-hexamer to the core by LRC [67, 80]. LRs have two distinct functional domains, the N-terminal part attaches to PC-hexamers, and the C-terminal part links consecutive PC-hexamers in the rod [66].

In PEC-containing cyanobacteria, specific rod-linker polypeptide incorporates PEC hexamers into the rod substructures. This is encoded by the *pecC* gene.

In cyanobacteria capable to adapt to different light quality, PE hexamers are attached by three rod-linker polypeptides encoded by *cpeC, D* and *E* genes. Although rod linkers are generally non-pigmented, PE-II-containing PBS has been shown to possess chromophorylated linkers called γ-subunits [64].

Table 3. Linker polypeptides of a phycobilisome containing only PC.

| Name	Abbreviation	Gene	Role	Molecular weight
Core-membrane linker	LCM	*apcE*	Determinates core size, binds to membrane, terminal energy acceptor	~ 100 kDa
Small core linker	LC	*apcC*	Stabilizes core substructure	~ 8 kDa
Rod-core linker	LRC	*cpcG*	Mediates rod-core attachment	~ 27 kDa
Rod linker	LR	*cpcC*	Incorporates subsequent phycobiliprotein hexamers into rods	~ 30 kDa
Small rod linker		*cpcD*	Minimizes heterogeneity of rod lengths	~ 10 kDa

I. 3. B. PBS function and regulation

I. 3. B. 1. Energy transfer

Light energy, absorbed by the PBS, migrates through the rods into the core and then to Chl *a* in the thylakoid membrane. These events are nonradiative, efficient, and

unidirectional [45]. The crystal structure of PC has been determined in both the trimeric and hexameric assembly forms providing a basis for understanding of the functional properties of the phycobiliproteins and energy transfer in the PBS [4, 49]. Radiationless de-excitation pathways are minimized by the rigid framework in which the phycobilins are held in the protein. In a phycobiliprotein, the phycobilins which absorb light energy and transfer the excitation to other phycobilins are called donors; while those which absorb the excitation energy of the donors and transfer it to the next phycobiliprotein in the energy migration chain, are called acceptors [45]. These latter chromophores emit fluorescence when the phycobiliprotein is not incorporated into the PBS and unable to transfer its energy further.

In the rods α-84 and β-155 phycobilins are donors lying towards the periphery of the trimeric disc. On the other hand phycobilin β-84 is an acceptor extending into the center of the disc (Figure 10) [51]. Excitation energy absorbed by any of the phycobilins at the periphery of a PC disc is rapidly transferred to the centrally located acceptor phycobilins [45, 81, 82].
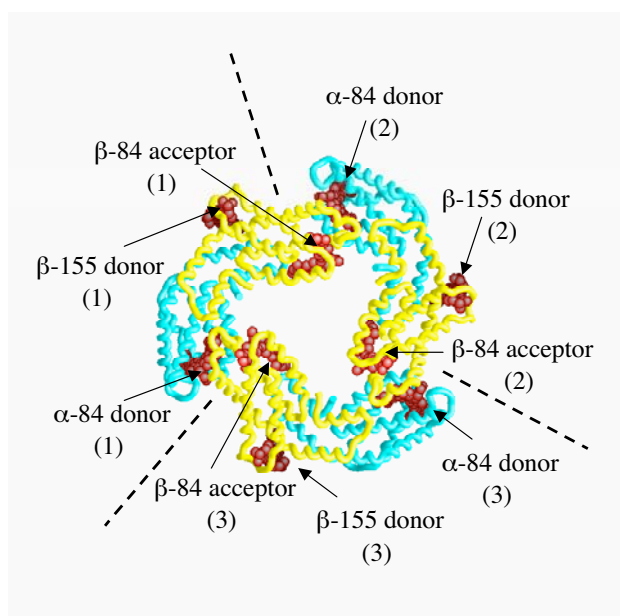
Figure 10. Structural model of Cα backbone of a PC trimer with its PCB donors and acceptors.

Dotted lines indicate the parts of the monomers and black arrows show the different types of chormophores. (α-subunit, blue; β-subunit, yellow and PCB chromophores, red) Kindly provided by Daniel Picot. [4, 5]

The rod is built up by stacked hexamers, and the β-84 phycobilins are arranged vertically above one another in an orientation favoring rapid energy transfer from each of the three acceptor phycobilins of the same disc to the acceptors in the disc below [4]. The large energy difference between different phycobiliproteins, such as between PE and PC, promotes unidirectional energy transfer. Whereas between the same types of phycobiliproteins, like between PC-hexamers, energy transfer is promoted by specifically attached linker polypeptides, modifying their absorption and fluorescence emission

properties. The LRC containing PC-hexamers are red shifted compared to those in the LR containing complexes [67, 68]. Consequently, the favored direction of transfer is from the core-distal to the core-proximal PC discs. The fluorescence emission properties of the LRC containing PC-hexamer and the absorption properties of APC indicate that the latter one functions as an efficient acceptor in the rod to core energy transfer. The same phycobilin is present in PC and APC complexes, but the spectrum of the phycobilins in each instance is "tuned" by the protein to absorb at different wavelengths, by maintaining the chromophores in specific conformations in the two different phycobiliprotein [5].

Energy transition in the core is probably similar to processes in the rods. It has been proposed that the spectral shift in allophycocyanin trimers is caused not only by the chromophore conformational change, i.e. by the aggregation of monomers to trimers, but also by excitonic interaction between the chromophores [83, 84]. In the core excitation energy is transferred from APC to α^{APCB} or *via* β^{18} to the phycobiliprotein domain of the LCM [85-87].

In summary, the energy absorbed by any phycobilin in the PBS is gathered on the terminal acceptor phycobilins of the core [45]. The emission of the terminal acceptors overlaps with the absorption maximum of the photosynthetic reaction centers. The light guide function of the PBS is achieved by the energy transfer from the terminal acceptors of the PBS to the reaction centers.

I. 3. B. 2. Adaptation to the environmental conditions

The composition of PBS in cyanobacteria changes in response to changes in (a) light intensity, (b) light quality and also (c) nutrient availability.

(a) For the more efficient absorption of light energy needed to maintaining high level electron transport, PBS-containing organisms can increase the size [88, 89] and/or number of phycobilisomes [90]. They may also alter the phycobiliprotein composition of PBS in response to change in light intensity. For example the ratio of PUB to PEB in the PE of *Callithamnion roseum* depends on the intensity of illumination, the PEB/PUB ratio increases when growth light is increased [90].

(b) The response to light quality is referred to as complementary chromatic adaptation. In this process the phycobiliprotein composition of the PBS changes in order to optimize the absorption of excitation energy [60, 91]. In *Calothrix* PCC7601, the PE to PC ratio reflects the spectral distribution of the light in their environment. When this strain is grown

under red light its PBS contains almost no PE and the PBS rods are built up from three PC-hexamers. However in green light, the phycobilisome is made of rods containing only one PC-hexamer each and up to three PE-hexamers (Figure 11). This change in rod composition is reversible and facilitates efficient harvesting of the prevalent wavelength component of light. In natural sunlight, the mixture of red and green light results in a PBS with rods containing both PC and PE [46].
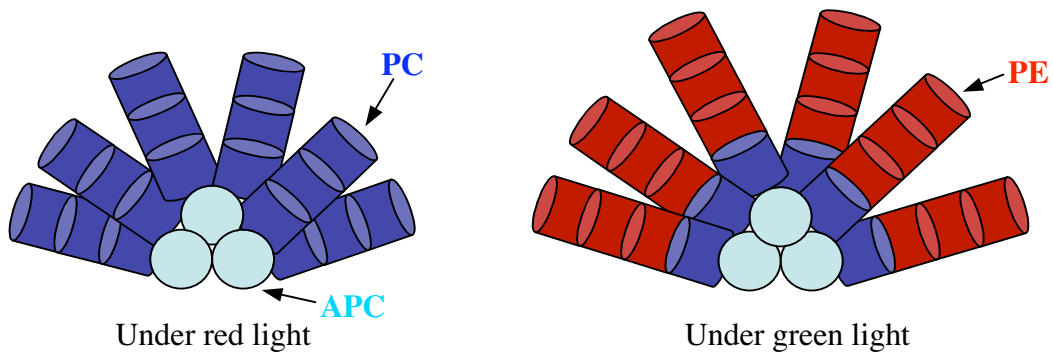
Figure 11. Chromatic adaptation.

Under red light the PBS rods are built up only from PC-hexamers, while under green light one PC-hexamer and three PE-hexamers built up the rods. (PE: red; PC: blue; APC: turquoise)

The PBS composition is controlled by the induction of various phycobiliprotein-encoding genes. The *cpeBA* genes are induced by green light in *Calothrix* PCC7601 [92]. There are three distinct *cpcBA* operons on the genome of the *Calothrix* PCC7601. The *cpcB1A1* operon is constitutively transcribed, the *cpcB2A2* operon is specifically active under red-light and inactive under green-light conditions [93, 94], and the *cpcB3A3* is only active during sulfur-limited growths [95].

(c) Cyanobacterial phycobilisomes are not only for light harvesting, they may also serve as protein storage under nutrient limited conditions. While phycobiliproteins are extremely abundant constituents of the cyanobacterial cells (50 % of the total soluble protein) under natural conditions, nitrogen- or sulfur-starvation causes rapid and almost complete loss of the PBS in *Synechococcus* PCC7942 [96, 97]. On the other hand, *Synechocystis* PCC6803 degrades its PBS under nitrogen-starvation but not under sulfur-starvation [98]. The *nblA* gene product is a polypeptide tagging the PBS for degradation during nitrogen starvation in several cyanobacterial species in a yet unknown way [46, 99]. This gene is induced and

essential for PBS degradation during nitrogen starvation. The degradation of the PBS under nitrogen starvation is a controlled process: starting with the degradation of the most distal PC-hexamers and associated linkers to the core [98, 100].

I. 3. C. Ferredoxin-NADP(H) oxidoreductase, a PBS associated protein

The *petH* gene product, ferredoxin-NADP(H) oxidoreductase (FNR), is a flavoprotein that catalyzes electron transfer between ferredoxin (or flavodoxin) and NADPH. Two isoforms of the FNR are found in photosynthetic as well as in non-photosynthetic plastids of higher plants, with a molecular mass ranging from 33 to 36 kDa [101, 102]. Despite the similarity in both biochemical properties and protein structure between cyanobacterial and plant FNRs [103], the cyanobacterial *petH* gene encodes a much larger (47 kDa) FNR than the chloroplastic one. The a 47 kDa FNR was found to be a constituent of purified PBSs, on the other hand FNR enzymes purified from several cyanobacterial strains were about 34 kDa: *Anabaena variabilis* [104, 105]; *Anabaena* sp. PCC7119 [106]; *Spirulina* sp. [107] and *Synechocystis* PCC6803 [108]. The 34-kDa enzyme was suggested to be a proteolytic product of the 47-kDa FNR.

The N-terminal domain of the 47 kDa FNR is similar to LR10, connected by a hinge-domain to the enzymaticaly active part [109]. A PEST-like sequence found on the hinge-domain of the *Synechocystis* PCC6803 FNR [110] seems to be frequent target site of proteolytic cleavage [111]. The LR10-like domain is responsible for the PBS binding of the enzyme [110]. According to van Thor *et al.*, each PBS of *Synechocystis* PCC6803 binds ~2.4 copies of FNR in average and 74 % of the FNR molecules is bound to PBS [112]. According to Gómez-Lojero *et al.* less than two FNRs could be specifically bound to the PBS in *Synechococcus* PCC7002, and 97 % of the FNR activity is associated to the PBS [113]. There is no consensus on the localization of the FNR binding site: it was suggested to be on the core-proximal PC-hexamer or even on the core itself [112], but other studies associated it to the core distal end of the rods [113]. The assumed association of FNR with the PBS would localize the FNR in close proximity to its ultimate source of reducing power, PSI [109].

Although the principal function of FNR is to catalyze the terminal step of electron transport [114], other functions have also been proposed for it. Among others it has been suggested that the FNR participates in cyanobacterial respiration [115], acting as an NADPH dehydrogenase [105], and takes part in cyclic electron transport [110].

Synechococcus PCC7002 and in *Synechocystis* PCC6803 mutant strains in which the *petH* gene was inactivated failed to segregate, indicating that the *petH* gene product is essential for the viability of both cyanobacteria [109, 116].

II. AIMS

Various linker polypeptides are associated with phycobiliproteins in the PBS: they are essential for stabilizing the PBS structure and for optimizing the efficiency of energy transfer. The aim of the present work was to study PBS assembly in *Synechocystis* PCC6803.

The PBS of *Synechocystis* PCC6803 consists of a core from which six rods radiate, each rod is composed of three stacked PC-hexamers and rod linkers. Two independent gene copies encode the rod-core linker (LRC) that attaches the proximal PC-hexamer to the core. Rod-linker polypeptides, LR33 and LR30, incorporate further PC-hexamers. An other small rod-linker, LR10 can bind to this complex. To our knowledge, this linker has never been studied in *Synechocystis* PCC6803. The PC subunits and the rod-linker polypeptides are encoded by the *cpc* operon. In order to study the biogenesis of the PBS rods we generated and characterized various mutants, in which genes encoding rods and rod-core linkers were inactivated.

Two isoforms of the ferredoxin-NADP(H)-oxidoreductase (FNR) were detected in *Synechocystis* PCC6803: a 46.3 kDa FNR, that is associated to the PBS, and a soluble 34.3 kDa FNR that was suggested to be the proteolytic product of the larger form. Site directed mutations of the *petH* gene, encoding the FNR, were constructed to find out the reason why these two isoforms exist.

The main questions addressed by our study were the following:

  i. How do LR33 and LR30 participate in rod assembly following the attachment of the first hexamer by the LRC?

  ii. What is the structural function of LR10 in the PBS?

  iii. Does the absence of rod-linker polypeptides affect PC accumulation?

  iv. Does the insertion of the commonly used Km and Ω cassettes affect the transcription of the *cpc* operon?

  v. Are both LRC-encoding genes, *cpcG1* and *cpcG2* expressed? If so, are their products both functional in PBS rod biogenesis?

  vi. The amino-acid sequence of the 34.3 kDa FNR begins with a methionine (Matsuo, M. et al 1998). Could it be a translational product starting from an alternative initiation site?

  vii. The N-terminal part of the 46.3 kDa FNR is similar to LR10. Do they share the same binding site on the PBS rod? Would the FNR be capable of binding to the PBS core?

III. MATERIALS AND METHODS

III. 1. Growth conditions

Wild-type and mutant strains of the *Synechocystis* PCC6803 were grown photoautotrophically in an illuminated orbital incubator at 32 °C in a CO_2-enriched (~5 %) atmosphere under continuous light (40 μmol m^{-2} s^{-1}). We used a modified BG11 medium [117] containing: 30 μM ferric citrate, 3 μM EDTA-diNa, 30 mM sodium nitrate, 250 μM potassium phosphate, 250 μM magnesium sulphate, 250 μM calcium chloride, 200 μM sodium carbonate, 10 mM sodium bicarbonate and microelements as in BG11. All chemicals were purchased from Sigma. For growth on Petri dishes, the above medium was supplemented with 1.5 % (w/v) Difco Bacto-agar and 2-5 mM sodium thiosulphate. Petri dishes were incubated at 30 °C under continuous light (30 μmol m^{-2} s^{-1}). When appropriate, media were supplemented with 25 to 50 μg/ml kanamycin, 25 to 50 μg/ml spectinomycin and 5 to 10 μg/ml streptomycin.

Escherichia coli strains, DH5α and XL1-Blue, were used for molecular cloning and for the maintenance of the plasmids. Difco LB medium or SOC medium [118] supplemented with the required antibiotic (50-100 μg ml^{-1} ampicillin, 50 μg ml^{-1} kanamycin, 50 μg ml^{-1} spectinomycin and streptomycin) was used to grow them. For the growth on Petri dishes Difco LB Agar was used.

III. 2. Genetic transformation

3 ml of a *Synechocystis* PCC6803 culture ($OD_{580nm} \approx 1.0$) was harvested by centrifugation. The cell pellet was washed with 3 ml modified BG11 and resuspended in 150 μl of modified BG11. Approximately 2 μg of plasmid DNA was added to the cells. The mixture was incubated 6 to 12 hours under dim light then plated on modified BG11 Petri dishes. 12 to 24 hours later the antibiotic containing solution (250 μl) was layered under the agar [7].

III. 3. Genomic DNA isolation from *Synechocystis* PCC6803 cells

Genomic DNA isolation from *Synechocystis* PCC6803 cells was achieved as described by Cai and Wolk [119]: 5 ml from a culture ($OD_{580nm} \approx 1.0$) were pelleted by centrifugation (21000 g 1 min at room temperature). The cells were resuspended in 100 μl TE buffer containing 1 % SDS. 100 μl phenol and 100 μl glass beads (212-300 microns, G-1277 Sigma) were added and the mixture was vortexed for 1 min. The phenol and the aqueous

phases were separated with centrifugation for 5 min 21000 g at 18 °C. The aqueous phase was transferred in a new Eppendorf-tube and nucleic acids were precipitated by adding 0.1 volume of 3 M sodium-acetate and 2.5 volume of ethanol and nucleic acids were collected with centrifugation for 20 min 21000 g at 4 °C. The pellet containing total nucleic acids was washed with 70 % ethanol, dried, and then resuspended in 20 μl distillated water.

III. 4. Cloning, mutagenesis and plasmid constructions

Table 4. Wild-type and mutant *Synechocystis* strains and plasmids used in the PBS related work.

Strain or plasmid	Properties	Source or reference
Strains		
WT	Wild-type strain of *Synechocystis* PCC6803	PCC
30f	Δ*cpcC2*::*aphI* -deletion of 68 % of *cpcC2* (codon 21 to 208), *aphI* insertion (Km^r)	This work
30r	Δ*cpcC2*::*aphI* -as above but *aphI* in the opposite orientation (Km^r)	This work
Δ30D3	Δ*cpcC2, cpcD⁻*::Ω -deletion of 83 % of *cpcC2* (codon 2 to 230) and termination of the *cpc* operon transcription before *cpcD* (Sp^r, Sm^r)	This work
D3	*cpcD⁻*::Ω - Ω insertion between *cpcC1* and *cpcD*, transcription termination before *cpcD* (Sp^r, Sm^r)	This work
33	Δ*cpcC1*::*aphI* -deletion of 50 % of *cpcC1* (codon 77 to 220), *aphI* insertion (Km^r)	This work
CB	Δ*cpcC2C1*::*aphI* -total deletion of *cpcC2* and *cpcC1* (codon 2 of *cpcC2* to the last codon of *cpcC1*), *aphI* insertion (Km^r)	This work
33c	33 transcomplemented with *cpcC1* in the *psbAII* locus (Km^r, Sp^r, Sm^r)	This work
Cbc	CB transcomplemented with *cpcC1* in the *psbAII* locus (Km^r, Sp^r, Sm^r)	This work
D4	*cpcD⁻*::Ω - Ω insertion in *Hinc*II of *cpcD*, transcription termination within *cpcD* (Sp^r, Sm^r)	This work
WD	WT plus *cpcD* in the *psbAII* locus (Km^r)	This work
D3D	D3 plus *cpcD* in the *psbAII* locus (Km^r, Sp^r, Sm^r)	This work
D4D	D4 plus *cpcD* in the *psbAII* locus (Km^r, Sp^r, Sm^r)	This work
CK	Δ*cpc* operon :: aphI, sacB – deletion of 85 % of *cpc* operon, *aphI* and *sacB* insertion (Km^r, Sucrose^s)	This work
G1	*cpcG1⁻* :: Ω - Ω insertion in *Nru*I of *cpcG1* (Sp^r, Sm^r)	This work
G2	*cpcG2⁻* ::*aphI* insertion in *Bsp*1407I of *cpcG2* (Km^r)	This work
Plasmids		
pCPC	4 kb *Mfe*I-*Pst*I genomic fragment carrying the *cpc* operon (Ap^r)	This work
pC30K+	Derivative of pCPC with Km cassette inserted between *Xho*I-*Eag*I (Km^r, Ap^r)	This work
pC30K-	As above with *aphI* gene in an opposite orientation (Km^r, Ap^r)	This work
pΔC2Ω	2.7 kb *Age*I-*Pst*I fragment carrying part of the operon minus 685-nucleotides deletion from *cpcC2*. Ω was inserted 35 bp downstream *cpcC1* (Ap^r, Sm^r/Sp^r)	This work
pΔC30	Derivative of pCPC with deletion of *Xho*I-*Eag*I fragment	This work
pC33K+	Derivative of pCPC with Km cartridge inserted between *Msc*I-*Nae*I (Km^r, Ap^r)	This work
pCBK+	Derivative of pCPC with Km cartridge inserted between *Spe*I-*Nhe*I (Km^r, Ap^r)	This work
pUCDΩ	*Nhe*I-*Pst*I fragment carrying *cpcD* with Ω inserted at *Hinc*II site (Ap^r)	This work
pPSBA2	500-bp upstream and 500-bp downstream of the *psbAII* orf separated by a multiple cloning site cloned in pSL1180 (Ap^r)	[120]
pS1DK	*cpcD* and the Km cartridge inserted in the multiple cloning site of pPSBA2 (Ap^r, Km^r)	This work
pS1C1	*cpcC1* and the Ω cartridge inserted in the multiple cloning site of pPSBA2 (Ap^r, Sm^r/Sp^r)	This work
pUC4K	Origin of the Km^r cassette containing the *aphI* gene (Amp^r, Km^r)	[121]
pDW9	Origin of the Ω fragment containing the *aadA* gene plus strong translation-transcription terminators on both sides (Amp^r, Sm^r/Sp^r)	[122, 123]
pCK	Derivative of pCPC with *aphI* and *sacB* inserted between *Eco*47III and *Nhe*I (Km^r, Ap^r, Sucrose^s)	This work
pG1Ω	850 bp genomic fragment carrying the *cpcG1* gene with Ω casette ineserted at *Nru*I (Ap^r, Sp^r, Sm^r)	This work
pG2K	1305 bp genomic fragment carrying the cpcG2 gene with *aphI* inserted at *Bsp*1407I (Ap^r, Km^r)	This work

Table 5. *Synechocystis* mutant strains and plasmids used in the FNR related work.

Strain or plasmid	Properties	Source or reference
Strains		
I	Point mutation changing M 113 of FNR, to I, Ω casette insertion	This work
V	Point mutation changing V 102 of FNR, to non-initiating V, Ω casette insertion	This work
H	Ω casette insertion	This work
FS1	C insertion, codon 110 of the FNR is a stop codon	This work
FS2	C deletion, codon 113 of the FNR is a stop codon	This work
Plasmids		
pBKH	2742 bp genomic fragment carrying the *petH* gene (Ap^r)	This work
pMS	Derivative of pBKH with deletion of *Sac*I-*Msc*I fragment (Ap^r)	This work
pSB7	216 bp fragment carrying part of the *petH* gene (Cm^r)	This work
pSBH	Derivative of pSB7 with insertion of *Bam*HI-*Eco*RV fragment of pBKH (Cm^r)	This work
pM7	Carrying 572 bp *Xba*I-*Msc*I fragment of pBKH (Ap^r)	This work
pI	Derivative of pM7 with changement of M (ATG) to I (ATC) (Ap^r)	This work
pV	Derivative of pM7 with changement of V (GTG) to V' (GTC) (Ap^r)	This work
pHFS1	Derivative of pMS with insertion of a C at the *Alw*NI site of the *petH* (Ap^r)	This work
pHFS2	Derivative of pMS with removal of a C at the *Alw*NI site of the *petH* (Ap^r)	This work
pSBI	Derivative of pSBH with replacement of *Xba*I-*Mfe*I fragment with *Xba*I-*Mfe*I fragment of pI (Cm^r)	This work
pSBV	Derivative of pSBH with replacement of *Xba*I-*Mfe*I fragment with *Xba*I-*Mfe*I fragment of pV (Cm^r)	This work
pSBHΩ	Derivative of pSBH with Ω cassette inserted at *Bam*HI (Cm^r, Sp^r, Sm^r)	This work
pSBIΩ	Derivative of pSBI with Ω cassette inserted at *Bam*HI (Cm^r, Sp^r, Sm^r)	This work
pSBVΩ	Derivative of pSBV with Ω cassette inserted at *Bam*HI (Cm^r, Sp^r, Sm^r)	This work
pFS1	Derivative of pSBIΩ with replacement of *Eco*RI-*Sma*I frament with *Eco*RI-*Sma*I fragment of pHFS1 (Cm^r, Sp^r, Sm^r)	This work
pFS2	Derivative of pSBIΩ with replacement of *Eco*RI-*Sma*I frament with *Eco*RI-*Sma*I fragment of pHFS2 (Cm^r, Sp^r, Sm^r)	This work

III. 4. A. Plasmids used for cloning and antibiotic cartridge containing plasmids

Commercial plasmids used during our work were: pBluescript SK+ and pBC SK+ (Stratagene); pUC9 and pUC-4K (Pharmacia). The first three were used for cloning and pUC-4K contains the Km cassette between two multi-cloning sites.

Non-commercial plasmids which were used during our work: pDW9 which is described in [123] and contains the Ω cassette between two multi-cloning sites; pPSBA2 plasmid, which contains the *psbA* promoter, and pPSBA2KS plasmid, which contains *sacB* and *aphI* genes, were described in [120].

III. 4. B. Constructions to generate PBS rod-linker mutants

We constructed different plasmids to inactivate with interposon mutagenesis one or different combination of the rod-linker or rod-core linker encoding genes (Table 4 on page 39).

pCPC: A 4239-bp fragment containing the *cpc* operon was amplified by PCR from the genomic DNA of wild type *Synechocystis* PCC6803 with the oligonucleotides pcr (5'- CACACTCTCAACGGTTCCGG) and pcf (5'- GTAGGCTGTGGTTCCCTAGG). A 4047 bp *Mun*I-*Pst*I fragment of the PCR product was cloned into pUC9 plasmid between *Eco*RI and *Pst*I to create pCPC plasmid. The cpc operon containing part of this plasmid was sequenced to verify the fidelity of the PCR amplification.

pCBK+: 1726 bp fragment from *Spe*I to *Nhe*I was excised from pCPC and after a Klenow DNA polymerase treatment it was replaced with the kanamycin cassette containing *Eco*RI fragment of pUC4K. The resulting plasmid was called pCBK+.

pC30K+: A 559 bp fragment of *cpcC2* was excised with *Xho*I and *Eag*I from pCPC, and after Klenow DNA polymerase treatment the *Eco*RI kanamycin cassette fragment of pUC4K was inserted in the same direction as the transcription of the *cpc* operon to create pC30K+.

pC33K+: A 425 bp *Msc*I-*Nae*I fragment was removed from pCPC and replaced with *Eco*RI fragment of Km cassette.

pC30K-: It was created as pC30K+, except that the Km cassette was inserted in opposite orientation.

pCK: A 2877 bp *Eco*47III-*Nhe*I fragment from pCPC was replaced with 3380 bp *Nae*I-*Xba*I fragment containing *sacB* and *aphI* genes of pPSBA2KS.

pUCDΩ: A 675 bp *Pst*I-*Nhe*I fragment from pCPC was cloned into pUC9 between *Pst*I and *Xba*I site, then Ω cassette containing *Hin*cII fragment from pDW9 was inserted in the *cpcD* gene at *Hin*cII site.

pΔC2Ω: pCPC plasmid was digested with *Eag*I and treated with Bal 31 nuclease for 30 min. Then it was digested with *Spe*I, treated with Klenow DNA polymerase and ligated using T4 DNA ligase. This way 680 bp was deleted. 1572 bp was also deleted from the plasmid digesting it with *Nde*I and *Age*I. Finally the Ω cassette containing *Hin*cII fragment of pDW9 was inserted at the *Bse*RI site.

pS1DK: Primers FD and RD were used to amplify from the genomic DNA a 390-bp fragment containing the *cpcD* open-reading-frame plus 130 bp downstream its stop codon containing the transcription termination site. This fragment was cloned in the *Eco*RV site of pBCSK+. The plasmid was sequenced to check the fidelity of the PCR reaction. A 380 bp *Nde*I-*Bam*HI fragment was cloned in pPSBA2 plasmid (4350 bp) between the 5' and the 3' ends of the *psbAII* gene to be under the control of the *psbA* promoter, and then a *Bam*HI fragment containing the Km cassette was introduced in the *Bam*HI site downstream to *cpcD*.

FD: 5'- GGAATTC**CATATG**TTAGGTCAATCTTC introduces an *Nde*I site.

RD: 5'- CG**GGATCC**TGACTCGATGGCTATTC introduces a *Bam*HI site.

pS1C1: A 3363 bp *Hin*cII fragment containing *cpcC1*, the Ω cassette and part of *cpcD* from pΔC2Ω; was inserted into pPSBA2 plasmid at *Hpa*I site to be under the control of the *psbA* promoter. The orientation of the insertion was checked by digestion with *Nhe*I, *Spe*I and *Hpa*I.

III. 4. C. Constructions of the rod-core linker mutants

pG1Ω: The *cpcG1* gene was amplified from the WT genome by PCR using G1F (5'-GCCAACGATTAGGACCCTTCC) and G1R (5'- CCTCTGACCTTAGTGCCTAGC) oligonucleotides. This 850 bp was cloned into pBluescript SK+ plasmid at *Eco*RV site and then the Ω cassette-containing *Hin*cII fragment of pDW9 was inserted at *Nru*I site.

pG2K: The *cpcG2* gene was amplified from the WT genome by PCR using G2F (5'-CAGCGGCAAATCATCCTCCAC) and G2R (5'- GATTGATACCACTGCCGATCC) oligonucleotides. This 1305 bp fragment was cloned into pBluescript SK+ plasmid at *Eco*RV site and the plasmid what we got this way was called pG2. Then the Km cassette containing *Pst*I fragment of pUC4K was inserted at *Bsr*GI site to create pG2K.

III. 4. D. Plasmid constructions to generate *petH*-mutant strains.

We constructed different plasmid to generate wit point mutation different *Syenchocystis petH*-mutant strains (Table 5 on page 40).

III. 4. D. 1. Construction of the basic plasmids

pBKH: BE (5'- GCTCTGGGATCCAGGGCGGTG) and EB (5'-GCTCTACGGTTCCATCAGACC) oligonucleotides were used to amplify from the wild-type genomic DNA a 2742-bp fragment containing the *petH* gene (1246 bp orf plus 710 bp upstream and 786 bp downstream). This fragment was cloned into the *Eco*RV site of pBluescript SK+ to create the pBKH plasmid. A *Sac*I-*Msc*I fragment was deleted to create pMS and a *Hin*cII-*Msc*I fragment was deleted to create pMH. The *petH* gene containing part of both plasmids were sequenced to check the fidelity of the PCR amplification and ascertain that the 2742-bp fragment carried in pBKH had a correct sequence.

pSB7: SB (5'- GTTCTAGCCAGAGATATAGCC) and BS (5'-GGATAGTCTAA<u>GGATCC</u>ATCAGTCATG) primers were used to amplify a 458-bp fragment containing a 5'-fragment of *petH* (339 bp upstream and 119 bp of its orf). The BS oligonucleotide added a <u>*Bam*HI</u> (underlined) site 106 bp upstream from the translation start point, which gave us the possibility to create a repeat in our construct. The amplified fragment was inserted in the *Eco*RV site of pBC SK+ creating pSB. A 216 bp *Spe*I-<u>*Bam*HI</u> fragment of pSB was transferred to pBC (between *Xba*I and *Bam*HI) to create pSB7. This fragment contains part of the *prk* gene, which is transcribed in the opposite direction to *petH*. The *prk* is an essential gene encoding phosphoribulokinase, therefore this part had to be kept intact in the mutants as it was described in [110].

pSBH: a 2561 bp *Bam*HI-*Eco*RV fragment of pBKH was inserted in pSB7 between <u>*Bam*HI</u> and *Eco*RV creating pSBH.

III. 4. D. 2. Directed mutagenesis

pM7: was constructed by subcloning a 572 bp *Xba*I-*Msc*I fragment of pBKH in pBluescript SK+ (between *Xba*I and *Eco*RV). PCR mutagenesis was performed with overlapping oligonucleotides on pM7. The oligonucleotides generate base substitutions in order to modify amino acids of the FNR. A single base-pair change generating a silent mutation and eliminating an *Alw*NI site was introduced in the mutagenic-oligonucleotides

to provide a rapid screen for the resulting plasmids. Only plasmids that were not digested by *Alw*NI were considered for sequencing.

pI: oligonucleotides WTRN (5'- ATTCAGGGGCGGGATTAGCCACCGCTTCTGAA CCA) and IFN (5'- CCCGCCCCTGAATCTAACAAAACCATCACAACAAC) were used to change an ATG codon of a methionine (M113) located at the N-terminus of the enzymatically active form of the FNR to ATC which encodes an isoleucine in the pM7 plasmid using Pfu Ultra DNA polymerase (Stratagene).

The PCR conditions were as follows:

95 °C 3.5 min   95 °C 40 s

62 °C 1 min   1 cycle   62 °C 40 s   25 cycles   72 °C 6 min 1cycle

72 °C 1 min   72 °C 4 min

The PCR products were digested with *Dpn*I to remove the original plasmids.

The *petH* containing part of the pI plasmid was sequenced.

pV: oligonucleotides WTF (5'- CTAATCCCGCCCCTGAATCTAACAAAACCATGACAACAACC) and VR (5'- GTTAGATTCAGGGGCGGGATTAGCGACCGCTTCTGAACCAC) were used to change a GTG codon of a valine 102 (V102) in the pM7 plasmid using Pfu Ultra. The GTG was changed to GTC, which also encodes a valine but is not an initiation codon.

The PCR conditions were as follows:

95 °C 3.5 min   95 °C 40 s

62 °C 1 min   1 cycle   62 °C 40 s   25 cycles   72 °C 6 min 1cycle

72 °C 1 min   72 °C 4 min

The PCR products were digested with *Dpn*I to remove the original plasmids.

The *petH* gene containing part of the pV plasmid was sequenced.

pHFS1: Oligonucleotides SHR (5'-TTCAGGGGGCTGGATTGC-3') and SHF (5'-CCAGCCCCCTGAATCTAAC-3') were used to create a frame-shift by introducing one more C at the *Alw*NI site (317 bp from the beginning of *petH*) by PCR on the pM7 plasmid using Pfu Ultra. The *Alw*NI site was eliminated and a stop codon was created 10 bp before the M113.

The PCR conditions were as follows:

95 °C 1 min   95 °C 40 s

55 °C 1 min   1cycle   55 °C 40 s   25 cycles

72 °C 4.5 min   72 °C 4.5 min   72 °C 6 min   1cycle

The PCR product was digested with *Dpn*I to remove the original plasmids.

44

The *petH* gene containing part of the pHFS1 plasmid was sequenced.

pHFS2: Oligonucleotides SIF (5'-CCAGCCCTGAATCTAAC) and SIR (5'-TTCAGGGCTGGATTAGC) were used to create a frame-shift by removing a C at the *Alw*NI site (317 bp from the beginning of *petH*) by PCR on the pM7 plasmid using Pfu Ultra. The *Alw*NI site was destroyed and a stop codon was created 337 bp from the start codon and 1 bp after M113.

The PCR conditions were as follows:

95 °C 1 min	95 °C 40 s	
55 °C 1 min 1cycle	55 °C 40 s 25 cycles	
72 °C 4.5 min	72 °C 4.5 min	72 °C 6 min 1cycle

The PCR product was digested with *Dpn*I to remove the original plasmids.

The *petH* gene containing part of the pHFS2 plasmid was sequenced.

III. 4. D. 3. Construction of the cargo plasmids

pSBI and pSBV: The 420 bp *Xba*I-*Mfe*I fragments of pI or pV were used to replace the *Xba*I-*Mfe*I fragment in pSBH resulting in pSBI or pSBV, respectively.

pSBHΩ, **pSBIΩ and pSBVΩ:** The cargo plasmids, pSBHΩ, pSBIΩ and pSBVΩ were constructed by inserting the Ω cassette (2 kb *Bam*HI fragment of pDW9) in the *Bam*HI sites of the respective plasmids.

pFS1 and pFS2: The *Eco*RI-*Sma*I fragment of pSBIΩ was replaced by the 835-bp *Eco*RI-*Sma*I fragment of pHFS1 and pHFS2 to create pFS1 and pFS2, respectively. The *Eco*RI-*Sma*I part of these plasmids were sequenced to check the mutation.


Primers were designed based on the published complete genome sequence of *Synechocystis* PCC6803, available at

(http://www.kazusa.or.jp/cyano/Synechocystis/index.html).

III. 5. Construction of *Synechocystis* mutant strains

III. 5. A. Construction of the PBS rod mutant strains

The WT *Synechocystis* PCC6803 strain was transformed with pCBK+, pC30K+, pC30K-, pC33K+, pΔC2Ω, pUCDΩ and pCK plasmids to create CB, 30+, 30-, 33, D3, D4 and CK strains, respectively (Figure 12). Transformation of the CB strain with pΔC2Ω resulted in the Δ30 mutant strain. The 33 and CB mutant were transformed with pS1C1 plasmid to construct the 33c and CBc mutant strains, respectively. The D3 and D4 strains were complemented with the pS1DK construction to create D3D and D4D strains. WT *Synechocystis* PCC6803 was also transformed with pS1DK to construct WD (Table 4 on page 39). Complete segregation of the mutated strains was checked by PCR.
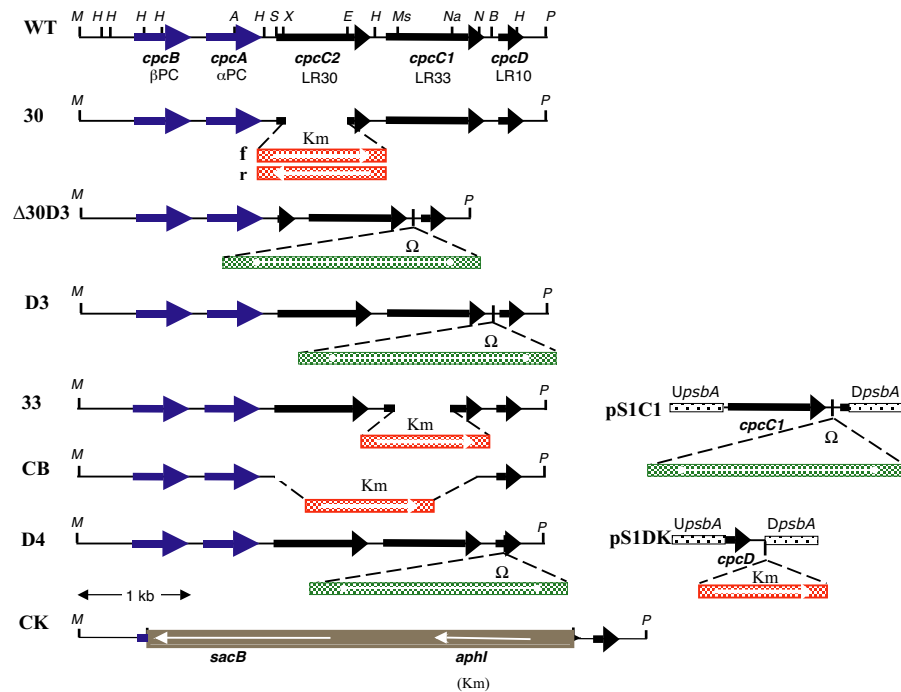
Figure 12. Maps of DNA fragments containing the *cpc* operon in the wild type and mutant strains, and the pS1C1 and the pS1DK construct.

WT, the wild-type *cpc* operon and. **30**, 560 bp *Xho*I-*Eae*I fragment from *cpcC2* replaced by the Km cassette (f and r indicate orientations of the *aphI* gene transcription in the respective strains); **Δ30D3**, 685 bp deleted from *cpcC2* plus Ω cassette inserted in the *Bse*RI site; **D3**, Ω cassette inserted in the *Bse*RI site. **33**, 425 bp *Msc*I-*Nae*I fragment from *cpcC1* replaced by the Km cassette; **CB**, 1.7 kb *Spe*I-*Nhe*I fragment containing both *cpcC2* and *cpcC1* replaced by the Km cassette; **pS1C1**, transcriptional fusion of *cpcC1* to the *psbAII* promoter. U*psbA*, upstream *psbAII*; D*psbA*, downstream *psbAII*. **CK**, 1.7 kb *Spe*I-*Nhe*I fragment containing both *cpcC2* and *cpcC1* replaced by the *aphI* and *sacB* containing construct **D4**, Ω cassette inserted in the *Hinc*II site of *cpcD*; **pS1DK**, translational fusion of the *cpcD* orf to the *psbAII* initiation codon. Phycocyanin-subunits encoding genes are represented as blue arrows; rod-linker encoding genes as black arrows, Ω cassette as white line in a green rectangle, and the Km cassette as white line in a red rectangle, the *aphI* and *sacB* genes as white lines in a brown rectangle, an arrowhead indicates the direction of gene transcription. Abbreviations: A; *Age*I, B; *Bse*RI, E, *Eae*I; H, *Hinc*II; M; *Mfe*I; Ms, *Msc*I; Na, *Nae*I; N, *Nhe*I; P, *Pst*I; S, *Spe*I; X, *Xho*I.

46

The WT *Synechocystis* PCC6803 strain was transformed with pG1Ω and pG2K plasmid to create G1Ω and G2K mutants, respectively (Table 4 on page 39). Complete segregation of the mutants was checked by PCR (see Figure 30 in Results and Discussion).

III. 5. B. Construction of the *petH* mutant strains

Transformation of the WT *Synechocystis* PCC6803 strain with pSBHΩ, pSBIΩ, pSBVΩ, pFS1 and pFS2 plasmids resulted in the H, I, V (see Figure 36 in Results and Discussion), FS1 and FS2 strains, respectively (Table 5 on page 40).

The structure of the genomic fragments around *petH* in the H, I and V strains were verified by Southern hybridization. Genomic DNA was digested with *Eco*RV and *Alw*NI, separated on an agarose gel and transferred to a Millipore ImmobilonTM-Ny+ Transfer membrane. The membrane was hybridized with a 683 kb *Mfe*I-*Spe*I fragment of *petH* (Probe H) labeled with [α-^{32}P]-dCTP.

The mutants were further checked by sequencing a 479-bp PCR product that was amplified from each strain by the oligonucleotides HSF (5'- GTAGTGGCAGCACGTTCATC) and HSR (5'- CACCGTGTCTGGTGGAAGC) to ensure that the required substitution occurred.

III. 6. RNA isolation from *Synechocystis* PCC6803

Total RNA was isolated from wild-type and the mutant cells as it was described in [124] with some modification. 40 ml of the cells at $OD_{580nm}= 0.8$ were harvested by 5 min centrifugation with 10 ml crushed ice at 4 °C with 8000 g. The pellet was frozen in liquid nitrogen then thawed on ice. The cells were washed with 500 μl 10 mM sodium acetate (pH 4.5), then pelleted again by 1 min centrifugation at 4 °C with 21000 g. The pellet was resuspended in 250 μl 10 mM sodium acetate (pH 4.5) and 37.5 μl 500 mM Na_2-EDTA and the suspension was incubated on ice for 5 min. 375 μl Lysis buffer (10 mM sodium acetate (pH 4.5) and 2 % SDS) was added and then the solution was incubated at 65 °C for 3 min. After the incubation 700 μl of hot (65 °C) water equilibrated, acidic phenol was added and the vortexed mixture was incubated at 65 °C for 3 min. The tubes were cooled rapidly on ice briefly and the phases were separated by 1 min centrifugation at 21000 g. The aqueous phase was transferred in a new Eppendorf tube. Then it was mixed with 700 μl room-temperature phenol: chloroform (1:1) and the phases were separated by 1 min

centrifugation at 21000 g. The upper phase was collected carefully to a new tube. The phenol: chloroform treatment was repeated. Then 0.1 volume of 10 M LiCl and 2.5 volume of ethanol were added and the solution was incubated at –20 °C for 30 min. After centrifugation at 4 °C (30 min at 21000 g) the pellet was washed with 70 % ethanol and dried at room temperature. The pellet was re-suspended in 54 μl H_2O. The solution was treated with RNase-free DNase (Invitrogene Deoxyribonuclease I Amplification Grade). After the DNase treatment the RNA was precipitated with LiCl and ethanol and resuspended in 17 μl H_2O. The concentration of the RNA samples was measured by the absorption at 260 nm. The RNA samples were stored at –80 °C.

All solution used for RNA isolation were treated with 0.1 % v/v diethyl pyrocarbonate (DEPC) (Sigma) by incubating at 37 °C for 1h with gentle agitation, and then autoclaved for 20 min. RNase free barrier tips and sterile tubes were used during the preparation; when it was possible the samples were kept at low temperature, and we used gloves.

III. 7. Northern blot

For Northern-blot analysis 9 μg of total RNA was denatured with glyoxal/DMSO as it was suggested in [118]. Briefly, to 4.5 μl RNA samples 5.4 μl 6 M glyoxal, 16 μl DMSO, 3 μl 100 μM sodium phosphate (pH 7.0) and 0.9 μl of DEPC treated H_2O were added and the mixture was incubated for 1h at 50 °C. During the incubation time 0.8 % agarose gel were prepared. 1 g agarose was dissolved in 108 ml H_2O and 12 ml 100 mM sodium phosphate (pH 7.0) by heating. Then the solution was cooled down to 70 °C and 0.25 g sodium iodoacetate was added. The gel was poured when the solution was around 50 °C.

The denatured RNA samples were cooled down on ice then centrifuged for 30 sec. 3 μl 10 x glyoxal/DMSO gel-loading buffer (50 % glycerol 10 mM sodium phosphate pH 7.0, 0.25 % bromphenol blue and 0.25 % xylene cyanol FF) was added and the samples were loaded immediately into the wells of the gel.

The gel was run at 45 V for 6.5 h in 10mM sodium phosphate buffer (pH 7.0). To maintain the pH during the migration the buffer was circulated.

After electrophoresis the gel was soaked in 200 ml 0.025 M NaOH solution for 15 min, rinsed with distillated water then soaked in 200 ml 20 x SSC [118] for 15 min. The RNA was transferred from the gel to a nitrocellulose filter by capillarity blot using 20 x SSC solution and Millipore ImmobilonTM-Ny+ Transfer membrane [118].

After capillarity blotting the RNA was linked to the membrane surface using Stratalinker UV Crosslinker Model 2400 with 1200 µJ (x 100). The hybridization procedure was as recommended by Millipore. The membrane was placed side facing in a hybridization bottle and prehybridized with 30 ml Hybridization Buffer (0.5 M sodium phosphate pH 7.1; 2 mM EDTA; 7 % (w/v) SDS and 0.1 % (w/v) sodium pyrophosphate) at 68 °C for 1 hour. To label the probes we used the Amersham Biosciences ready-To-Go-DNA labeling (-dCTP) kit. The prehybridization solution was replaced with 15 ml fresh Hybridization Buffer preheated to 68 °C and the labeled probe was added. The blot was hybridized for 16 hours at 68 °C. After removing the hybridization solution the membrane was rinsed twice with Wash Solution I (1 x SSC and 0.1 % w/v SDS) for 5 min at room temperature. The hybridization tube was filled halfway with Wash Solution II (0.2 x SSC and 0.1 % w/v SDS) preheated to 68 °C. After 15 min incubation the membrane was washed again for 15 min at 68 °C with Wash Solution II. Radioactivity was detected by Molecular Dynamics STORM 860 Phosphorimager.

For probe stripping 250 ml 0.1 % (w/v) SDS was boiled. Then poured on the membrane and incubated for 15 min with gentle agitation. The stripping process was repeated once more and we checked if the membrane was clean.

Control hybridization of the filter was carried out with constitutively-expressed *rnpB* gene [125].

Probes for the Northern blot analysis:

Probe 1: Contains two fragments, an 80 bp *Hpa*I and *Spe*I fragment, containing *cpcA-cpcC2* intergenic region, and a 350 bp *Nhe*I and *Hpa*I fragment, containing *cpcC1-cpcD* intergenic region and 200 bp of *cpcD*.

Probe 2: 600 bp *Nae*I and *Hpa*I fragment from *cpcC1* to *cpcD*.

Probe K: The Km cassette-containing *Pst*I fragment from pUC4K.

Probe *rnpB*: 500 bp *Hin*dIII and *Eco*RI fragment containing *rnpB*.

Probe D: 350 bp *Nhe*I and *Hpa*I fragment, containing *cpcC1-cpcD* intergenic region and 200 bp of *cpcD*.

Probe G1: 850 bp fragment containing *cpcG1* gene amplified by PCR

Probe G2: 1407 bp *Kpn*I and *Sac*I fragment of pG2 containing the *cpcG2* gene.

III. 8. Reverse transcription-PCR

To check if there is transcription from *cpcG1* and *cpcG2*, cDNA was prepared from 5 µg of total RNA of WT strain with StrataScript™ Reverse Transcriptase (Stratagene) according to the manufacturer's protocol with Oligonucleotide1 (see in the table 6). For negative controls the same procedure was performed with Oligonucleotide2. One-fifth of the reaction products was used as template for PCR with RedTaq™ DNA polymerase (Sigma) using Oligonucleotide1 and Oligonucleotide2. For positive controls the same PCR reaction was performed with genomic DNA. The PCR reaction mixture was prepared as it was suggested in the RedTaq™ DNA polymerase technical bulletin.

The PCR conditions were as follows:

95°C 1 min		95°C 30 s		
55°C 1 min	1 cycle	55°C 30 s	30 cycles	
72°C 1 min		72°C 1 min		72°C 4 min 1 cycle

Then one-fifth of the PCR product was loaded on a 1 % agarose gel. After electrophoresis a photo was taken with CCD camera.

Table 6. The oligonucleotides of the RT-PCR.

Transcription of	Oligonucleotide1	Oligonucleotide2	Product size
cpcG1	G1RT (5'-GCGGAAACCT TGGGAATGG-3')	G1FT (5'-GGCTCTGAAG AGAAGCCTG-3')	654 bp
cpcG2	G2RT (5'-CAACGGTAAG TTAACGGAGC-3')	G2FT (5'-CTGGAGATGA ACACGCTCG-3')	550 bp

III. 9. Southern hybridization

5 µg of DNA, isolated from wild-type or mutant cells, was digested with the required restriction enzymes. The DNA fragments were separated by electrophoresis through a 0.8 % agarose gel in 0.5 % TAE buffer (Tris-Acetate-EDTA Buffer). DNA fragments were transferred to Millipore ImmobilonTM-Ny+ Transfer membrane as described in [118]. The blotting time was around 3 hours, then the membrane was washed with 5 % SSC and dried on room temperature. Hybridization was as described in the chapter of Northern hybridization, except the prehybridization and hybridization solution was as described in [118]: 6 x SSC, 5 x Denhard's reagent, 0.5 % SDS and 100 µg/ml denatured salmon sperm DNA. To label the probes we used the Amersham Biosciences ready-To-Go-DNA (-dCTP) kit.   Probe H: 683 bp *Spe*I and *Mfe*I fragment of pMS.

III. 10. PBS isolation

The PBS from wild-type and mutant cells were purified as described in [48, 126, 127] with some modifications.

500 ml of cyanobacterial culture at OD_{580nm} = 0.8-0.9 were harvested by centrifugation at room temperature (6500 g for 5 min). The cells were resuspended in 10 ml of 0.8 M potassium/sodium phosphate buffer (pH 8.0), and transferred into a 50 ml polypropylene tube and centrifuged again at room temperature (6500 g for 5 min). After removing the supernatant, the pellet was frozen at –20 °C. The cells were thawed at room temperature and resuspended in 5 ml 0.8 M potassium phosphate buffer. Three ml glass beads (212-300 μm diameter, G-1277 Sigma) and 550 μl freshly made 10 x Complete™ (Roch) protease inhibitor solution were added. The mixture was wortexed 6 times (1 min each) to break the cells.

After breaking the cells, one of the following procedures was applied:

1. The solution was centrifuged at room temperature (1500 g for 2 min) to remove the glass beads and any unbroken cells and the supernatant was transferred to a 15 ml tube Triton-100 was added to the supernatant to a final concentration of 2 % (v/v), and the mixture was incubated for 20 min at room temperature in the dark, then it was transferred to a polycarbonate tube and centrifuged for 15 min (31000 g at 18 °C) in a Beckman JA-25.50 rotor. The supernatant was removed carefully with a 1 ml pipette from underneath the floating chlorophyll containing layer. Two ml supernatant aliquots were layered on a sucrose step gradient in a Beckman Ultra Clear™ Tube 14x89 mm, with the following sucrose molarities: 2.0 M (3 ml); 1.0 M (2 ml); 0.5 M (2 ml); 0.25 M (3 ml). The sucrose was dissolved in 0.8 M potassium/sodium phosphate buffer (pH 8.0) in all layers.

2. Then the solution was centrifuged at room temperature (1500 g for 2 min) to remove the glass beads and any unbroken cells and the supernatant was transferred to a 15 ml tube The glass beads and unbroken cells were washed with 5 ml 0.8 M potassium/sodium phosphate buffer (pH 8.0), then centrifuged again (1500 g for 2 min at 20 °C). The supernatant was added to the earlier one. This solution was centrifuged for 30 min at 20°C with 15000 g to pellet the membranes. The pellet was resuspended in 2 ml 0.8 M potassium/sodium phosphate buffer (pH 8.0) and 220 μl 10 x Complete™ (Roch) protease

inhibitor solution. Triton was added to the solution to a final concentration of 2 % (v/v) and the mixture was incubated at room temperature in the dark for 20 min. It was centrifuged in Eppendorf tubes (21000 g for 15 min at 20 °C). The supernatant, containing the PBS was removed carefully with a 1 ml pipette from underneath the floating chlorophyll containing layer. Two ml PBS containing samples were layered on a sucrose step gradient in a Beckman Ultra Clear™ Tubes 14x89 mm, with the following sucrose molarities: 1.0 M (3.5 ml); 0.75 M (3 ml); 0.5 M (2.5 ml); 0.25 M (2 ml). The sucrose was dissolved in 0.8 M potassium/sodium phosphate buffer (pH 8.0).

The PBS containing blue bands were collected with syringe from the gradients in Eppendorf tubes.

III. 11. Absorption spectra

200 μl PBS containing samples collected from the sucrose gradients were diluted with 1800 μl 0.8 M potassium/sodium phosphate buffer (pH 8.0). Absorption spectra were recorded in 1 ml cuvettes, using a Varian Cary-5E double-beam spectrophotometer, with a data interval of 0.5 nm.

III. 12. Fluorescence emission spectra

Cells in exponential growth phase, either from wild-type or mutant cells were rapidly vacuum-sucked onto a paper filter (to form a monolayer less than 8×10^7 cells/cm^2) then immediately frozen in liquid nitrogen and fluorescence emission spectra were recorded at 77 K using a Hitachi spectrofluorometer with 580 nm excitation with a data interval of 0.5 nm.

III. 13. Protein gels

To analyze the protein composition of the isolated PBS, we used either 10-20 % Tris-Glycine gels were used with running buffer and samples buffer as described earlier [128], or Invitrogene NuPAGE® Novex Bis-Tris Gels 4-12 % with NuPAGE®MES running buffer.

Thirty μl PBS sample with $OD_{620nm}= 10$ (with exception of PBS complex from the rod less mutants, when we used 7.5 μl with $OD_{650nm}= 10$) was precipitated on ice for 5 min after adding an equal volume of 20 % TCA. This was followed by a 2 min centrifugation (at

21000 g at 4 °C) then the supernatant was removed and the pellet was resuspended in the loading buffer, heated for 5 min at 85 °C and finally loaded on the gel.

The gels were stained with Bio-SafeTM Coomassie G250 (BIO-RAD) as it was proposed in its manual. The NuPAGE® Novex Bis-Tris Gels were also colored with the Invitrogene SimplyBlue staining. After destaining the gels were photo-documented with a CCD camera. As the composition of wild-type PBS is well known, PBS bands from the mutants were identified by comparing their positions on the gel with those of the wild-type PBS protein bands. These were identified by their size compared to the molecular-weight marker. The fluorescence of phycobiliproteins was detected on the gel, in the presence of $ZnSO_4$, as described previously [3].

IV. RESULTS AND DISCUSSION

IV. 1. Mutants deficient in PBS-rod subunits

PBSs are not essential for phototrophic growth [70, 129], so mutations affecting various linkers are of special interest because they provide the opportunity for observing PBS biogenesis under normal growth conditions. The phycobilisome of *Synechocystis* PCC6803 consists of a three-cylindrical core with six rods, each rod being composed of three stacked PC-hexamers [48]. In *Synechocystis* PCC6803, two independent genes (*cpcG1* and *cpcG2*) encode the rod-core linker (LRC), which attaches the proximal PC-hexamer to the core. The remaining rod-subunit-encoding genes are clustered in the *cpc* operon. This operon contains five genes: *cpcB* and *cpcA* encode the β^{PC} and α^{PC} subunits, respectively, while *cpcC2*, *cpcC1* and *cpcD* encode the rod linkers LR30, LR33 and LR10, respectively. The remaining two PC-hexamers could be linked by LR30 and LR33 in two ways: (i.) LR33 and LR30 are interchangeable, which means either can be present in the intermediary as well as in the distal PC-hexamers, (ii.) the intermediary PC-hexamers contain only one linker type, with the other specifically present in the distal PC-hexamers. Characterization of the PBS assembly process in mutants deficient in the above linkers should support one of the above models. In order to study this, various rod-linker-deficient mutants were constructed.

## IV. 1. A. Construction of a PBS rod-less mutant

The *cpc* operon was inactivated by replacing a 2877-bp fragment, containing the *cpcBAC1C2* genes, with a fragment containing *aphI* and *sacB* genes. The resulting mutant, denoted CK, grew slowly and had a distinct "olive" color (Table 4 on page 39 and Figure 13)
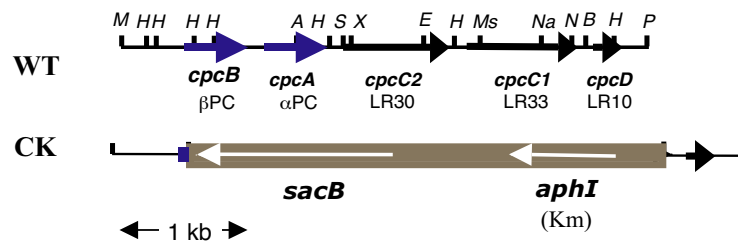
Figure 13. Maps of DNA fragments containing the *cpc* operon in the wild type and rod-less *Synechocystis* mutant strain.

WT, the wild-type *cpc* operon and **CK**, 1.7 kb *Spe*I-*Nhe*I fragment containing both *cpcC2* and *cpcC1* replaced by the *aphI* and *sacB*-containing construct. Phycocyanin-subunits encoding genes are represented as blue arrows; rod-linker encoding genes as black arrows, the *aphI* and *sacB* genes as white lines in a brown rectangle, an arrowhead indicates the direction of gene transcription. Abbreviations: A; *Age*I, B; *Bse*RI, E, *Eae*I; H, *Hin*cII; M, *Mfe*I; Ms, *Msc*I; Na, *Nae*I; N, *Nhe*I; P, *Pst*I; S, *Spe*I; X, *Xho*I.

Sucrose gradients of PBS preparations from the CK mutant contained a unique turquoise band at the bottom of the 0.5 M sucrose layer, significantly higher (i.e. towards lower sucrose) on the gradient than the dark-blue PBS band from the wild type, which is usually located in the 1 M sucrose layer (Figure 14).
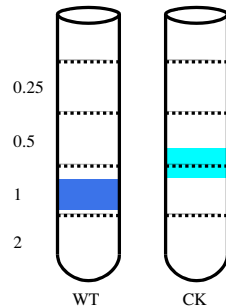
Figure 14. Sucrose gradient profiles of the phycobiliprotein complexes from wild type and rod-less strain of *Synechocystis* PCC6803.

The wild-type PBS is located at the bottom of the 1 M sucrose layer. The core complex isolated from CK is located at the bottom of the 0.5 M sucrose layer.

In addition to the phycobiliproteins (PC and APC) in the 20 kDa range, the SDS-PAGE of purified wild-type PBS contained seven polypeptides: LC, core linker; LR10 small rod linker; LRC, rod-core linker; LR30, 30 kDa rod linker; LR33, 33 kDa rod linker; FNR, ferredoxin-NADP(H)-oxidoreductase and LCM, core-membrane linker. The PBS complex of CK contained the core polypeptides (LC, allophycocyanin subunits and the LCM) and some additional contaminant proteins only (Figure 15. A).
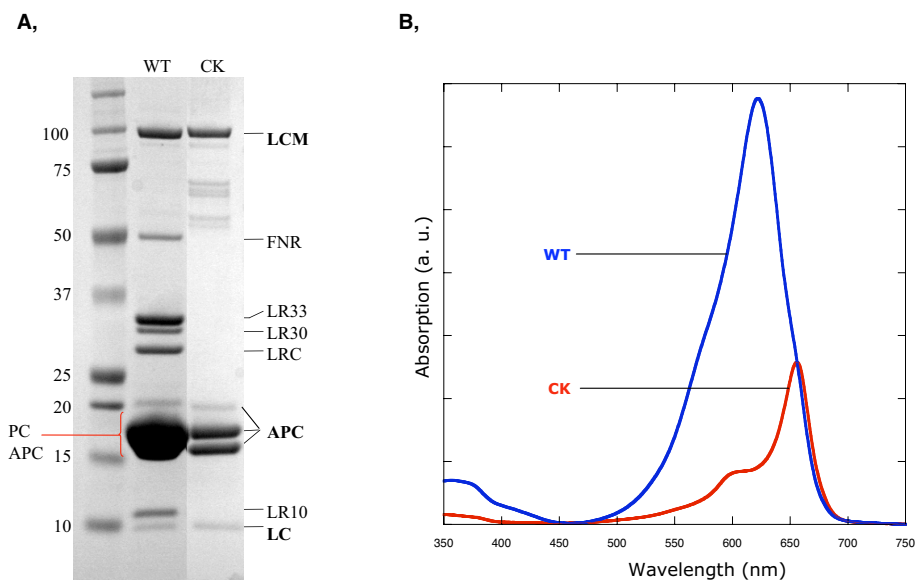
Figure 15. SDS-PAGE and absorption spectra of wild-type and CK PBS.

A, Polypeptide composition of purified PBSs from wild type (WT) and CK strain analyzed on an SDS-PAGE (NuPage 4-12 % acrylamide gradient in Bis-Tris-HCl). The identities of polypeptides are labeled on the right. Masses of the molecular marker are indicated in kDa on the left. **B,** Absorption spectra of purified PBSs from wild type and CK. The core complex isolated from CK gave the typical absorption spectra of APC (λmax, 650 nm). The spectra were normalized to the 650 nm absorption.

The isolated CK complex had an absorption spectrum with a maximum at 650 nm characteristic to APC. On the other hand wild-type PBS, containing a large amount of PC besides APC, had an absorption maximum at 620 nm (Figure 15. B).

These results showed that the CK is a rod-less mutant, containing only the core of the PBS. Similar mutants have already been isolated from *Synechocystis* PCC6803 by chemical mutagenesis [48, 130, 131]. Our CK strain was constructed in order to complement with plasmids carrying deletions in the different rod-linker encoding genes present in the *cpc* operon.

Unfortunately, the CK strain was not transformable. Therefore, we needed an other method and we used antibiotic resistance cartridge insertion for the construction of the rod-linker mutants.

IV. 1. B. LR30-deficient strains

The *cpcC2* gene, encoding the LR30 linker, was inactivated by replacing a 559-bp integral fragment with Km cassette to create 30f (Figure 16). Analysis of the protein composition of the PBS of this mutant showed lower amounts of proteins encoded downstream from the inactivated gene than the wild-type PBS. The decreased amount of these proteins could be due to either the absence of the LR30 polypeptide or to the effect of the inactivation on the *cpc* operon transcription. Therefore, in order to estimate the polar effect on flanking genes, two other strategies were used to inactivate *cpcC2*. The 30r strain carried the same deletion in *cpcC2* as 30f, except that the orientation of the Km cassette was opposite (Table 4 on page 39 and Figure 16).

Figure 16. Maps of DNA fragments containing the *cpc* operon in the wild-type, 30, Δ30D3 and D3 mutant *Syenchocystis* strains

WT, the wild-type *cpc* operon; **30**, 560 bp *Xho*I-*Eae*I fragment from *cpcC2* replaced by the Km cassette (f and r indicate orientations of the *aphI* gene transcription in the respective strains); **Δ30D3**, 685 bp deleted from *cpcC2* plus Ω cassette inserted in the *Bse*RI site; **D3**, Ω cassette inserted in the *Bse*RI site. Phycocyanin-subunits encoding genes are represented as blue arrows; rod-linker encoding genes as black arrows, Ω cassette as white line in a green rectangle, and the Km cassette as white line in a red rectangle, an arrowhead indicates the direction of gene transcription.

Abbreviations: A; *Age*I, B; *Bse*RI, E, *Eae*I; *H*, *Hin*cII; M, *Mfe*I; Ms, *Msc*I; Na, *Nae*I; N, *Nhe*I; P, *Pst*I; S, *Spe*I; X, *Xho*I.

57
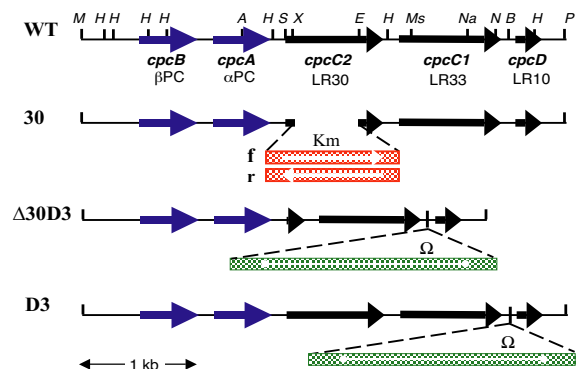
The Δ30D3 strain contained a deletion in *cpcC2* plus the Ω cartridge inserted between *cpcC1* and *cpcD*. As a control we used a strain designated D3, containing only the Ω insertion (Table 4 on page 39 and Figure 16).

The PBSs were purified from each mutants in order to determine their polypeptide composition. Sucrose gradients of the PBS preparations contained a dark blue band in the 1 M sucrose layer at positions near that expected for a complete PBS, indicating that PBSs were assembled in the mutants as well (Figure 17).
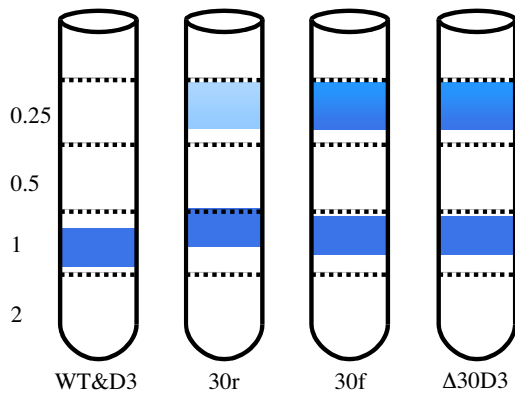
Figure 17. Sucrose gradient profiles of the phycobiliprotein complexes from wild type and rod-linker deficient strains of *Synechocystis* PCC6803.

The wild-type and D3 PBSs are located at the bottom of the 1 M sucrose layer. The 30r, 30f and Δ30D3 PBSs are located slightly higher on the gradient. The sucrose gradients of the latter preparations also contained a free PC containing band at 0.25 M sucrose layer.

However, these assembled particles were at slightly higher positions on the sucrose gradient than those of the wild type or the D3 strain, indicating that the absence of LR30 resulted in the assembly of a smaller PBS. This reduction in the PBS size was accompanied by the appearance of a free PC band on the top of the gradient tubes, in the 0.25 M sucrose layer; suggesting that a certain amount of synthesized PC was not incorporated into rods. Mutant 30r contained less free PC than 30f and Δ30D3.
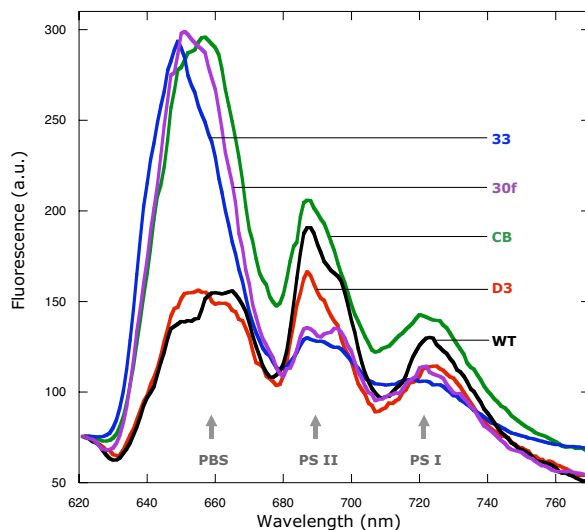

Figure 18. Fluorescence emission spectra of the wild-type and rod-linker mutant cells.

Cells were excited at 570 nm at 77 K. D3 fluorescence emission spectra was similar to the wild type, but 30f, 33 and CB showed high emission from PC. (Grey arrows indicates the emission from PBS, PSII and PSI).

Fluorescence emission from PC upon excitation with biliprotein-sensitizing light (570 nm) was more intense in *cpcC2*-deficient cells compared to the wild type or D3, confirming the presence of free, unincorporated PCs in these strains (Figure 18).

The polypeptide composition of purified PBSs from the mutants was analyzed by SDS-PAGE. In addition to the phycobiliproteins (PC and AP) in the 20 kDa range, wild-type PBS contained seven polypeptides (Figure 19. A lane WT). Four of these polypeptides, not encoded by the *cpc* operon: LC, core linker; LRC, rod-core linker; FNR, ferredoxin-NADP(H)-oxidoreductase and the LCM, core-membrane linker were invariably present in all strains. As expected, the LR30 polypeptide was absent from the three *cpcC2*-deleted strains: Δ30D3, 30f, and 30r. These strains exhibited lower amounts of the LR33 polypeptide than wild type, gradually decreasing as Δ30D3 > 30f > 30r ≥ 0 (Figure 19. A). Among the mutants the LR10 polypeptide was detected only in the 30f PBS but in lesser amount than in the WT PBS.
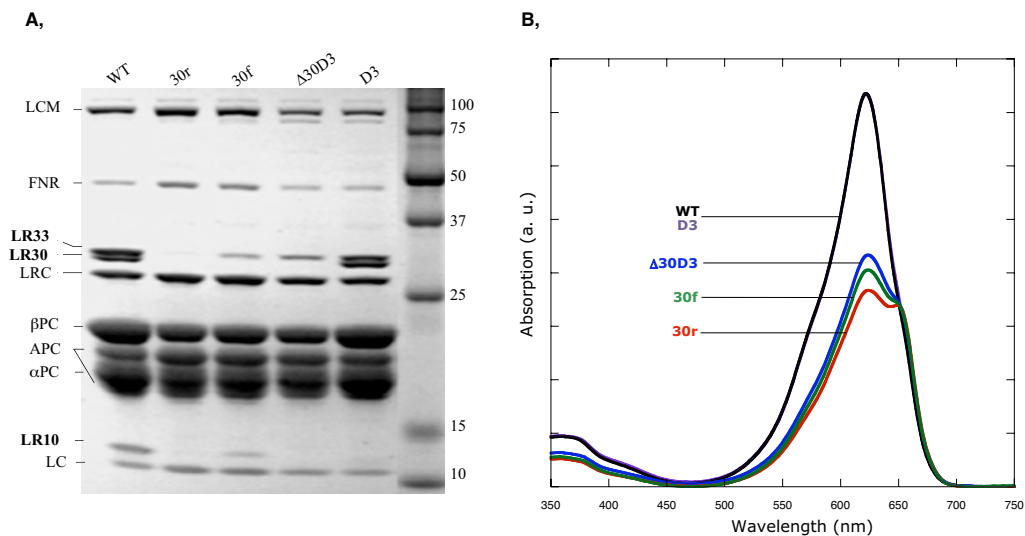
Figure 19. SDS-PAGE and absorption spectra of wild-type, 30R, 30f, Δ30D3 and D3 PBS.

A, Polypeptide composition of purified PBS from wild type (WT), and from rod-linker-deficient strains: 30r, 30f, Δ30D3 and D3, analyzed on an SDS-PAGE (10-20 % linear acrylamide gradient in Tris-HCl). Polypeptides are labeled on the left. Molecularnass markers in kDa are on the right. **B,** Absorption spectra of purified PBSs from wild type and rod-linkers-deficient strains normalized to the 655 nm absorption. Wild-type and D3 PBSs have similar absorption spectra (λmax, 620 nm), the lower amounts of PC incorporated in the Δ30D3, 30f and 30r PBSs indicated by the contribution of AP (λmax = 650 nm) to their absorption spectra. Decreasing intensities of the 620 nm peaks reflects decreasing amounts of PC in the PBS.

The PBSs purified from the mutants were further characterized by comparing their absorption spectra to that of the wild type. In wild-type PBS, PC (λ_{max} = 620 nm) is the

major phycobiliprotein (~75 %). As PBSs from the *cpcC2*-deleted strains had less PC than the PBS of wild type, the contribution of APC absorption at 650 nm, was more dominant and it became visible. Among the *cpcC2*-deleted strains the relative amount of PC was the lowest in 30r PBS, 30f had an intermediate amount, while Δ30D3 PBS contained the largest amount of PC (Figure 19. B). The amounts of PC incorporated into the PBSs of the three allelic mutants, 30r, 30f and Δ30D3, were proportional to the amounts of the LR33 polypeptide detected in their PBSs (Figure 19).

Since LR33 is the product of *cpcC1*, located downstream of the inactivated *cpcC2* gene, different amounts of LR33 in the *cpcC2*-inactivated strains might reflect different polar effects of the *cpcC2* mutations on *cpcC1* expression.

The steady-state level of *cpc* transcripts was monitored in the mutants by Northern blot (Figure 21). The wild-type *cpc* operon generates three transcripts from one transcription initiation site (Figure 21 a). This site was mapped 251-bp upstream from the starting point of translation for *cpcB* in *Synechocystis* PCC6714 [132], a strain that is closely related to *Synechocystis* PCC6803.

Sequence analysis identified a stable stem-loop structure downstream from *cpcA*, which might act as a transcriptional terminator (not followed by a poly-T stretch) or as a 3'-stabilizer to an abundant 1.6 kb transcript containing *cpcB* and *cpcA* (Figure 20).

This structure was intact in all mutants, which explains the constant amount of this transcript in these strains. Two larger and less abundant transcripts, which contain the linker-encoding genes *cpcC2*, *cpcC1* and *cpcD*, are detected at 3.4 and 3.8 kb in the wild type (Figure 21 b. panel 1 and 2, lane WT). These transcripts are generated by a readthrough of the above RNA structure and two rho-independent terminations downstream of *cpcC1* and *cpcD*, where significant stem-loops and poly-T stretches are detected (Figure 20).

Figure 20. The stem-loop structures and poly-T stretches on the *cpc* operon.

The stem-loop structures are highlighted with yellow and green. The yellow parts are complementer with the green parts, and the order is signaled with numbers. The poly-T streches are highlighted with grey.

60
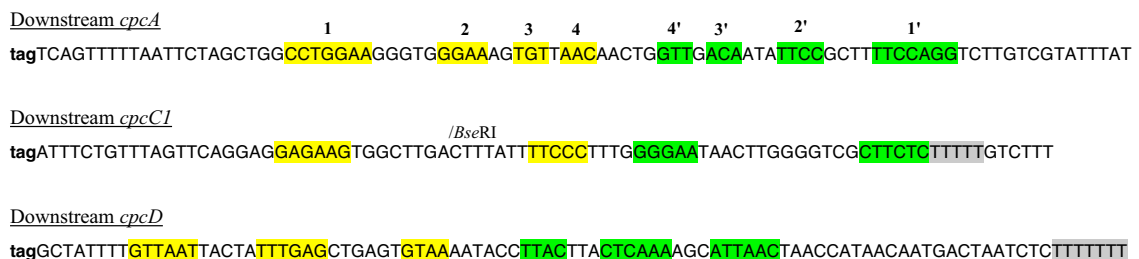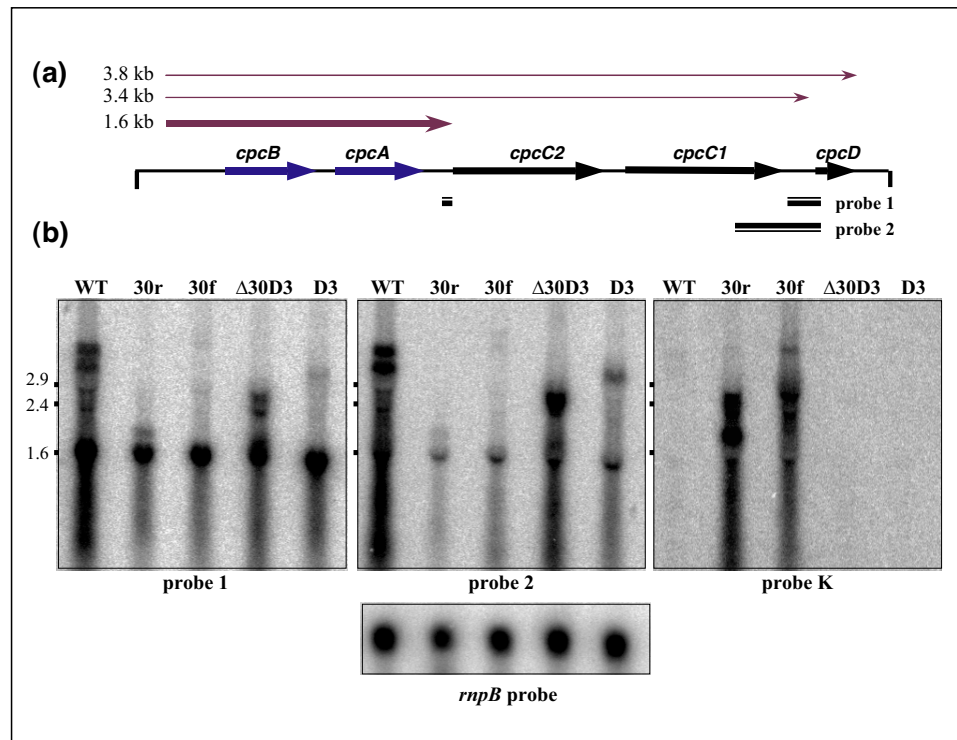
Figure 21. Northern-blot analysis of the *cpc* transcripts.

(a) The three mRNAs produced from the *cpc* operon in *Synechocystis* PCC6803. Positions of two of the DNA probes used in panel b are shown below a map of the operon. **(b)** Northern-hybridization analysis of the *cpc* operon in the wild type and four rod-linker-deficient strains. DNA probes were chosen to be general for all the *cpc* transcripts (probe 1), specific for the large *cpc* transcripts (probe 2), specific for the Km cassette containing transcripts (probe K) and the *rnpB* gene to estimate the loading of the samples. Approximately 10 μg of total RNA were loaded per lane. (Probes are described in Materials and Methods). The same blot was used for all four hybridizations. Positions of the rRNAs are indicated on the left of each blot (2.9, 2.4 and 1.6 kb). Note that signal clouds are detected at the positions of the rRNA contain degradation products of larger RNA molecules.

The size and relative abundance of these transcripts varied in the mutants. In the 30r and 30f strains they are expected to be about 0.6 kb larger due to the deletion in *cpcC2* and the Km cassette insertion, consequently their sizes should be 4 and 4.4 kb. These were not detected in the 30r strain and were present in a drastically reduced amount in strain 30f (Figure 21 b. panel 2), which could explain the decreased amounts of LR33 and LR10 in their PBSs (Figure 19. A). In Δ30D3, a shorter form of this transcript (2.7 kb due to the deletion in *cpcC2*) was detected and seemed fairly abundant. In D3, the 3.8 kb transcript was absent due to the strong transcription terminators present in Ω, while the 3.4 kb transcript seemed less abundant than in the WT (Figure 21 b. panel 2). This might be due to a stem-loop affected by the Ω insertion and suggests that the Ω terminator does not provide a 3'-stabilizer effect.

The blot was hybridized with a Km probe and over-exposed to detect mRNAs containing the Km cassette (Figure 21 b. panel K). In the 30f mutant two major transcripts were detected at 4 and 2.9 kb. While in strain 30r the 4 kb transcript was barely detectable and the 2 kb transcript, that also hybridized to the probe 1, was obvious. Larger bands (around 2.5 kb) could be the products of abortive transcription and degradation of the full operon transcript. The 4 kb transcript corresponds to the transcription of the whole operon through the Km cassette. Their low amounts demonstrate that the insertion of the Km cassette destabilizes those transcripts. The 2.9 and 2 kb transcripts, in 30f and 30r, respectively, are the products of read-through transcription from the *aphI* promoter. The 2.9 kb transcript detected in 30f terminates at the end of the *cpc* operon; it should then contribute to the translation of *cpcC1* and *cpcD*. The lower amount of LR33 and LR10 in its PBS (Figure 19. A) suggests that the transcripts initiating from the *aphI* promoter are either less abundant or unstable. The size of the 2 kb one in 30r implies that it terminates within *cpcB*. Part of this transcript is an antisense RNA to the 1.6 kb mRNA containing *cpcB* and *cpcA*, which explains the lower PC content in this strain. It is important to note, that this *aphI* transcript terminates in *cpcB* (where a significant stem-loop structure and a poly-T stretch are detected) and not at the stem-loop structure downstream of *cpcA*. This observation suggests that the latter structure is an RNA-processing site rather than a terminator. The same role was also suggested for the *cpc* operon of *Anabaena* PCC7120 [133].

The detected lower amounts of LR33 in the PBS of the three allelic mutants, 30r, 30f and Δ30D3 than in the wild type (Figure 19. A) were due to different expression levels of *cpcC1*. The Km cassette inserted upstream of *cpcC1* in 30f and 30r and the Ω cassette insertion downstream from *cpcC1* in Δ30D3 induce polar effect on the *cpcC1* expression. These polar effects resulted in a decreased amount of the *cpcC1* product, LR33 and consequently the amount of PC incorporated into the PBS decreased. This result suggests that transcriptional regulation of the rod-linker genes could adjust the light-harvesting capacity of the PBS by modulating the amount of PC incorporated into the rods. In *Anabaena* PCC7120 high light induced a decrease in the level of the *cpc* operon larger transcript as compared to the smaller one [133]. The relative level of the transcripts could be modulated through transcription termination at the stem-loop downstream of *cpcA* or by RNA processing at this site followed by degradation of the linker-encoding mRNA. In PBS of *Synechocystis* PCC6803 and *Synechococcus* PCC6301 strains, the LR30 to LR33

ratio was repeatedly <1, decreasing under high-light conditions further ([88] and our observations). Regarding the *cpcC2* and *cpcC1* co-transcription, a feasible possibility of regulation is the down regulation of *cpcC2* first. Endoribonuclease processing downstream of *cpcA* followed by a 5'→3' progressing degradation of the linker-encoding RNA [134] could accomplish this, since *cpcC2* would be down-regulated first and *cpcC1* would be protected by the 3'-stem-loop structures. Further experiments are needed to test this hypothesis.

IV. 1. C. LR33-deficient strains

The *cpcC1* gene encoding the LR33 linker was inactivated by replacing a 425 bp internal fragment with the Km cassette, the resulting mutant was denoted 33. A strain in which both *cpcC2* and *cpcC1* genes were totally deleted and replaced by the Km cassette was also constructed and denoted CB (Table 4 on page 39 and Figure 22). The CB mutant is similar to the An112 mutant of *Synechococcus* PCC6301 [76] and the PR6009 mutant of *Synechococcus* PCC7002 [78].
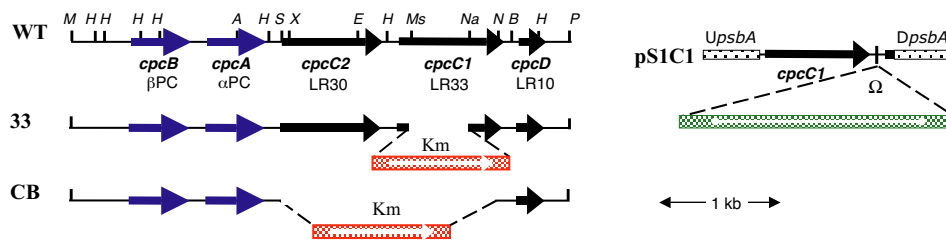
Figure 22. Maps of DNA fragments containing the *cpc* operon in the wild-type, 33 and CB *Synechocystis* PCC6803 strains.

WT, the wild-type *cpc* operon; **33**, 425 bp *Msc*I-*Nae*I fragment from *cpcC1* replaced by the Km cassette; **CB**, 1.7 kb *Spe*I-*Nhe*I fragment containing both *cpcC2* and *cpcC1* replaced by the Km cassette; **pS1C1**, transcriptional fusion of *cpcC1* to the *psbAII* promoter. U*psbA*, upstream *psbAII*; D*psbA*, downstream *psbAII*. Genes are represented as on the Figure15. Abbreviations: A; *Age*I, B; *Bse*RI, E, *Eae*I; H, *Hin*cII; M, *Mfe*I; Ms, *Msc*I; Na, *Nae*I; N, *Nhe*I; P, *Pst*I; S, *Spe*I; X, *Xho*I.

Figure 23. Sucrose gradient profiles of the phycobiliprotein complexes from wild type and rod-linker deficient strains of *Synechocystis* PCC6803.

The wild-type PBSs are located at the bottom of the 1 M sucrose layer. The CB and 33 PBSs are located slightly higher on the gradient. The sucrose gradients of CB and 33 also contained a free PC containing diffuse band at 0.25 M sucrose layer.

63
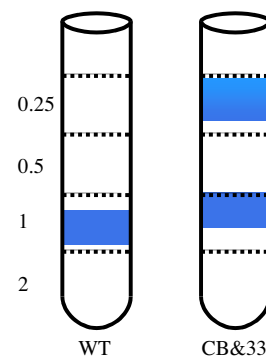
Sucrose gradient patterns of PBS preparation from 33 and CB contained a dark blue band at a position significantly higher on the gradient than that of the wild type PBS indicating, that assembled PBSs were much smaller in size in the mutants (Figure 23). Free PC bands at the top of the gradients indicate the presence of unincorporated PC in these mutants. The presence of unincorporated PC in these strains was confirmed by fluorescence emission upon excitation at 570 nm showing higher emission from PC than in the wild-type cells (Figure 18).

The SDS-PAGE of purified PBSs showed no trace of either LR33 or LR30 in CB. Surprisingly, both linkers were also absent in strain 33. The relative amounts of LR10 were also significantly reduced in both mutants (Figure 24. A lane 33 and CB). PBSs from 33 and CB have identical absorption spectra; these are represented by same trace in Figure 24. B and were similar to the spectrum of 30r (shown on Figure 19. B).
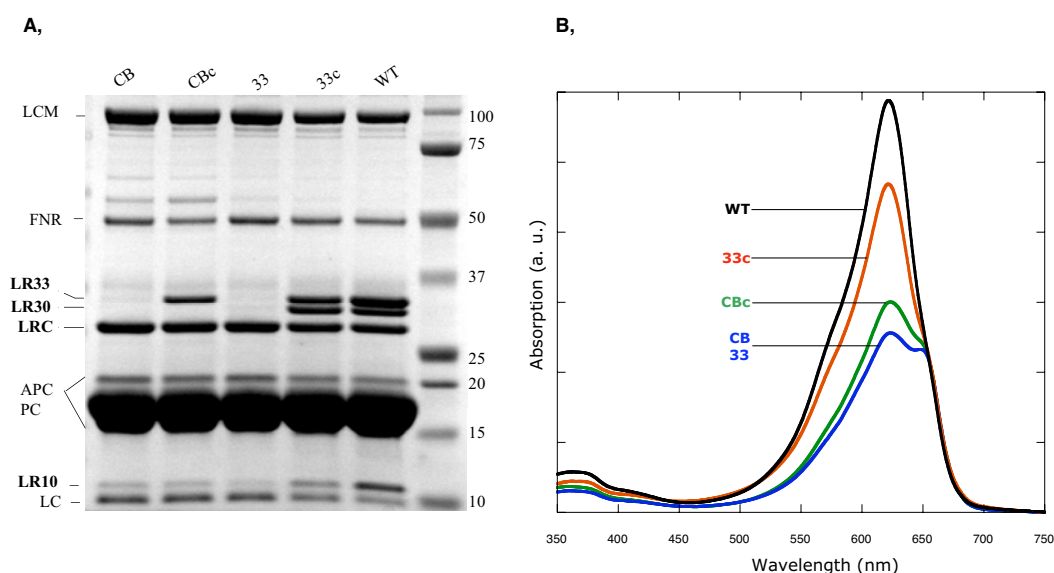
Figure 24. SDS-PAGE and absorption spectra of wild-type, CB, CBc, 33 and 33c PBS.

A, Polypeptide composition of purified PBS from wild type, WT, rod-linker-deficient and complemented strains: CB, CBc, 33, 33c, analyzed on an SDS-PAGE (NuPage 4-12 % acrylamide gradient in Bis-Tris-HCl). The identities of polypeptides are labeled on the left. Masses of the molecular marker are indicated in kDa on the right. **B,** Absorption spectra of purified PBSs from wild type, rod-linkers-deficient and complemented strains, the absorption spectra of CB and 33 contained the lowest amounts of PC (λmax, 620 nm). The increasing height of the 620 nm peaks reflects the increasing amount of PC in the PBSs of the complemented strains, CBc and 33c. The spectra were normalized to the 655 nm absorption.

The absence of LR30 in the PBS from strain 33 suggests that LR30 was not incorporated into the PBS in the absence of LR33. In order to corroborate this hypothesis and to exclude any polar effect of the *cpcC1* mutation, both CB and 33 were complemented with a

transcriptional fusion in which *cpcC1* was placed under the control of the strong *psbAII* promoter in the *psbAII* locus (Figure 22, pS1C1). The resulting strains were denoted CBc and 33c. This insertion was neutral to *Synechocystis* PCC6803 since it was shown that *psbAIII* can support photoautotrophic growth in the absence of *psbAII* [135]. The SDS-PAGE demonstrated that CBc PBSs recovered LR33, indicating that the ectopic *cpcC1* gene was expressed and capable of complementing the deleted gene (Figure 24. A lane CBc). PBSs from 33c recovered both LR33 and LR30, confirming that the absence of both linkers in 33 was due only to the deletion of *cpcC1* (Figure 24. B lane 33c). Absorption spectra showed increased amounts of PC in CBc and 33c PBSs compared to their parent mutants CB and 33, respectively (Figure 24. B). The extent of this increase is more spectacular in 33c, since in this mutant two rod linkers and their associated PC-hexamers were recovered. These results demonstrated that *cpcC2* was functional in strain 33, the absence of its product, LR30 in PBS was due to an epistatic effect of *cpcC1* on *cpcC2*. It is noteworthy that the relative amount of LR10 also increased in the PBSs of 33c compared to that of CB, CBc and 33 (Figure 24. A).

LR30 and LR33 deficient mutants constructed in *Synechococcus* PCC7942 suggested that LR30 could replace LR33 in its absence [136, 137]. On the other hand the results presented here suggest that following the core-proximal PC-hexamer, attached by the LRC, the intermediary PC-hexamer contains specifically LR33 and that the LR30 specifically attaches the distal PC-hexamer. This was demonstrated by two observations, (i.) the absence of LR33 prevented the attachment of LR30 in strain 33, and (ii.) transcomplementation of strain 33 with *cpcC1* restored the attachment of both LR33 and LR30. This model is also in agreement with results obtained upon nitrogen starvation, where sequential loss of PC and associated linkers occurs. LR30 disappears first from the PBS of *Synechocystis* PCC6803 and *Synechococcus* PCC6301 during the initial steps of nitrogen starvation, suggesting that this linker is associated with the peripheral PC-hexamer [98, 100]. In terms of genetics, *cpcC2* and *cpcC1* might have been produced by gene duplication in an ancestral strain that contained only one *cpcC*, such as *Synechococcus* PCC7002. The resulting genes then acquired different functions and *cpcC1* became epistatic to *cpcC2*. The domain that determines the specificity of LR30 and LR33 may lie within the C-terminal third of their sequences, since it is less conserved than the remaining two-thirds (28 % and 55 % identity for each, respectively). Specific interactions between these rod linkers seem to exclude their random insertion in

Synechocystis PCC6803 but not in *Synechococcus* PCC7942 mutants. Amino acid sequence comparison of LR33 and LR30 from *Synechocystis* PCC6803 to *Synechococcus* PCC7942 did not provide an explanation for the differing results obtained in these strains.

LR10 was present in PBSs lacking the core-distal (30f) or both the intermediary and the core-distal PC-hexamers (33 and CB) but in smaller amounts than in the wild type. The reduced level of LR10 was first attributed to the polar effect of the Km cassette on *cpcD* expression in these strains. But the increased amount of LR10 in the 33c PBS compared to CBc (Figure 24. A) suggests that, although the polar effect exists, LR10 might have a higher affinity to a PC-hexamer containing LR30. Indeed, LR10 was proposed to be associated with the distal end of the rods [78].

IV. 1. D. LR10-deficient strains and trans-complemented strains.

The D3 strain (described in IV.I.B.) was almost indistinguishable from the wild type with respect to its growth rate and fluorescence emission characteristics (Figure 18). The polypeptide profile of its PBS confirmed the absence of the LR10 linker and revealed a small decrease in the LR33 to LR30 ratio (Figure 19. A). Examination of the D3 PBS absorption spectra revealed a higher contribution from APC (shoulder at 650 nm), which means that the D3 PBS contained less PC (Figure 26. B). In this mutant, the Ω cassette was inserted upstream of *cpcD*, destroying a stem-loop structure that might stabilize the 3.4 kb mRNA where *cpcC1* is at the 3'-end (Figure 20). In order to verify this possibility, a mutant was created by inserting the Ω cassette into the *cpcD* orf (Table 4 on page 39 and Figure 25).
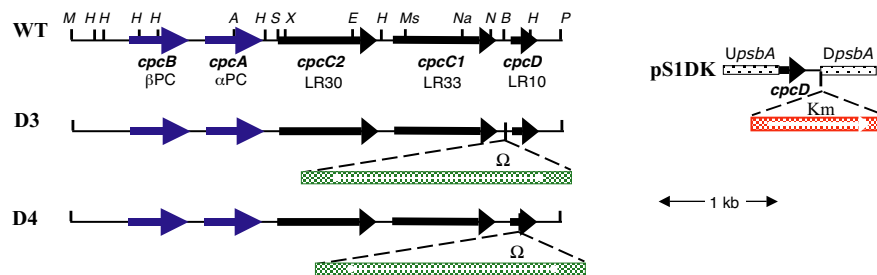
Figure 25. Maps of DNA fragments containing the *cpc* operon in the wild-type, D3 and D4 *Synechocystis* PCC6803 strains, and pS1DK construct.

D3 Ω cassette inserted in the *Bse*RI site; **D4**, Ω cassette inserted in the *Hinc*II site of *cpcD*; **pS1DK**, translational fusion of the *cpcD* orf to the *psbAII* initiation codon. U*psbA*, upstream *psbAII*; D*psbA*, downstream *psbAII*. Genes are represented as on Figure 16. Abbreviations: A; *Age*I, B; *Bse*RI, E, *Eae*I; H, *Hinc*II; M, *Mfe*I; Ms, *Msc*I; Na, *Nae*I; N, *Nhe*I; P, *Pst*I; S, *Spe*I; X, *Xho*I.

PBSs from this D4 mutant lacked LR10 but contained a normal LR33 to LR30 ratio and the absorption spectra of these PBSs were identical to that of the wild type (Figure 26. A and B). Therefore, the decrease in LR33 and the modified absorption spectra observed in D3 were due to the absence of the stem-loop in the 3.4 kb mRNA. Similar results were obtained in *Synechococcus* PCC7002 mutants in which the stem-loop between *cpcC* and *cpcD* was deleted [78].
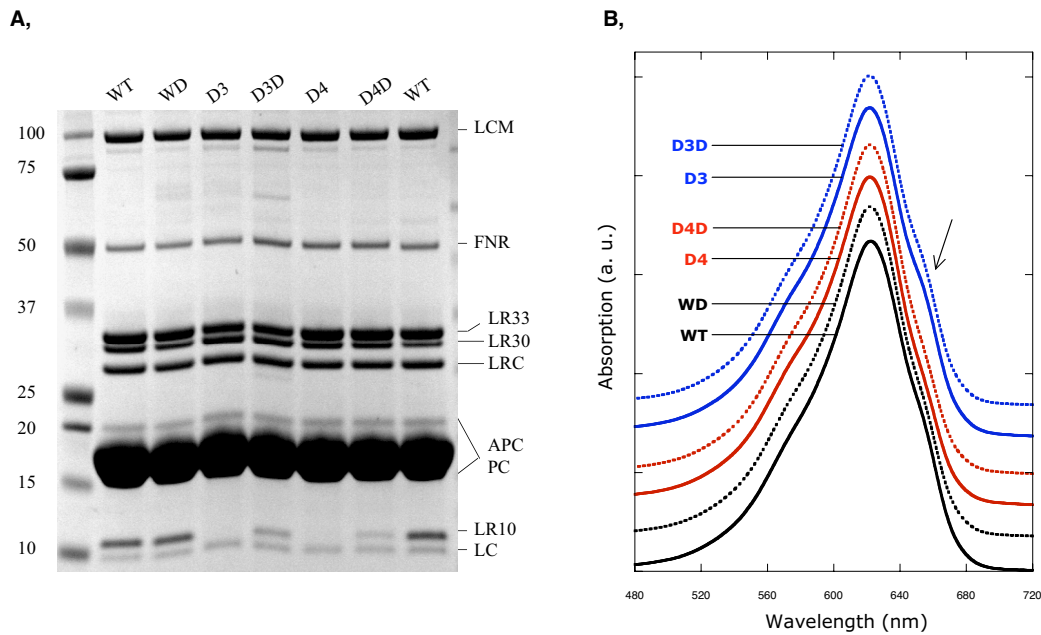
Figure 26. SDS-PAGE and absorption spectra of wild-type, WD, D3, D3D, D4 and D4D PBS.

A, Polypeptide composition of purified PBSs from *cpcD*-mutant strains analyzed on an SDS-PAGE (NuPage 4-12 % acrylamide gradient in Bis-Tris-HCl). The identities of polypeptides are labeled on the right. Masses of the molecular marker are indicated in kDa on the left. **B,** Absorption spectra of purified PBSs. The contribution of APC (arrow at 650 nm) was more obvious in the D3 and D3D spectra. The spectra were shifted for better viewing.

Since the loss of LR10 does not affect either the assembly or the function of PBS in *Synechocystis* PCC6803, over-expression of *cpcD* might elucidate its role. A fragment starting at the *cpcD* initiation codon and ending downstream of its transcription terminator was used to produce a construct placing *cpcD* under the control of the *psbAII* transcriptionally and translationally in plasmid pS1DK (Figure 25). Transformation of the wild type with this construct generated the WD strain. This strain produced a high level of a 0.4 kb mRNA containing *cpcD*, indicating that the ectopic *cpcD* was transcribed at the level expected from the *psbAII* promoter (Figure 27). PBSs from WD were indistinguishable from those from the wild type regarding either their polypeptide composition or their absorption spectra (Figure 26. A and B). In order to estimate the

67

production of LR10 polypeptide from the ectopic *cpcD* gene, the *cpcD* deficient strains D3 and D4 were transformed with pS1DK resulting in strains D3D and D4D, respectively. PBSs from both strains recovered LR10, but the PBSs of these strains contained lower amounts of LR10 than the wild type (Figure 26. A and B). These results indicated that although the ectopic gene over-produced an mRNA containing *cpcD*, the LR10 polypeptide was not proportionally translated or was degraded before its incorporation into the PBS. When the LR10 is produced *in trans* proteolysis might prevent its association to the PBS; it is known that linker polypeptides are highly sensitive to proteolysis when they are not associated to phycobiliproteins. Therefore, over-expression of a linker polypeptide should be achieved by placing the ectopic gene as close as possible to the *cpc* operon as it was done earlier in *Synechococcus* PCC7942 [79] although these authors did not check the ability of their ectopic *cpcD* gene to complement a *cpcD* deficient strain.
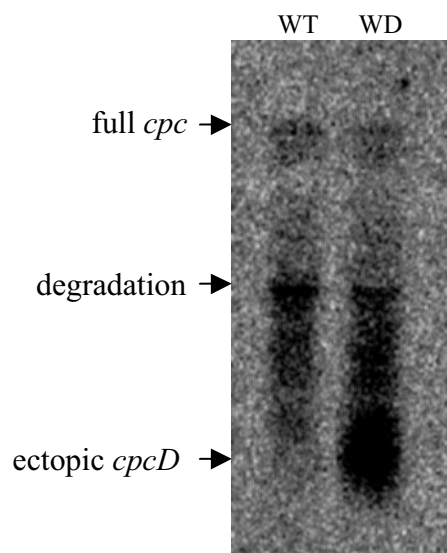
Figure 27. Northern-hybridization analysis of the *cpcD* gene expression in the wild type and D4 mutant strain.

DNA probe were chosen to be specific for *cpcD* (ProbeD). Approximately 15 µg of total RNA were loaded per lane (6 nm well width). Arrows indicates the full *cpc* transcript, degradation product of the *cpc* transcript and the transcript of the ectopic gene. Strong signal in the case of D4 mutant (WD) at the ectopic gene transcript indicated that the ectopic *cpcD* was transcribed at the level expected from the *psbAII* promoter.

IV. 1. E. LRC-deficient strains

LRC has a crucial role in the function of the PBS, which might explain the presence of several genes encoding the LRC. In *Synechococcus* WH8102 two genes were found to encode the LRC and both genes product were detected in the PBS [65]. *Anabaena* PCC7120 has four *cpcG* genes, but only three LRCs were detected [77]. It is not yet elucidated whether the different LRCs have different roles in specific interactions between the different core subunits (see Figure 28) and the rods. The core-proximal PC-hexamers of

the rods are in interaction with two APC-trimers, therefore in *Synechocystis* PCC6803 two different rod-core interactions could be postulated.

A.

1: $(\alpha\beta)_3^{APC} \bullet LC$

2: $(\alpha\beta)_3^{APC}$

3: $(\alpha\beta)_3^{APC} \bullet \beta^{18} \bullet LCM$

4: $(\alpha\beta)_3^{APC} \bullet \alpha^{APCB} \bullet LC$

B.
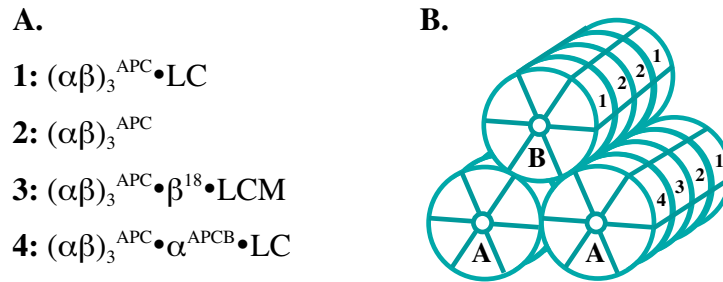
Figure 28 The composition of the core complex of the *Synechocystis* PCC6803.

A. Each of the three core cylinders in the PBS of *Synechocystis* is composed of four different subcomplexes. **B.** The PBS of the *Synechocystis* has two types of cylinder A and B depending on their composition. (A rod is in interaction with two APC-trimers, therefore it could interact with the 1 and 2 type trimers or with 4 and 3 type trimers).

In *Synechocystis* PCC6803, two genes encode LRC, *cpcG1* and *cpcG2*, which raise the question whether these are active alleles as in the case of *psbAII* and *psbAIII* or whether one of them is not transcribed as the *psbAI* [135, 138, 139].

Using specific primers, RT-PCR assays were performed to check whether the LRC encoding *cpcG1* and *cpcG2* genes are transcribed in *Synechocystis* PCC6803. The RT-PCR analysis produced bands with the expected size for each gene, 650 bp and 550 bp with *cpcG1* and with *cpcG2*, respectively, indicating that both of these genes are transcribed in the wild type (Figure 29).
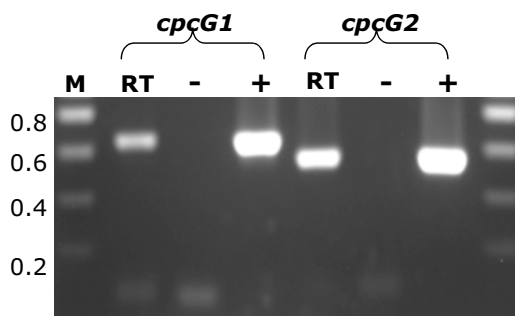
Figure 29. RT-PCR analysis of *cpcG1* and *cpcG2* transcription.

RT: RT-PCR product, which indicates that the gene was transcribed
-: negative control, which do not contain Reverse Transcriptase and indicates if we have DNA in our RNA preparation
+: positive control, which contained genomic DNA of *Synechocystis* and indicates that our PCR was working.

In order to study whether the two LRCs, encoded by these genes have different roles in the PBS structure by mediating different rod-core interactions, the two genes were inactivated one by one. In the G1 mutant the *cpcG1* gene was inactivated by the insertion of the Ω cassette, and in the G2 mutant the *cpcG2* gene was inactivated by the insertion of the Km cassette (Table 4 on page 39 and Figure 30).

Northern-blot hybridization showed that both genes are transcribed as monocistronic mRNAs of about 1 kb in the wild type and that each mutant lacked the mRNA corresponding to the inactivated gene (Figure 31).
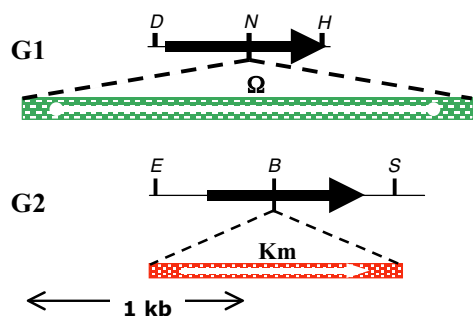
Figure 30. Restriction maps of *Synechocystis* PCC6803 rod-core linker mutant strains.

G1, Ω cassette inserted into the *cpcG1* gene at *Nru*I site; **G2**, Km cassette inserted into the *cpcG2* gene at *Bsr*GI site. *cpcG* genes are represented as black arrows, Ω cassette as white line in a green rectangle and the Km cassette as white arrow in a red rectangle, an arrowhead indicates the direction of gene transcription. Abbreviations: B, *Bsr*GI; E, *Eae*I; H, *Hinc*II; N, *Nru*I; D, *Dra*I; S, *Spe*I.
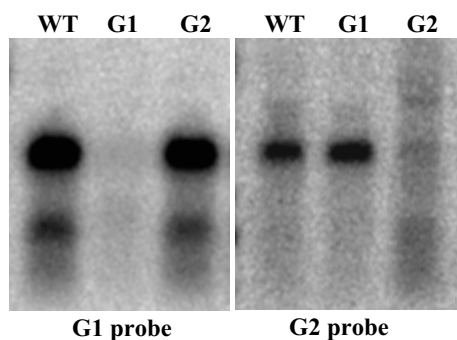

Figure 31. Northern-blot analysis of the *cpcG1* and *cpcG2* transcription in the wild-type and G1 and G2 mutant strains.

Left panel shows the transcription of *cpcG1* and the right panel shows the transcription of *cpcG2*, indicating that both genes are transcribed in the wild type.
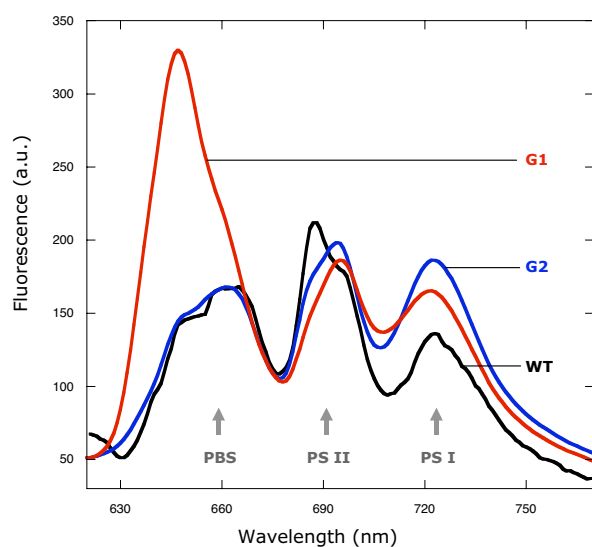
Figure 32. Fluorescence emission spectra of wild-type, G1 and G2 cells at 77 K excited at 570 nm.

Cells were excited at 570 nm at 77 K. Fluorescence emission spectra of G2 was similar to the wild type, but G1 showed high emission from PC. (Grey arrows indicates the emission from PBS, PSII and PSI).

Fluorescence emission spectra upon excitation with biliprotein-sensitizing light (570 nm) of G2 cells were similar to the wild type. On the other hand fluorescence emission spectrum of G1 cells showed higher emission from PC than those of the wild-type or G2 cells, indicating that in G1 PC were unable to transfer its energy to the PBS core (Figure 32).

PBSs were purified from both strains in order to determine their polypeptide composition. Sucrose gradient pattern from the PBS preparation of G2 contained a dark-blue band at the position where the wild-type PBS was expected, indicating that complete PBS were assembled in this strain. Suc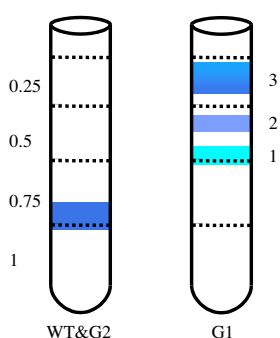rose gradient pattern of G1 preparation did not contain this dark-blue band; but had two bands in the 0.5 M sucrose layer, a turquoise band near the 0.75 M layer (band 1, Figure 33) and a blue band near the 0.25 M layer (band 2, Figure 33). The gradient also contained a diffuse blue band at the top, with free phycobiliproteins (band 3, Figure 33).

Figure 33. Sucrose gradient profiles of the phycobiliprotein complexes from wild-type, G1 and G2 mutant strains.

The wild-type and G2 PBSs are located at the bottom of the 0.75 M sucrose layer. The sucrose gradient of G1 contained: a turquoise band at the bottom of the 0.5 M sucrose layer, a blue band near to the top of the 0.5 M sucrose layer and a blue band in the 0.25 M sucrose layer.

The polypeptide composition of purified complexes was analyzed by Coomassie-stained SDS-PAGE. The compositions of the wild-type and G2 PBSs were identical (Figure 34. A). The turquoise band of G1 preparation contained the PBS core polypeptides, APC, LCM, LC and some contaminant proteins as well. The dark blue band of the G1 PBS preparation contained PC, LR30, LR33, small amount of LR10 and some contaminant proteins in the 50 kDa range. None of the complexes from G1 contained LRC (Figure 34. A).

The absorption spectrum of the purified PBS of G2 is similar to that of the WT (Figure 34. B). The complex from the turquoise band showed an absorption spectrum characteristic to the APC containing core (Figure 34. B, G1c), identical to the spectrum of cores isolated from CK (Figure 15. B). The absorption maximum of the dark-blue band 2 was at 620 nm, indicating that it contained PC (Figure 34. B, G1r).
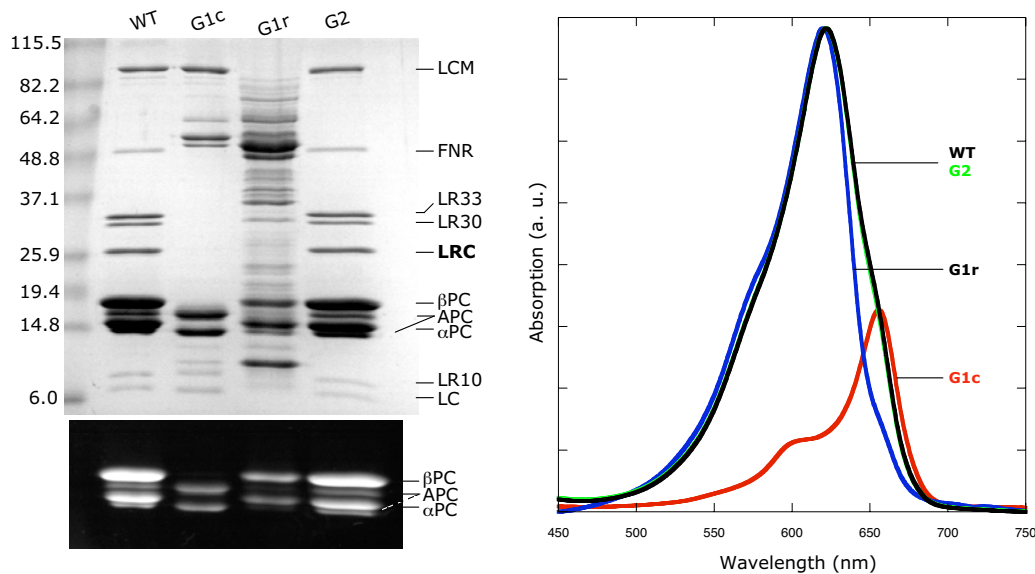
Figure 34. SDS-PAGE and absorption spectra of wild-type, G1c, G1r and G2 PBS complexes.

A, Polypeptide composition of purified PBS from wild type (WT), *cpcG1* inactivated strain (turquoise band 1: G1c, blue band 2: G1r) and *cpcG2* inactivated strain (G2); analyzed on SDS-PAGE (8-18 % linear acrylamide gradient Tris-HCl). The identities of polypeptides are labelled on the right. Masses of the molecular marker are indicated in kDa on the left. Under the commassie-stained gel: the fluorescence of phycobiliproteins in the presence of $ZnSO_4$ [3].

B, Absorption spectra of purified PBSs from wild-type, G1 and G2 strains. Wild-type and G2 PBSs have similar absorption spectra (λmax, 620 nm). The turquoise band of the G1 PBS isolation gradient have a typical absorption spectra of a core (λmax, 650 nm), while the blue band showed absorption spectra of PC (λmax, 620 nm). The spectra were normalized to the 655 nm absorption.

Our results indicate that only the *cpcG1* encoded LRC participates in the PBS structure in *Synechocystis* PCC6803. Inactivation of *cpcG2* did not alter the PBS composition but the sucrose gradient of the G1 PBS preparation contained the core complex and the rods of the PBS separately, indicating that the inactivation of *cpcG1* prevented the attachment of the rods to the core. We could not assign a role to the LRC encoded by *cpcG2*, even under high-light or nitrogen-starvation conditions. These results raise the question whether LRC is translated from the *cpcG2* gene.

The LRC (band from an SDS-PAGE) of wild-type PBS was sequenced in the Institut Pasteur (Paris). The N-terminal amino-acid sequence of this band was determined as: ALPL, which corresponds to the N-terminal amino-acid sequence of the LRC encoded by *cpcG1*. There was no indication of the presence of other amino-acid sequence in this band, as confirmed by mass spectroscopy analysis.

When we analyzed the sequence of the upstream region of *cpcG2* we could not find a Shine-Dalgarno sequence, which could promote positioning the ribosome for translational initiation. However, not all bacterial genes have Shine-Dalgarno sequence, its absence might prevent the translation of *cpcG2*. Translational fusion of *cpcG2* with the promoter of *psbAII* is under way to elucidate this question.

In summary, the construction and characterization of rod-core-linker and rod-linker mutant strains enabled us to construct the following model of *Synechocystis* PCC6803 PBS (Figure 35).
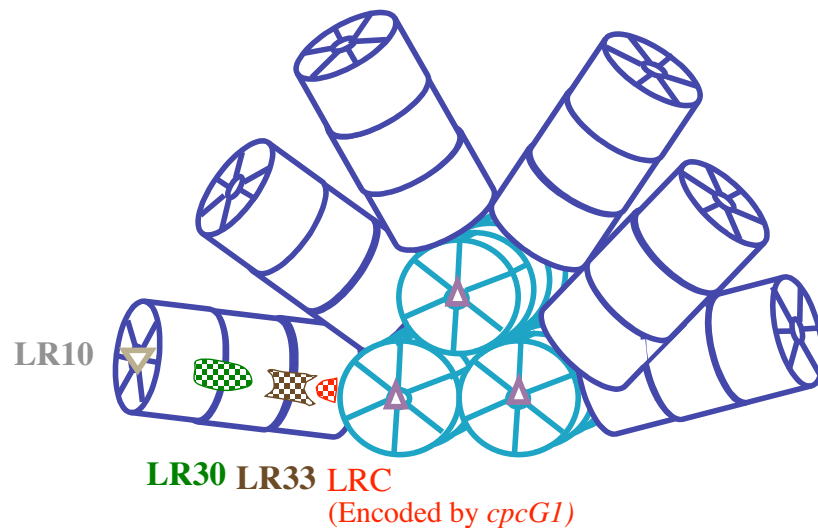
Figure 35. Schematic representation of the *Synechocystis* PBS.

The APC containing core is turquoise and the PC-containing rods are blue. The first PC-hexamer is attached by the *cpcG1* encoded LRC (red), the second hexamer is attached by the LR33 (brown) and the third and core-distal PC-hexamer is attached by the LR30 (green). The LR10 (grey) binds to the core distal end of the rods and LR10 has higher affinity to the LR30 containing PC-hexamers that the LR33-containing PC-hexamers.

IV. 2. Preliminary results obtained with the FNR mutants

There are two isoforms of ferredoxin-NADP(H)-oxidoreductase (FNR) in *Synechocystis* PCC6803. The 46.3 kDa form, containing an LR10-like domain, binds to the PBS and the smaller, 34.3 kDa FNR, which was suggested to be a proteolytic product of the larger one [110]. The N-terminal of this protein was determined as MTTTPKEK [108]. The analysis of the *petH* gene sequence indicates two other potential initiating sites besides the initiating methionine 1, these are valine 102, coded by GTG, and methionine 113, coded by ATG. In order to determine whether these sites are functional initiation sites, mutant strains called I and V were constructed, in which methionine 113 (M113) was replaced by isoleucine (coded by ATC), and valine 102 (V102) was changed to a non-initiating valine (coded by GTC) (Table 5 on page 40 and Figure 36).
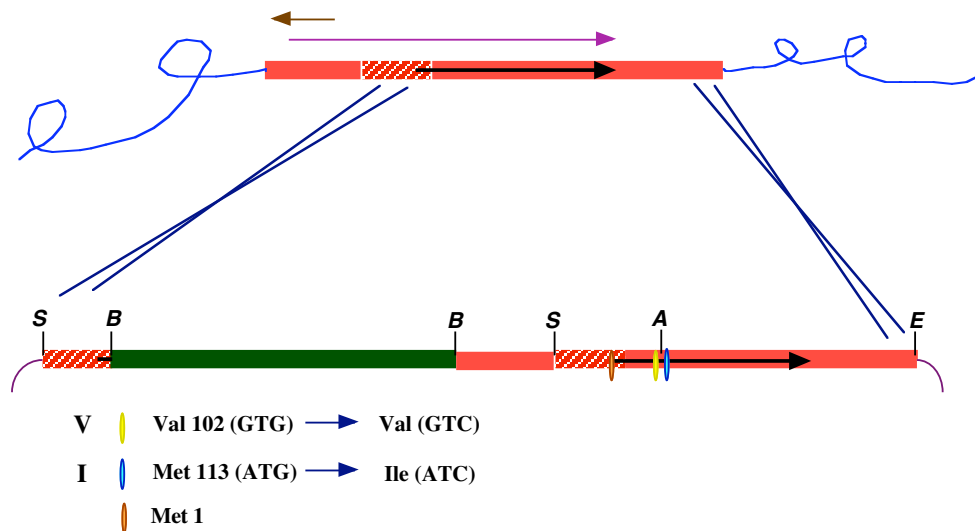
Figure 36. Schematic representation of the construct for the *petH* gene mutagenesis.

The *petH*-containing PCR-amplified fragment is represented in red, and the repeated domain of the construct is marked with white lines. The *petH* gene is represented as a black arrow, the Ω cassette is represented in green. The purple arrow indicates the *petH* gene transcript and the brown arrow the beginning of the *prk* gene transcript. Dark blue lines indicate where the double recombination should take place. In the V mutant valine 102 (indicated by yellow ellipsis) coded by GTG was replaced by valine coded by GTC. In the I mutant methionine113 (indicated by blue ellipsis) coded by ATG was replaced by isoleucine coded by GTC. The H mutant strain contained the same construct without any alteration on the gene sequence. Abbreviations: *A*, *Alw*NI; *B*, *Bam*HI; *E*, *Eco*RV; *S*, *Spe*I; Met, methionine; Ile, isoleucine; Val, valine.

The 5' end of the *petH* transcript in *Synechocystis* PCC6803 is located within the open reading frame of the phosphoribulokinase encoding *prk* gene, which is transcribed in an opposite orientation [116]. When creating the FNR mutant strains it was important not to disturb the *prk* gene transcription, because the phosphoribulokinase is essential for the

74

cells. Therefore a system, similar to the one used by van Thor [110] was used, in which a *prk-petH* intergenic region is duplicated. Integration of the constructs into the chromosome by double recombination resulted in fully segregated mutants that carried a modified *petH* gene and the Ω cassette (Figure 36). Note that since these strains carry an 815-bp duplication on both sides of the Ω cartridge, single recombination could result in its excision in the absence of selective pressure (antibiotics) yielding strains, which still carry the introduced mutation, but not the Ω cassette (Figure 37).

The wild type cells were also transformed with a construct containing the wild-type *petH* sequence to create the control H strain (Table 5 on page 40).
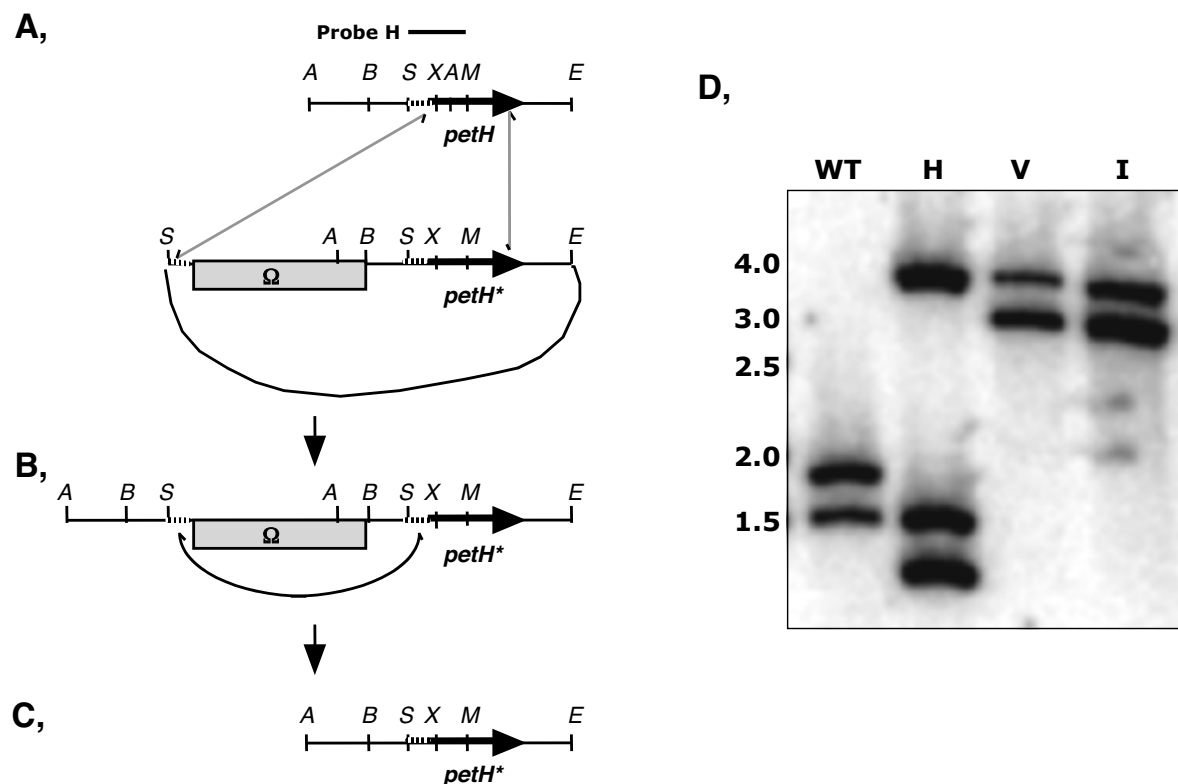
Figure 37. The construction of the FNR mutants.

A, Mutant construct and the *petH* gene on the genome. Double recombination indicated by grey arrows.
B, The genome after the double recombination, on which single recombination might occur resulting in the lost of the Ω cassette.
C, The genome after the above-mentioned single recombination. Abbreviations: *A*, *Alw*NI; *B*, *Bam*HI; *E*, *Eco*RV; *S*, *Spe*I; *X*, *Xba*I; *M*, *Msc*I.
D, Southern-blot analysis with Probe H, which indicates the complete segregation of the mutant strains after double recombination. The genomic DNA isolated from the wild-type, H, V and I mutant strains was digested with *Alw*NI and *Eco*RV. (In the H mutant the orientation of the Ω cassette was opposite, to that of the I and V mutants).

75

SDS-PAGE analysis of the purified PBSs from these strains confirmed that they had completely assembled PBS with the FNR attached, similar to the PBS of the wild type (Figure 38).
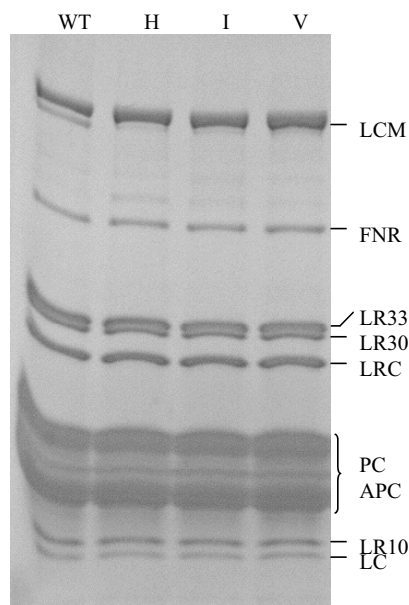
Figure 38. Polypeptide composition of purified PBS from WT, and H, I and V mutant strains.

PBS composition was analyzed on an SDS-PAGE (10-20 % linear acrylamide gradient in Tris-HCl). The identities of polypeptides are labelled on the right.

The FNR content of whole cell extracts from the mutant strains and wild-type cells was detected by Western-blot analysis (performed in collaboration with Dr J.-C. Thomas using *Synechocystis* PCC6803 FNR antibodies kindly provided by Dr B. Lagoutte).
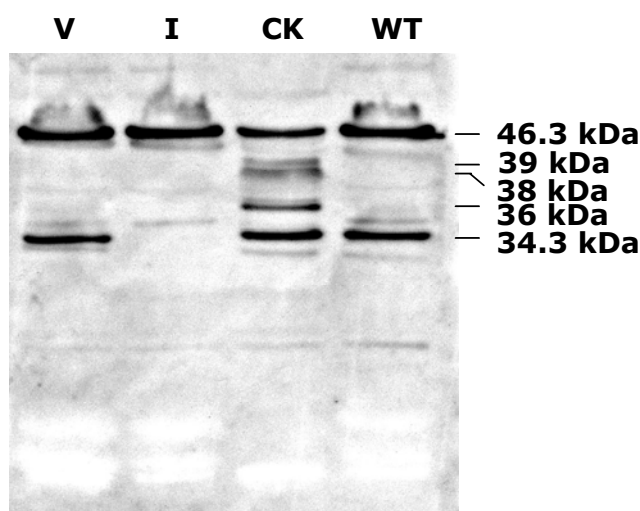
Figure 39. Western-blot analysis of the FNR content of whole cell extracts from the *petH* mutated strains, the rod-less strain and wild-type cells.

Synechocystis PCC6803 FNR specific antibody was used for the Western-blot analysis. Masses of the detected bands are indicated in kDa on the right. The molecular masses of the FNRs (46.3 and 34.3 kDa) were calculated from the *petH* encoded polypeptides, while the masses of the degradation products were estimated from their positions on the gel.

The wild type and V mutant gave a strong signal of the 46.3 kDa protein and somewhat weaker signal of the smaller 34.3 kDa protein (Figure 39). The H mutant gave the same signals as the wild type (not shown). Cell extracts from CK contained both the 34.3 kDa

and the 46.3 kDa protein, as well as degradation products of the latter one. If the larger form of the FNR can not bind to the PBS its linker domain is target of proteolysis. The degradation product in CK indicates that in this rod-less mutant the FNR do not bind to the PBS. The lack of the 34.3 kDa protein from the I strain support the idea that methionine 113 might be an alternative initiation site. On the other hand the replacement of the methionine to isoleucine may also prevent the proteolysis if methionine is the specific site of the proteolysis.

We have also created mutant strains by the insertion and deletion of a cytosin in *petH* in which, stop codons were generated at codon 110 and codon 113, respectively, (Table 5 on page 40). In these strains, the stop codon terminates the translation from methionine 1, but translation from methionine 113 is still possible, since its codon was not altered. Complete segregation of these strains was only possible with a second initiation from methionine 113, since the FNR is essential for the cells. The *petH* frame-shift mutants did segregate, which proved our hypothesis to be correct.

These FS1 and FS2 mutants produced only the 34.3 kDa FNR isoform and their PBSs were devoid of FNR. Preliminary results indicated that under heterotrophic and nitrogen-starved growth conditions the amount of the 34.3 kDa FNR form increased in the wild type. Further experiments are needed to determine the function of the two FNR isoforms. In future studies, parallel characterization of wild type, I and FS mutant strains in *Synechocystis* PCC6803 may elucidate the function of the two isoforms, since the wild type contains both, while the I and the FS mutant strains contain only the 46.3 and 34.3 kDa FNR forms, respectively.

As mentioned above, the N-terminal domain of the larger FNR shows high similarity to LR10 (about 32 % identity and 75 % similarity over 80 amino acids), while lower similarities were found to the C-terminal domains of LR33 and LR30 and even to the core-associated linker LC. FNR was proposed to share the same binding site with LR10 in the PBS of *Synechococcus* PCC7002 [113]. Consequently, one could expect the relative amount of FNR to increase in the absence of LR10, however, this was not observed in our LR10-deficient mutants (Figure 26. A). It was also suggested that FNR binds to the core-proximal PC-hexamer or even directly to the core in *Synechocystis* PCC6803 [112]. But FNR did not co-purify with the PBS-core complexes of G1 nor CK (see Figure 15. A and Figure 34. A). These results suggest that FNR does not share the same binding site with the

LR10 and that it is not able to bind to the core either, it is rather located on the rods in a core-proximal position.

V. CONCLUSIONS AND PERSPECTIVES

V. 1. Conclusions

Based on characterization of various PBS rod and FNR related mutant strains we came to the following conclusions:

i. There is a special order of PBS rod development during the biogenesis of the PBS in *Synechocystis* sp. strain PCC6803. Our results clearly demonstrated that the rod linkers are inserted in a specific order during PBS rod growth, i. e. when the first PC-hexamers are attached by the LRC to the core, the LR33 binds the intermediary PC-hexamer. This is followed by the binding of the third core-distal PC-hexamer by LR30. LR33 and LR30 are not interchangeable.

This result contradicts studies on mutants of *Synechococcus* sp. strain PCC7942 lacking rod-linker genes in which it was proposed that LR30 and LR33 could occupy interchangeable positions within the rods [136, 137]. On the other hand, our model is in a good agreement with results obtained with wild-type *Synechocystis* PCC6803 under nitrogen starvation, where sequential loss of PC-hexamer and associated linkers occurs and LR30 disappearing first from the PBS [98].

ii. We demonstrated that the LR10 has higher affinity to LR30 containing than to LR33 containing PC-hexamers. LR10 has already been proposed to be associated with the distal end of the rods [78], and our results proved that the LR30 binds to the core distal PC hexamer. The absence of LR10 did not affect either the PBS structure or function.

iii. We have shown that PC biosynthesis was not co-regulated by the synthesis of the rod-linker polypeptides under our experimental condition.

iv. We demonstrated that the insertion of the commonly used Km cassette, regardless of its orientation, had a polar effect on the *cpc* operon transcription. The Ω terminator did not provide a 3'-stabilizer effect to transcripts.

v. Our results showed that in *Synechocystis* PCC6803 although both LRC encoding genes, *cpcG1* and *cpcG2* were expressed, only *cpcG1* product participated in the PBS structure formation. Similarly to *Synechocystis* PCC6803, LRC is encoded by more than one gene in other cianobacterial strains as well. In *Synechococcus* WH8102, two genes encode the LRC and both genes product were detected in the PBS [65]. *Anabaena* PCC7120 has four *cpcG* genes, but only three LRCs were detected [77], however the expression of these genes were not examined in this strain.

vi.   We demonstrated that the 34.3 kDa form of the FNR, in contrast to the earlier assumptions, is not produced by proteolysis of the 46.3 kDa form, but the two isoforms of the FNR are the products of alternative translation initiations.

vii.   Based on the characterization of various rod-linker and rod-less mutant strains, we suggest that the 46.3 kDa from of the FNR do not share the same binding site with the LR10 on the PBS rods and it is not able to bind directly to the core, rather it must be located in a core proximal position on the rods.

V. 2. Perspectives

The production and characterization of various *Synechocystis* PCC6803 mutant strains enable us to answer several questions related to PBS biogenesis and to the two FNR isoforms. Our conclusions were summarized in chapter V. A. However, there are several further issues to address. Because the absence of LR10 did not affect either the assembly or the function of *Synechocystis* PCC6803 PBS, further experiments considering the instability of the protein, might be essential to elucidate the function of this linker, such as LR10 over-expression in close proximity to the *cpc* operon. The structure analysis in the PBS of the LR10 mutant strains by electron microscopy might also uncover the function of the LR10 in the termination of the rod growth.

It is generally accepted that the amount of the linker polypeptides determines the amount of phycobiliproteins incorporated into the PBS and therefore the efficiency of energy transfer to the photosynthetic reaction centers. LR33, encoded by the *cpcC1*, binds the second PC hexamer and LR30 encoded by *cpcC2* binds the third PC hexamer in the PBS rods. Therefore under high-light conditions *cpcC2* should be down-regulated first in order to diminish the light-harvesting capacity of the PBS rods. Since *cpcC2* and *cpcC1* are co-transcribed, there should be a transcriptional regulation mechanism assuring that *cpcC2* is down-regulated first. Endoribonuclease processing downstream of *cpcA* followed by a 5'→3' progressing degradation of the linker-encoding RNA could accomplish this, since the *cpcC2* part of the transcript would be degraded before the *cpcC1* part of the transcript protected at its 3' end by the stem-loop structure. The expression of the linker encoding part from the *psbA* promoter in our rod-linker deficient strain (CB) may prove this hypothesis. In such mutant, the ratio of LR30 and LR33 should be around 1 and should not decrease under high light conditions.

The LRC has a crucial role in the PBS structure and light harvesting efficiency. It is an interesting question why the *cpcG2* encoded LRC does not participate in the PBS structure, although the gene is transcribed. The upstream region of *cpcG2* gene does not contain a Shine-Dalgarno sequence, which might prevent the translation of this gene. Translational fusion of *cpcG2* in the *psbAII* locus might elucidate whether this is the reason of the absence of the *cpcG2* encoded LRC from the PBS structure.

Synechococcus WH8102 has two rod-core linker encoding genes and both genes product were detected in the PBS. It would be interesting to study the role of the different

LRCs in the PBS of *Synechococcus* WH8102 by inactivating the respective genes. Comparison of absorption spectra, polypeptide composition and electron-microscopic analysis of PBS purified from these mutants might elucidate the role of these linker polypeptides.

Our FNR mutant strains provided us with good experimental background to study the role of the two FNR isoforms as well. The wild type contains both forms, while the I mutant contains only 46.3 kDa form and the FS mutant contains only the 34.3 kDa form of the FNR. Characterization of these mutant strains under different growth conditions may reveal whether one form participated in linear or cyclic electron transport in photosynthesis or in respiration and may also indicate other roles. Western-blot analysis of the FNR content of the wild type grown under different conditions - such as heterotrophic growth, different light conditions, salt stress or nitrogen starvation - could indicate which form is more functional under such conditions.

Fluorescence emission, fluorescence induction, photosynthetic oxygen evolution and P700 measurements of the mutant strains could show how the lack of one FNR form would affect the electron transport. It would also be interesting to purify each of the two forms, the 46.3 kDa form attached to a PC hexalmer and the 34.3 kDa form, in order to characterize their enzymatic activity *in vitro*.

REFERENCES

1.   Blankenship, R.E., 2002. Antenna Complexes and Energy Transfer Processes, in *Molecular Mechanism of Photosynthesis*. Blackwell Science. p. 61-94.

2.   Reuter, W., G. Wiegand, R. Huber, and M.E. Than, 1999. Structural analysis at 2.2 A of orthorhombic crystals presents the asymmetry of the allophycocyanin-linker complex, AP.LC7.8, from phycobilisomes of *Mastigocladus laminosus*. Proc Natl Acad Sci U S A, **96**(4): p. 1363-1368.

3.   Raps, S., 1990. Differentiation between Phycobiliprotein and colorless Linker Polypeptides by Fluorescence in the Presence of $ZnSO_4$. Plant Physiol, **92**: p. 358-362.

4.   Schirmer, T., R. Huber, M. Schneider, W. Bode, M. Miller, and M.L. Hackert, 1986. Crystal structure analysis and refinement at 2.5 A of hexameric C-phycocyanin from the cyanobacterium Agmenellum quadruplicatum. The molecular model and its implications for light-harvesting. J Mol Biol, **188**(4): p. 651-676.

5.   Brejc, K., R. Ficner, R. Huber, and S. Steinbacher, 1995. Isolation, crystallization, crystal structure analysis and refinement of allophycocyanin from the cyanobacterium *Spirulina platensis* at 2.3 A resolution. J Mol Biol, **249**(2): p. 424-440.

6.   Whitton, B.A. and M. Potts, 2000. Introduction to the Cyanobacteria, in *The Ecology of Cyanobacteria*, B.A. Whitton and M. Potts, Editors. Kluwer Academic Publishers: Dordrecht. p. 1-11.

7.   Shestakov, S.V. and N.T. Khyen, 1970. Evidence for genetic transformation in blue-green alga *Anacystis nidulans* R2. Molec Gen Genet, **107**: p. 372-375.

8.   Thiel, T., 1994. Genetic Analysis of Cyanobacteria, in *The Molecular Biology of Cyanobacteria*, D.A. Bryant, Editor. Kluwer Academic Publishers: Dordrecht. p. 581-611.

9.   Lewin, R.A., 1981. Prochloron and the theory of symbiogenesis. Ann N Y Acad Sci, **361**: p. 325-329.

10.   Lokstein, H., C. Steglich, and W.R. Hess, 1999. Light-harvesting antenna function of phycoerythrin in *Prochlorococcus marinus*. Biochim Biophys Acta, **1410**: p. 97-98.

11.   La Roche, J., G.M.W. Vanderstaay, F. Partensky, A. Ducret, R. Aeberssold, R. Li, S.S. Golden, R.G. Hiller, P.M. Wrench, A.W.D. Larkum, and B.R. Green, 1996. Independent evolution of the prochlorophyte and green plant Chlorophyll *a/b* light-harvesting protein. Proc Natl Acad Sci U S A, **93**: p. 15244-15248.

12.   Miyashita, H., H. Ikemoto, N. Kurano, K. Adachi, M. Chihara, and S. Miyachi, 1996. Chlorophyll *d* as a major pigment. Nature, **383**: p. 402-402.

13.   Grigorieva, G.A. and S.V. Shestakov, 1982. Transformation in the cyanobacterium *Synechocystis* PCC 6803. FEMS Microbiol Lett, **13**: p. 367-370.

14.   Awramik, S.M., 1992. The oldest records of photosynthesis. Photosynth Res, **33**: p. 75-89.

15. Ke, B., 2001. Photosynthesis. Photobiochemistry and Photobiophysics. Kluwer Academic Publishers.

16. Blankenship, R.E., 2002. Photosynthetic Organisms and Organelles, in *Molecular Mechanism of Photosynthesis*. Blackwell Science. p. 11-25.

17. Blankenship, R.E., 2002. Carbon Metabolism., in *Molecular Mechanism of Photosynthesis*. Blackwell Science. p. 171-203.

18. Calvin, M., 1962. The Path of Carbon in Photosynthesis. Science, **135**(3507): p. 879-889.

19. Blankenship, R.E., 2002. Reaction Center complexes, in *Molecular Mechanism of Photosynthesis*. Blackwell Science. p. 95-123.

20. Hankamer, B., J. Barber, and E.J. Boekema, 1997. Structure and membrane organization of photosystem II in green plants. Annu Rev Plant Physiol Plant Mol Biol, **48**: p. 641-671.

21. Nugent, J.H., 1996. Oxygenic photosynthesis. Electron transfer in photosystem I and photosystem II. Eur J Biochem, **237**(3): p. 519-531.

22. Barber, J., 1998. Photosystem two. Biochim Biophys Acta, **1365**(1-2): p. 269-277.

23. Zouni, A., H.T. Witt, J. Kern, P. Fromme, N. Krauss, W. Saenger, and P. Orth, 2001. Crystal structure of photosystem II from Synechococcus elongatus at 3.8 A resolution. Nature, **409**(6821): p. 739-743.

24. Ferreira, K.N., T.M. Iverson, K. Maghlaoui, J. Barber, and S. Iwata, 2004. Architecture of the photosynthetic oxygen-evolving center. Science, **303**(5665): p. 1831-18318.

25. Stroebel, D., Y. Choquet, J.L. Popot, and D. Picot, 2003. An atypical haem in the cytochrome b(6)f complex. Nature, **426**(6965): p. 413-418.

26. Kurisu, G., H. Zhang, J.L. Smith, and W.A. Cramer, 2003. Structure of the cytochrome *b6f* complex of oxygenic photosynthesis: tuning the cavity. Science, **302**(5647): p. 1009-1014.

27. Scheller, H.V., P.E. Jensen, A. Haldrup, C. Lunde, and J. Knoetzel, 2001. Role of subunits in eukaryotic Photosystem I. Biochim Biophys Acta, **1507**(1-3): p. 41-60.

28. Chitnis, P.R., 1996. Photosystem I. Plant Physiol, **111**(3): p. 661-669.

29. Jordan, P., P. Fromme, H.T. Witt, O. Klukas, W. Saenger, and N. Krauss, 2001. Three-dimensional structure of cyanobacterial photosystem I at 2.5 A resolution. Nature, **411**(6840): p. 909-917.

30. Ben-Shem, A., F. Frolow, and N. Nelson, 2003. Crystal structure of plant photosystem I. Nature, **426**(6967): p. 630-635.

31.   Fromme, P., A. Melkozernov, P. Jordan, and N. Krauss, 2003. Structure and function of photosystem I: interaction with its soluble electron carriers and external antenna systems. FEBS Lett, **555**(1): p. 40-44.

32.   Noji, H., R. Yasuda, M. Yoshida, and K. Kinosita, Jr, 1997. Direct observation of the rotation of F1-ATPase. Nature, **386**(6622): p. 299-302.

33.   Wada, Y., Y. Sambongi, and M. Futai, 2000. Biological nano motor, ATP synthase F(o)F(1): from catalysis to gammaepsilonc(10-12) subunit assembly rotation. Biochim Biophys Acta, **1459**(2-3): p. 499-505.

34.   Boyer, P.D., 2000. Catalytic site forms and controls in ATP synthase catalysis. Biochim Biophys Acta, **1458**(2-3): p. 252-262.

35.   Groth, G. and E. Pohl, 2001. The structure of the chloroplast F1-ATPase at 3.2 A resolution. J Biol Chem, **276**(2): p. 1345-1352.

36.   Allen, J.F., 2002. Photosynthesis of ATP-electrons, proton pumps, rotors, and poise. Cell, **110**(3): p. 273-276.

37.   Scheer, H., 2003. The Pigments, in *Light-Harvesting Antennas in Photosynthesis*, B. Green and W. Parson, Editors. Kluwer Academic Publishers: Printed in The Netherlands.

38.   Green, B.R., J.M. Anderson, and W.W. Parson, 2003. Photosynthetic Membranes and Their Light-Harvesting Antennas., in *Light-Harvesting Antennas in Photosynthesis*, B. Green and W. Parson, Editors. Kluwer Academic Publishers: Printed in Netherlands. p. 1-28.

39.   Fromme, P., E. Schlodder, and S. Jansson, 2003. Structure and Function of the Antenna System in Photosystem I, in *Light-Harvesting Antennas in Photosynthesis*, B. Green and W. Parson, Editors. Kluwer Academic Publishers: Printed in The Netherlands. p. 253-279.

40.   Robert, B., R.J. Cogdell, and R. Grondelle, 2003. The Light-Harvesting System of Purple Bacteria, in *Light-Harvesting Antannas in Photosynthesis*, B. Green and W. Parson, Editors. Kluwer Academic Publishers: Printed in The Netherlands. p. 169-194.

41.   Gantt, E., B. Grabowski, and F.X. Cunningham, Jr, 2003. Antenna System of Red Algae: Phycobilisomes with Photosystem II and Chlorophyll Complexes with Photosystem I, in *Light-Harvesting Antennas in Photosynthesis*, B. Green and W. Parson, Editors. Kluwer Academic Publishers: Printed in The Netherlands. p. 307-322.

42.   Macpherson, A.N. and R.G. Hiller, 2003. Light-Harvesting Systems in Chlorophyll *c*-Containing Algae, in *Light-Harvesting Antennas in Photosynthesis*, B. Green and W. Parson, Editors. Kluwer Academic Publishers: Printed in The Netherlands. p. 323-352.

43.   Blankenship, R.E. and K. Matsuura, 2003. Antenna Complexes from Green Photosynthetic Bacteria, in *Light-Harvesting Antennas in Photosynthesis*, B. Green and W. Parson, Editors. Kluwer Academic Publishers: Printed in The Netherlands. p. 195-217.

44.   Sidler, W.A., 1994. Phycobilisome and Phycobiliprotein Structures, in *The Molecular Biology of Cyanobacteria*, D. Bryant, Editor. Kluwer Academic Publishers: Dordrecht. p. 139-216.

45.   Glazer, A.N., 1989. Light guides. Directional energy transfer in a photosynthetic antenna. J Biol Chem, **264**(1): p. 1-4.

46.   Grossman, A.R., L.G. van Waasberger, and D. Kehoe, 2003. Environmental Regulation of Phycobilisome Biosynthesis, in *Light-Harvesting Antennas in Photosynthesis*, B. Green and W. Parson, Editors. Kluwer Academic Publishers: Printed in Netherlands. p. 471-493.

47.   Tandeau de Marsac, N. and G. Cohen-Bazire, 1977. Molecular Composition of Cyanobacterial Phycobilisomes. Proc Natl Acad Sci U S A, **74**(4): p. 1635-1639.

48.   Elmorjani, K., J.-C. Thomas, and P. Sebban, 1986. Phycobilisomes of wild type and pigemnt mutants of the cyanobacterium *Synechocystis* PCC 6803. Arch Microbiol, **146**: p. 186-191.

49.   Schirmer, T., W. Bode, R. Huber, W. Sidler, and H. Zuber, 1985. X-ray crystallographic structure of the light-harvesting biliprotein C-phycocyanin from the thermophilic cyanobacterium Mastigocladus laminosus and its resemblance to globin structures. J Mol Biol, **184**(2): p. 257-277.

50.   Pastore, A. and A.M. Lesk, 1990. Comparison of the structures of globins and phycocyanins: evidence for evolutionary relationship. Proteins, **8**(2): p. 133-155.

51.   Schirmer, T., W. Bode, and R. Huber, 1987. Refined three-dimensional structures of two cyanobacterial C-phycocyanins at 2.1 and 2.5 A resolution. A common principle of phycobilin-protein interaction. J Mol Biol, **196**(3): p. 677-695.

52.   Koller, K.P., W. Wehrmeyer, and E. Morschel, 1978. Biliprotein assemble in the disc-shaped phycobilisomes of Rhodella violacea. On the molecular composition of energy-transfering complexes (tripartite units) forming the periphery of the phycobilisome. Eur J Biochem, **91**(1): p. 57-63.

53.   Lundell, D.J. and A.N. Glazer, 1983. Molecular architecture of a light-harvesting antenna. Quaternary interactions in the Synechococcus 6301 phycobilisome core as revealed by partial tryptic digestion and circular dichroism studies. J Biol Chem, **258**(14): p. 8708-8713.

54.   Ley, A.C., W.L. Butler, D.A. Bryant, and A.N. Glazer, 1977. The isolation and function of allophycocyanin B or Porphyridium cruentum. Plant Physiol, **59**: p. 974-980.

55.   Lundell, D.J. and A.N. Glazer, 1981. Allophycocyanin B. A common beta subunit in Synechococcus allophycocyanin B (lambda max 670 nm) and allophycocyanin (lambda max 650 nm). J Biol Chem, **256**(23): p. 12600-12606.

56.   Lundell, D.J., G. Yamanaka, and A.N. Glazer, 1981. A terminal energy acceptor of the phycobilisome: the 75,000-dalton polypeptide of *Synechococcus* 6301 phycobilisomes--a new biliprotein. J Cell Biol, **91**(1): p. 315-319.

57.   Yamanaka, G., D.J. Lundell, and A.N. Glazer, 1982. Molecular architecture of a light-harvesting antenna. Isolation and characterization of phycobilisome subassembly particles. J Biol Chem, **257**(8): p. 4077-4086.

58.   Ong, L.J. and A.N. Glazer, 1987. R-phycocyanin II, a new phycocyanin occurring in marine Synechococcus species. Identification of the terminal energy acceptor bilin in phycocyanins. J Biol Chem, **262**(13): p. 6323-6327.

59.   Bryant, D.A., 1981. The photoregulated expression of multiple phycocyanin species. A general mechanism for the control of phycocyanin synthesis in chromatically adapting cyanobacteria. Eur J Biochem, **119**(2): p. 425-429.

60.   Bryant, D.A. and G. Cohen-Bazire, 1981. Effects of chromatic illumination on cyanobacterial phycobilisomes. Evidence for the specific induction of a second pair of phycocyanin subunits in *Pseudanabaena* 7409 grown in red light. Eur J Biochem, **119**(2): p. 415-424.

61.   Bryant, D.A., 1982. Phycoerythrocyanin and phycoerythrin: Properties and occurrence in cyanobacteria. J Gen Microbiol, **128**: p. 835-844.

62.   Ong, L.J. and A.N. Glazer, 1991. Phycoerythrins of marine unicellular cyanobacteria. I. Bilin types and locations and energy transfer pathways in *Synechococcus* spp. phycoerythrins. J Biol Chem, **266**(15): p. 9515-9527.

63.   Swanson, R.V., L.J. Ong, S.M. Wilbanks, and A.N. Glazer, 1991. Phycoerythrins of marine unicellular cyanobacteria. II. Characterization of phycobiliproteins with unusally high phycourobilin content. J Biol Chem, **266**(15): p. 9528-9534.

64.   Wilbanks, S.M. and A.N. Glazer, 1993. Rod structure of a phycoerythrin II-containing phycobilisome. II. Complete sequence and bilin attachment site of a phycoerythrin gamma subunit. J Biol Chem, **268**(2): p. 1236-1241.

65.   Six, C., J.-C. Thomas, L. Thion, Y. Lemoine, F. Zal, and F. Partensky, 2005. Two novel phycoerythrin-associated linker proteins in the marine cyanobacterium *Synechococcus* sp. WH8102. J Bacteriol, **187**(5): p. 1685-1694.

66.   Yu, M.H. and A.N. Glazer, 1982. Cyanobacterial phycobilisomes. Role of the linker polypeptides in the assembly of phycocyanin. J Biol Chem, **257**(7): p. 3429-3433.

67.   Lundell, D.J., R.C. Williams, and A.N. Glazer, 1981. Molecular architecture of a light-harvesting antenna. In vitro assembly of the rod substructures of Synechococcus 6301 phycobilisomes. J Biol Chem, **256**(7): p. 3580-3592.

68.   Yu, M.H., A.N. Glazer, and R.C. Williams, 1981. Cyanobacterial phycobilisomes. Phycocyanin assembly in the rod substructures of *Anabaena variabilis* phycobilisomes. J Biol Chem, **256**(24): p. 13130-13136.

69.   Bald, D., J. Kruip, and M. Rögner, 1996. Supramolecular Architecture of Cyanobacterial Thylakoid Membranes: How is the Phycobilisome Connected with the photosystems? Photosynth Res, **49**: p. 103-118.

70.   Ajlani, G. and C. Vernotte, 1998. Deletion of the PB-loop in the L(CM) subunit does not affect phycobilisome assembly or energy transfer functions in the cyanobacterium *Synechocystis* sp. PCC6714. Eur J Biochem, **257**(1): p. 154-9.

71.   Capuano, V., J.-C. Thomas, N. Tandeau de Marsac, and J. Houmard, 1993. An in vivo approach to define the role of the LCM, the key polypeptide of cyanobacterial phycobilisomes. J Biol Chem, **268**(11): p. 8277-8283.

72.   Houmard, J., V. Capuano, M.V. Colombano, T. Coursin, and N. Tandeau de Marsac, 1990. Molecular characterization of the terminal energy acceptor of cyanobacterial phycobilisomes. Proc Natl Acad Sci U S A, **87**(6): p. 2152-2156.

73.   Capuano, V., A.S. Braux, N. Tandeau de Marsac, and J. Houmard, 1991. The "anchor polypeptide" of cyanobacterial phycobilisomes. Molecular characterization of the *Synechococcus* sp. PCC 6301 apce gene. J Biol Chem, **266**(11): p. 7239-7247.

74.   Reuter, W., C. Nickel, and W. Wehrmeyer, 1990. Isolation of allophycocyanin B from Rhodella violacea results in a model of the core from hemidiscoidal phycobilisomes of rhodophyceae. FEBS Lett, **273**(1-2): p. 155-158.

75.   Maxson, P., K. Sauer, J.H. Zhou, D.A. Bryant, and A.N. Glazer, 1989. Spectroscopic studies of cyanobacterial phycobilisomes lacking core polypeptides. Biochim Biophys Acta, **977**(1): p. 40-51.

76.   Yamanaka, G., A.N. Glazer, and R.C. Williams, 1980. Molecular architecture of a light-harvesting antenna. Comparison of wild type and mutant Synechococcus 6301 phycobilisomes. J Biol Chem, **255**(22): p. 11104-11110.

77.   Bryant, D.A., V.L. Stirewalt, M. Glauser, G. Frank, W. Sidler, and H. Zuber, 1991. A small multigene family encodes the rod-core linker polypeptides of *Anabaena* sp. PCC7120 phycobilisomes. Gene, **107**(1): p. 91-99.

78.   de Lorimier, R., D.A. Bryant, and S.E. Stevens, Jr, 1990. Genetic analysis of a 9 kDa phycocyanin-associated linker polypeptide. Biochim Biophys Acta, **1019**(1): p. 29-41.

79.   Bhalerao, R.P. and P. Gustafsson, 1994. Factors influencing the phycobilisome rod composition of the cyanobacterium *Synechococcus* sp. PCC 7942: Effects of reduced phycocyanin content, lack of rod-linkers and over-expression of the rod-terminating linker. Physiol Plant, **90**: p. 187-197.

80.   Yamanaka, G. and A.N. Glazer, 1981. Dynamic aspects of phycobilisome structure: modulation of phycocyanin content of *Synechococcus* phycobilisomes. Arch Microbiol, **130**: p. 23-30.

81.   Glazer, A.N., R.C. Williams, S.W. Yeh, and J.H. Clark, 1985. Kinetics of energy flow in the phycobilisome core. Science, **230**: p. 1051-1053.

82.   Glazer, A.N., S.W. Yeh, S.P. Webb, and J.H. Clark, 1985. Disk-to-disk transfer as the rate-limiting step for energy flow in phycobilisomes. Science, **227**: p. 419-423.

83.   Csatorday, K., R. MacColl, V. Csizmadia, J. Grabowski, and C. Bagyinka, 1984. Exciton interaction in allophycocyanin. Biochemistry, **23**(26): p. 6466-6470.

84.   MacColl, R., 2004. Allophycocyanin and energy transfer. Biochim Biophys Acta, **1657**(2-3): p. 73-81.

85.   Mimuro, M., C. Lipschultz, and E. Gantt, 1986. Energy flow in the phycobilisome core of *Nostoc* sp. (MAC): two independent terminal pigments. Biochim Biophys Acta, **852**(1): p. 126-132.

86.   Gindt, Y.M., J. Zhou, D.A. Bryant, and K. Sauer, 1994. Spectroscopic studies of phycobilisome subcore preparations lacking key core chromophores: assignment of excited state energies to the Lcm, beta 18 and alpha AP-B chromophores. Biochim Biophys Acta, **1186**(3): p. 153-162.

87.   Ashby, M.K. and C.W. Mullineaux, 1999. The role of ApcD and ApcF in energy transfer from phycobilisomes to PSI and PSII in a cyanobacterium. Photosynth Res, **61**: p. 169-179.

88.   Lönneborg, A., L.K. Lind, R. Kalla, P. Gustafsson, and G. Öquist, 1985. Acclimation processes in the light-harvesting system of the cyanobacterium *Anacystis nidulans* following a light shift from white to red. Plant Physiol, **78**: p. 110-114.

89.   Garnier, F., J.-P. Dubacq, and J.-C. Thomas, 1994. Evidence for a transient association of new proteins with the *Spirulina maxima* phycobilisome in relaton to light intensity. Plant Physiol, **106**: p. 747-754.

90.   Grossman, A.R., 1990. Chromatic adaptation and the events involved in phycobilisome biosynthesis. Plant Cell Environ, **13**: p. 651-666.

91.   Sobczyk, A., G. Schyns, N. Tandeau de Marsac, and J. Houmard, 1993. Transduction of the light signal during complementary chromatic adaptation in the cyanobacterium Calothrix sp. PCC 7601: DNA-binding proteins and modulation by phosphorylation. EMBO J, **12**(3): p. 997-1004.

92.   Mazel, D., G. Guglielmi, J. Houmard, W. Sidler, D.A. Bryant, and N. Tandeau de Marsac, 1986. Green light induces transcription of the phycoerythrin operon in the cyanobacterium *Calothrix* 7601. Nucleic Acids Res, **14**(21): p. 8279-8290.

93.   Conley, P.B., P.G. Lemaux, and A. Grossman, 1985. Cyanobacterial light-harvesting complex subunits encoded in two red light-induced transcripts. Science, **230**: p. 550-553.

94.   Casey, E.S. and A. Grossman, 1994. In vivo and in vitro characterization of the light-regulated *cpcB2A2* promoter of *Fremyella diplosiphon*. J Bacteriol, **176**(20): p. 6362-6374.

95.   Mazel, D. and P. Marlière, 1989. Adaptive eradication of methionine and cysteine from cyanobacterial light-harvesting proteins. Nature, **341**(6239): p. 245-248.

96.   Collier, J.L. and A.R. Grossman, 1992. Chlorosis induced by nutrient deprivation in *Synechococcus* sp. strain PCC 7942: not all bleaching is the same. J Bacteriol, **174**(14): p. 4718-4726.

97.   Collier, J.L. and A.R. Grossman, 1994. A small polypeptide triggers complete degradation of light-harvesting phycobiliproteins in nutrient-deprived cyanobacteria. EMBO J, **13**(5): p. 1039-1047.

98.   Richaud, C., G. Zabulon, A. Joder, and J.-C. Thomas, 2001. Nitrogen or Sulfur Starvation Differentially Affects Phycobilisome Degradation and Expression of the nblA Gene in Synechocystis Strain PCC 6803. J Bacteriol, **183**(10): p. 2989-2994.

99.   Luque, I., J.A.G. Ochoa de Alba, C. Richaud, G. Zabulon, J.-C. Thomas, and J. Houmard, 2003. The NblAI protein from the filamentous cyanobacterium *Tolypothrix* PCC 7601: regulation of its expression and interactions with phycobilisome components. Mol Microbiol, **50**(3): p. 1043-1054.

100.   Yamanaka, G. and A.N. Glazer, 1980. Dynamic aspects of phycobilisome structure. Phycobilisome turnover during nitrogen starvation in *Synechococcus* sp. Arch Microbiol, **124**: p. 39-47.

101.   Carrillo, N. and R.H. Vallejos, 1982. Interaction of ferredoxin-NADP oxidoreductase with the thylakoid membrane. Plant Physiol, **69**: p. 210-213.

102.   Aliverti, A., V. Pandini, and G. Zanetti, 2004. Domain exchange between isoforms of ferredoxin-NADP+ reductase produces a functional enzyme. Biochim Biophys Acta, **1696**(1): p. 93-101.

103.   Ceccarelli, E.A., A.K. Arakaki, N. Cortez, and N. Carrillo, 2004. Functional plasticity and catalytic efficiency in plant and bacterial ferredoxin-NADP(H) reductases. Biochim Biophys Acta, **1698**(2): p. 155-165.

104.   Sancho, J., M.L. Peleato, C. Gomez-Moreno, and D.E. Edmondson, 1988. Purification and properties of Ferredoxin-NADP$^+$ Oxidoreductase from the nitrogen-fixing cyanobactria *Anabaena variabilis*. Arch Biochem Biophys, **260**(1): p. 200-207.

105.   Scherer, S., I. Alpes, H. Sadowski, and P. Böger, 1988. Ferredoxin-NADP$^+$ Oxidoreductase is the respiratory NADPH Dehydrogenase of the cyanobacterium *Anabaena variabilis*. Arch Biochem Biophys, **267**(1): p. 228-235.

106.   Morales, R., M.H. Charon, G. Hudry-Clergeon, Y. Petillot, S. Norager, M. Medina, and M. Frey, 1999. Refined X-ray structures of the oxidized, at 1.3 A, and reduced, at 1.17 A, [2Fe-2S] ferredoxin from the cyanobacterium *Anabaena* PCC7119 show redox-linked conformational changes. Biochemistry, **38**(48): p. 15764-73.

107.   Yao, Y., T. Tamura, K. Wada, H. Matsubara, and K. Kodo, 1984. *Spirulina* ferredoxin-NADP+ reductase. The complete amino acid sequence. J Biochem, **95**(5): p. 1513-1516.

108.   Matsuo, M., T. Endo, and K. Asada, 1998. Properties of the respiratory NAD(P)H dehydrogenase isolated from the cyanobacterium Synechocystis PCC6803. Plant Cell Physiol, **39**(3): p. 263-7.

109.   Schluchter, W.M. and D.A. Bryant, 1992. Molecular characterization of ferredoxin-NADP+ oxidoreductase in cyanobacteria: cloning and sequence of the petH gene of

Synechococcus sp. PCC 7002 and studies on the gene product. Biochemistry, **31**(12): p. 3092-3102.

110.   van Thor, J.J., R. Jeanjean, M. Havaux, K.A. Sjollema, F. Joset, K.J. Hellingwerf , and H.C. Matthijs, 2000. Salt shock-inducible photosystem I cyclic electron transfer in Synechocystis PCC6803 relies on binding of ferredoxin:NADP(+)reductase to the thylakoid membranes via its CpcD phycobilisome-linker homologous N-terminal domain. Biochim Biophys Acta, **1457**(3): p. 129-144.

111.   Rogers, S., R. Wells, and M. Rechsteiner, 1986. Amino Acid Sequences Common to Rapidly Degraded Proteins: The PEST Hypothesis. Science, **234**: p. 364-368.

112.   van Thor, J.J., O.W. Gruters, H.C. Matthijs, and K.J. Hellingwerf, 1999. Localization and function of ferredoxin:NADP(+)reductase bound to the phycobilisomes of Synechocystis. EMBO J, **18**(15): p. 4128-4136.

113.   Gomez-Lojero, C., B. Perez-Gomez, G. Shen, W.M. Schluchter, and D.A. Bryant, 2003. Interaction of ferredoxin:NADP+ oxidoreductase with phycobilisomes and phycobilisome substructures of the cyanobacterium *Synechococcus* sp. strain PCC 7002. Biochemistry, **42**(47): p. 13800-13811.

114.   Morand, L.Z., R.H. Cheng, D.W. Krogman, and K.K. Ho, 1994. Soluble electron transfer catalysts of cyanobacteria, in *The Molecular Biology of Cyanobacteria*, D.A. Bryant, Editor. Kluwer Academic Publishers: Dordrecht. p. 381-407.

115.   González De La Vara, L. and C. Gómez-Lojero, 1986. Participation of plastoquinone, cytochrome c_{553} and ferredoxin-NADP$^+$ oxido-reductase in both photosynthesis and respiration in *Spirulina maxima*. Photosynth Res, **8**: p. 65-67.

116.   van Thor, J.J., K.J. Hellingwerf , and H.C. Matthijs, 1998. Characterization and transcriptional regulation of the *Synechocystis* PCC 6803 petH gene, encoding ferredoxin-NADP+ oxidoreductase: involvement of a novel type of divergent operator. Plant Mol Biol, **36**(3): p. 353-363.

117.   Allen, M.M., 1968. Simple conditions for growth of unicellular blue-green algae on plates. J Phycol, **4**: p. 1-4.

118.   Sambrook, J., E.F. Fritsch, and T. Maniatis, 1989. Molecular Cloning: a Laboratory Manual. 2 ed. NY: Cold Spring Harbor Laboratory Press: Cold Spring Harbor.

119.   Cai, Y. and C.P. Wolk, 1990. Use of a conditionally lethal gene in *Anabaena* sp. strain PCC 7120 to select for double recombinants and to entrap insertion sequences. J Bacteriol, **172**: p. 3138-3145.

120.   Lagarde, D., L. Beuf, and W. Vermaas, 2000. Increased production of zeaxanthin and other pigments by application of genetic engineering techniques to *Synechocystis* sp. strain PCC 6803. Appl Environ Microbiol, **66**(1): p. 64-72.

121.   Oka, A., H. Sugisaki, and M. Takanami, 1981. Nucleotide sequence of the kanamycin resistance transposon Tn*903*. J Mol Biol, **147**: p. 217-226.

122.   Golden, J.W. and D.R. Wiest, 1988. Genome rearrangement and nitrogen fixation in *Anabaena* blocked by inactivation of *xisA* gene. Science, **242**: p. 1421-1423.

123.   Prentki, P. and H.M. Krisch, 1984. In vitro insertional mutagenesis with a selectable DNA fragment. Gene, **29**: p. 303-313.

124.   Aiba, H., S. Adhya, and B. de Crombrugghe, 1981. Evidence for two functional *gal* promoters in intact *Escherichia coli* cells. J Biol Chem, **256**: p. 11905-11910.

125.   Vioque, A., 1992. Analysis of the gene encoding the RNA subunit of ribonuclease P from cyanobacteria. Nucl Acids Res, **20**: p. 6331-6337.

126.   Ajlani, G., C. Vernotte, L. DiMagno, and R. Haselkorn, 1995. Phycobilisome core mutants of *Synechocystis* sp. PCC 6803. Biochim Biophys Acta, **1231**: p. 189-196.

127.   Glazer, A.N., 1988. Phycobilisomes. Methods Enzymol, **167**: p. 304-312.

128.   Fling, S.P. and D.S. Gregerson, 1986. Peptide and protein molecular weight determination by electrophoresis using a high-molarity tris buffer system without urea. Anal Biochem, **155**: p. 83-88.

129.   Bruce, D., S. Brimble, and D.A. Bryant, 1989. State transitions in a phycobilisome-less mutant of the cyanobacterium *Synechococcus* sp. PCC 7002. Biochim Biophys Acta, **974**: p. 66-73.

130.   Rogner, M., P.J. Nixon, and B.A. Diner, 1990. Purification and characterization of photosystem I and photosystem II core complexes from wild-type and phycocyanin-deficient strains of the cyanobacterium *Synechocystis* PCC 6803. J Biol Chem, **265**(11): p. 6189-6196.

131.   Plank, T. and L.K. Anderson, 1995. Heterologous assembly and rescue of stranded phycocyanin subunits by expression of a foreign *cpcBA* operon in Synechocystis sp. strain 6803. J Bacteriol, **177**(23): p. 6804-6809.

132.   Imashimizu, M., S. Fujiwara, R. Tanigawa, K. Tanaka, T. Hirokawa, Y. Nakajima, J. Higo, and M. Tsuzuki, 2003. Thymine at -5 is crucial for cpc promoter activity of *Synechocystis* sp. strain PCC 6714. J Bacteriol, **185**: p. 6477-6480.

133.   Belknap, W.R. and R. Haselkorn, 1987. Cloning and light regulation of expression of the phycocyanin operon of the cyanobacterium *Anabaena*. EMBO J, **6**: p. 871-884.

134.   Rauhut, R. and G. Klug, 1999. mRNA degradation in bacteria. Microbiol Rev, **23**: p. 353-370.

135.   Mohamed, A. and C. Jansson, 1989. Influence of light on accumulation of photosynthesis-specific transcripts in the cyanobacterium *Synechocystis* 6803. Plant Mol Biol, **13**(6): p. 693-700.

136.   Bhalerao, R.P., T. Gillbro, and P. Gustafsson, 1991. Structure and energy transfer of the phycobilisome in a linker protein replacement mutant of cyanobacterium *Synechococcus* 7942. Biochim Biophys Acta, **1060**(1): p. 59-66.

137. Bhalerao, R.P., L.K. Lind, C.E. Persson, and P. Gustafsson, 1993. Cloning of the phycobilisome rod linker genes from the cyanobacterium *Synechococcus* sp. PCC 6301 and their inactivation in *Synechococcus* sp. PCC 7942. Mol Gen Genet, **237**(1-2): p. 89-96.

138. Mohamed, A. and C. Jansson, 1991. Photosynthetic electron transport controls degradation but not production of *psbA* transcripts in the cyanobacterium *Synechocystis* 8803. Plant Mol Biol, **16**(5): p. 891-897.

139. Mohamed, A., J. Eriksson, H.D. Osiewacz, and C. Jansson, 1993. Differential expression of the *psbA* genes in the cyanobacterium *Synechocystis* 6803. Mol Gen Genet, **238**(1-2): p. 161-168.

SUMMARY

Phycobilisome assembly in *Synechocystis* sp. strain PCC6803

Cyanobacteria are prokaryotes that perform oxygenic photosynthesis. Photosynthesis starts with the absorption of light energy by specialized macromolecular complexes, called antennae. In cyanobacteria and red-algae the phycobilisome (PBS) harvests light energy for photosynthesis. The PBS is a huge protein complexes (5-10 x 10^6 Da), twice as big as the ribosome. The light energy, is used for the generation of NADPH and ATP. Energy transfer in PBS is unidirectional and its efficiency approaches 95 %. This supramolecular complex is composed of two main structural elements: a core substructure, and the peripheral rods. The main part of the PBS consists of the chromophore-containing phycobiliproteins, which are attached by smaller amount of color-less linker polypeptides. Phycobiliproteins are soluble proteins containing open-chain tetrapyrroles, known as phycobilins. The fundamental assembly units of PBS are trimeric or hexameric aggregates of phycobiliporteins. Two main questions arise regarding the structure and function of the PBS. One is how this huge protein complex assembles, the other is how its structure allows such efficient energy transfer. It is believed that the linker polypeptides have important function in these processes. The linker polypeptides induces face-to-face aggregation of phycobiliprotein trimers and cause the tail-to-tail joining of hexamers. Linker polypeptides modulate the spectral properties of the phycobiliproteins, and these small spectral changes may support the unidirectional transfer of excitation energy from the rod periphery to the core of the PBS.

The PBS of the cyanobacterium *Synechocystis* PCC6803, which was the target of our investigations, consists of a three-cylindrical core from which six rods radiate. Each rod is composed of three stacked phycocyanin (PC) hexamers. In this strain two independent genes, *cpcG1* and *cpcG2*, encode the rod-core linker (LRC) that binds the proximal PC-hexamer to the core. The remaining rod-subunit-encoding genes are clustered in the *cpc* operon. This operon contains five genes, *cpcB* and *cpcA* (encoding the β^{PC} and α^{PC} subunits respectively), and *cpcC2*, *cpcC1* and *cpcD* (encoding the rod linkers LR30, LR33 and LR10, respectively).

The ferredoxin-NADP(H)-oxidoreductase (FNR) catalyzes the electron transfer between ferredoxin and NADP$^+$ in the last steps of photosynthesis. Two isoforms of the FNR have been detected in *Synechocystis* PCC6803 cells: a 46.3 kDa FNR that is associated to the

PBS and a soluble 34.3 kDa FNR. It is widely accepted that the 34.3 kDa isoform is produced by the proteolysis of the 46.3 kDa isoform of the FNR. Since the N-terminal amino-acid sequence of the 34.3 kDa FNR begins with methionine, which could be alternative translational event. The FNR participates in important physiological processes such as respiration and photosynthesis, and it is essential for the cells. The exact role of the two isiforms in the different processes is not known. The N-terminal domain of the 46.3 kDa FNR is similar to LR10, therefore it is believed to share the same binding site on the core-distal end of the rods.

In our work we set as an aim to understand the role of the rod-linker polypeptides in the PBS assembly in *Synechocystis* PCC6803. We studied the linker deficiency on the phycobiliprotein synthesis and the effect of Km (kanamycin resistance) and Ω (spectinomycin and streptomycin resistance) cassettes insertion on the transcription of the *cpc* operon. We examined whether the 34.3 kDa FNR is generated by proteolysis or by alternative translation. Furthermore we wished to determine the function of the two isoforms of the FNR, and we studied the localization of the FNR in relation to PBS, using molecular genetic and biochemical approaches.

In order to study the roles of the rod linkers we generated and characterized interposon mutants in the three rod-linker genes located in the *cpc* operon of *Synechocystis* PCC6803. We studied the fluorescence emission spectra of the wild-type and mutant cells, and analyzed the absorption spectra and protein composition of their PBSs. With the characterization of the PBS assembly process in the mutants we were able to deduce the sequential order of PBS-rod biogenesis in *Synechocystis* PCC6803.

Our results clearly demonstrated that the rod linkers are incorporated in a precise order during the biogenesis of the PBS rods; i. e. following the attachment of the core-proximal PC-hexamer by the LRC, only LR33 can bind the intermediary PC-hexamer, whereas only the LR30 attaches the distal PC-hexamer. Our data strongly suggest that the function of LR33 and LR30 are not interchangeable. Our model is in a good agreement with results obtained upon nitrogen starvation, where sequential loss of PC and associated linkers occurs, and LR30 disappears first from the PBS during the initial steps of nitrogen starvation.

We found that LR10 was present in PBSs lacking either the core-distal or both the intermediary and the core-distal PC-hexamers, however in smaller amounts. The reduced level of LR10 was first attributed only to the polar effect of the Km cassette on the expression of LR10 encoding *cpcD* in these strains. The loss of LR10 did not affect PBS assembly or function. Over-expression of this linker polypeptide in mutant strains in which *cpcD* was under the control of the highly active *psbAII* promoter indicate that when LR10 is produced *in trans* proteolysis prevents its association to the PBS. It is known, that linker polypeptides are highly sensitive to proteolysis when they are not associated to phycobiliproteins.

Fluorescence emission spectra of whole cells and the sucrose-gradient pattern of the PBS preparations indicated the presence of free PC in the rod-linker deficient strains. These observations demonstrate that under our culture condition, PC biosynthesis was not down-regulated in the absence of the rod-linker polypeptides.

In *cpc* operon mutants, containing Km cassette insertion, the PBS contained smaller amount of the linker polypeptides encoded by the genes located downstream from the inactivated gene. Therefore we examined whether this was due to the absence of the inactivated gene product or to the polar effect of the insertion. The Km cassette is commonly used for gene inactivation, but it was not measured in cyanobacteria how its insertion affects expression of adjacent genes. By monitoring steady state RNA levels in the mutants, we demonstrated that the insertion affected the gene expression in its vicinity regardless of orientation. The wild-type *cpc* operon generates three transcripts from one transcription initiation site. The most abundant 1.6 kb transcript contains only *cpcB* and *cpcA*. Two larger, less abundant transcripts, contain in addition PC subunits genes, LR30 and LR33 encoding *cpcC2* and *cpcC1* or these plus the LR10 encoding *cpcD*, respectively. The sizes and relative abundance of these transcripts varied in the mutants. Their low amounts demonstrate that the insertion of the Km cassette destabilizes the rod-linker transcripts. This is the reason why we found weaker incorporation of the flanking genes products into the PBS. Using Km-specific probe we detected transcripts, which were the products of read-through transcription from the *aphI* promoter driving Km expression. When the Km cassette was inserted in an opposite orientation to the operon transcription, the presence of an anti-sense mRNA effect was demonstrated. In such a case complementary mRNA can annealed to the original transcript, thereby preventing the translation of upstream genes.

99

We constructed two LR10 less-strains. In one the Ω cassette was inserted into the LR10 encoding *cpcD* gene, while in the other insertion took place upstream of *cpcD*, destroying a stem-loop structure. The PBS of the latter mutant contained slightly lesser PC than the other LR10-less strain and the wild type, which could be due to the destabilization of the linker-encoding mRNA. This observation suggests that the Ω terminator does not provide a 3' stabilizing effect to the transcript.

We demonstrated by Northern-blot analysis and RT-PCR that both LRC encoding *cpcG1* and *cpcG2* genes are transcribed. In the PBS structure formation only the *cpcG1* encoded LRC participates, since inactivation of *cpcG1* prevented the PC attachment to the core, while inactivation of *cpcG2* did not alter the PBS composition.

Site directed mutations of the *petH* gene, encoding the FNR, were constructed to identify the function of the two isoforms of the FNR. Analysis of the FNR encoding *petH* gene sequence indicates two other translational starts after the first methionine, valine 112 and methionine 113. In order to determine whether these sites are functional initiation sites, mutant strains I and V were constructed, in which methionine 113 (M113) was replaced by isoleucine, and valine 102 (V102) was changed to a non-initiating valine. SDS-PAGE analysis of the purified PBSs from these strains confirmed that they have assembled PBS with the FNR attached, similar to the PBS of the wild type. The FNR content of whole cell extracts from the mutant strains and wild-type cells was detected by Western-blot analysis using *Synechocystis* PCC6803 FNR antibodies. The I mutant strain contained only the 46.3 kDa isoform of the FNR. The lack of the 34.3 kDa protein in this strain supports the idea of an alternative initiation site corresponding to M113. On the other hand the replacement of the methionine to isoleucine may also prevent the proteolysis if the methionine is a specific site of the proteolysis. To confirm our hypothesis, we constructed two frame-shift mutant strains in which stop codons were created either at the codon 110 or 113, without the alteration of the ATG code of the original M113. In these strains translation from the first methionine is interrupted, but translation from methionine 113 is still allowed if it is a real initiation site. The frame-shift containing strains were able to segregate and they contained only the 34.3 kDa form of the FNR, suggesting that our hypothesis was correct. That means the 34.3 kDa form of the FNR, in contrast to the earlier assumptions, is not produced by the proteolysis of the 46.3 kDa form. We proved that the two isoforms of FNR are the products of different translation initiation sites.

The PBS of the LR10-less mutant strains contained the same amount of FNR as the wild-type PBS, and the FNR did not co-purify with the core-complex of the PBS. Therefore we suggest that FNR and LR10 do not share the same binding site, and the FNR it is not able to bind directly to the core, but it is located in a core-proximal position on the rods.

We were able to answer several questions related to PBS biogenesis and the existence of two FNR isoforms. On the other hand further over-expression experiments with LR10, considering the instability of the protein, might be essential to elucidate the function of this linker. The structure of the PBS of the LR10 mutant strains analyzed by electron microscopy might uncover the function of the LR10 in the termination of the rod growth.

It is interesting that, although, both LRC encoding genes are transcribed in *Synechocystis* PCC6803, only the *cpcG1* encoded LRC participates in the formation of PBS structure. The absence of Shine-Dalgarno sequence from the 5'-region of *cpcG2* may prevent the translation from this gene. Translational fusion of *cpcG2* with the promoter of *psbAII* might elucidate whether this is the reason for which *cpcG2* did not participate in the PBS structure. The construction of this mutant strain is in progress. *Synechococcus* WH8102 has also two rod-core linker encoding genes, but in this case both gene products were detected in the PBS. It would be interesting to study the function of these two LRCs in the PBS structure of *Synechococcus* WH8102.

It is still an open question whether the two isoforms of the FNR have different functions, like in the higher plants leave and root FNRs. Our FNR mutant strains provide good experimental background for studying of the role of each of the two FNR isoforms. The wild type contains both forms, mutant I contains only 46.3 kDa form, and the frame-shift mutant strains contain only the 34.3 kDa form. Characterization of these mutant strains could indicate how the absence of each FNR form can affect electron transport. In the wild type it is possible to study which form is more abundant and how the ratio between these two forms affected under specific condition. It would be also interesting to purify each of the two isoforms, the 46,3 kDa isoform attached to a PC-hexamer and the free 34,3 kDa isoform in order to characterize their enzymatic activity in vitro. These investigations might further elucidate the physiological role of each FNR isoform.

ÖSSZEFOGLALÁS

Synechocystis PCC6803 cianobaktérium fikobiliszóma rúdkötőfehérje és FNR mutánsok vizsgálata

A cianobaktériumok oxigén-termelő fotószintetizáló szervezetek, melyek több milliárd évvel ezelőtt jöttek létre a Földön. A fotoszintézis folyamatának köszönhető a Földet az UV sugárzástól védő ózonréteg kialakulása, a légkörünkben található oxigén és a Földön található szerves anyag nagy részének megjelenése. A fotoszintézis a napfény energiájának begyűjtésével kezdődik, amit úgynevezett fénybegyűjtő antenna fehérje-komplexek, a cianobaktérium sejtek esetében egy szupramolekuláris fehérje komplex, a fikobiliszóma végzi. A fikobiliszóma továbbítja a fotonok energiáját a fotoszintetikus apparátus reakciócentrumaiba, ahol a fényenergia kémiai energiává alakul át. Ez a hatalmas, körülbelül 5-20 x 10^6 Da tömegű fehérje komplex, mely 95 %-os hatékonysággal továbbítja a begyűjtött energiát, főként fikobiliproteinekből áll. A fikobiliproteinekben kovalensen kötött pigment molekula, nyílt láncú tetrapirrol, a fikobilin található. Minden fikobiliszóma stabilis alapegysége a trimerekbe és hexamerekbe szerveződött fikobiliprotein oligomer. A fikobiliszóma két fő szerkezeti egységét különböztethetjük meg, a magot és a róla elágazó rudakat. Az általunk vizsgált *Synechocystis* PCC6803 cianobaktérium törzsben a magot három, allofikocianin trimerekből álló henger alkotja, melyhez hat rúd kapcsolódik. A rudak három fikocianin hexamerből épülnek fel. A fikobiliszóma szerkezetével és működésével kapcsolatban két fő kérdés merül fel. Az egyik, hogyan áll össze ez a hatalmas komplex szerkezet; a másik, hogyan lehetséges ilyen nagy hatékonyságú energiatovábbítás ennyire korlátozott számú pigment és fehérje segítségével. A kevésbé ismert, úgynevezett kötőfehérjéknek lehet ezekben a folyamatokban meghatározó szerepük. Ezek a fehérjék indukálják a trimerek fej-fej kapcsolódását, valamint összetartják a hexamereket, ezáltal fontos szerepet töltenek be a fikobiliszóma szerkezetének kialakításában. A fikobiliproteinek spektroszkópiai tulajdonságainak módosításával kiemelkedő szerepük van az egyenletes energiatovábbításban is.

A *Synechocystis* PCC6803 cianobaktérium törzsben az első fikocanin hexamert a rúd-mag kötőfehérje kapcsolja a maghoz és további fikocianin hexamerek rudakhoz való kapcsolódásában a 33 és 30 kDa molekuláris tömegű rúdkötőfehérjéknek van szerepe. A rúd-mag kötőfehérjét két gén a *cpcG1* és *cpcG2* kódolja, melyek működését korábban nem vizsgálták. Nem ismert, hogy a különböző gének által kódolt rúd-mag kötőfehérjék

egymástól eltérő szerepet töltenek-e be. A rúdkötőfehérjéket kódoló gének a fikocianin alegységeit is kódoló *cpc* operonon találhatóak. Ezen az operonon öt gén található, a fikocianin β és α alegységét kódoló *cpcB* és *cpcA*, valamint a 30, 33 és 10 kDa-os rúdkötőfehérjéket kódoló *cpcC2*, *cpcC1* és *cpcD* gének. Az első fikocianin hexamer maghoz történő kapcsolódása után a további két fikocianin hexamer kapcsolódása két módon lehetséges. Az egyik lehetőség, a 33 és a 30 kDa-os kötőfehérjék felcserélhetők és bármelyik kapcsolhatja a középső, illetve a magtól távolabbi fikocianin hexamert. A másik lehetőség szerint a középső fikocianin hexamer kizárólag az egyik, míg a magtól távolabbi pedig csak a másik kötőfehérjét tartalmazza. A 10 kDa-os kis rúdkötőfehérjét még nem vizsgálták *Synechocystis* PCC6803 cianobaktériumban. Más cianobaktériumokon történt vizsgálatok alapján feltételezik, hogy a 10 kDa-os kötőfehérje a rudak végéhez kapcsolódik és a rudak egyforma hosszúságáért felelős.

A fikbiliszóma által begyűjtött fényenergiát a fotoszintetikus rendszer NADPH és ATP szintézisében hasznosítja. A fotoszintézis utolsó szakaszában a ferredoxin és a $NADP^+$ között az elektron átmenetet a ferredoxin-NADP(H)-oxidoreduktáz (FNR) katalizálja. Az FNR-t a *petH* gén kódolja. A *Synechocystis* PCC6803-ban az FNR-nak két formája található meg: a fikobiliszómához kapcsolódó 46,3 kDa-os forma és a szabad 34,3 kDa-os forma. Széles körben elfogadott, hogy a 34,3 kDa-os forma a 46,3 kDa-os forma lebontásával keletkezik. Lehetséges azonban, hogy a 34,3 kDa-os forma egy alternatív fehérjeátírás terméke, mivel ennek a fehérjének az N-terminális vége metioninnal kezdődik, mely a fehérjék átírásának kezdő kódja. A fikobiliszómához kötődő 46,3 kDa-os FNR-nak az N-terminális vége a 10 kDa-os kis rúdkötőfehérjével nagy hasonlóságot mutat. Emiatt a hasonlóság miatt feltételezik, hogy az FNR a kis rúdkötőfehérjével versenyben a rudak végéhez kapcsolódik; de az is felmerült, hogy az FNR közvetlenül a fikobiliszóma mag részéhez képes kapcsolódni.

Munkánk során célul tűztük ki, hogy meghatározzuk a különböző kötőfehérjék szerepét a fikobiliszóma rudak felépítésében, és a fikobiliproteinek szintézisében. Megvizsgáltuk azt is, hogy a széles körben használt Km (kanamicin rezisztencia) és Ω (spektinomicin és sztreptomicin rezisztencia) kazetta operonba történő beépítése miként befolyásolja az operonon kódolt gének átírását. Megvizsgáltuk az FNR fikobiliszómához való kötődését, valamint a 34,3 kDa-os forma képződését.

Molekuláris genetikai módszerek alkalmazásával, különböző fikobiliszóma rúdkötőfehérje mutánsokat hoztunk létre azért, hogy tanulmányozzuk a kötőfehérjék

szerepét a *Synechocystis* PCC6803 cianobaktériumban. Megvizsgáltuk a vadtípusú és a mutáns sejtek fluoreszcenciáját. Összehasonlítottuk a vadtípusból és a mutánsokból izolált fikobiliszóma komplexek abszorpciós spektrumát, és SDS poliakrilamid gélen megvizsgáltuk a fehérje-összetételüket. Így meghatároztuk a különböző rúdkötőfehérjék szerepét a fikobiliszóma biogenezisében és működésében. Vizsgálatainkkal bizonyítottuk, hogy a fikobiliszóma rudak felépülésekor a kötőfehérjék meghatározott sorrendben követik egymást. Az első fikocianin hexamer rúd-mag kötőfehérje által a maghoz történő kapcsolódása után a 33 kDa-os kötőfehérje kapcsolja a rudakhoz a második fikocianin hexamert, és csak ezután képes a 30 kDa-os kötőfehérje a harmadik, a rudak magtól távolabbi végén elhelyezkedő fikocianin hexamert beépíteni. A 33 és 30 kDa-os rúdkötőfehérjék nem helyettesítik egymást a fikobiliszóma rudak felépítésében. Eredményünk összhangban van nitrogén éheztetés során tapasztaltakkal, amikor legelőször a magtól távolabbi fikocianin hexamer és a 30 kDa-os kötőfehérje lebomlását majd ezt követően a következő fikocianin hexamer és a 33 kDa-os kötőfehérje lebomlását figyelték meg.

A 10 kDa-os rúdkötőfehérje hozzákapcsolódott azoknak a rúdkötőfehérje mutánsoknak a fikobiliszómáihoz is melyek rúdjai csak egy vagy két fikocianin hexamerből álltak. A mutánsok azonban kisebb mennyiségben tartalmazták a kis rúdkötőfehérjét, mint a vadtípus; amit kezdetben csak a beépített Km kazetta hatásával magyaráztunk. Ugyanakkor az, hogy nagyobb mennyiségben tartalmazta a kis rúdkötőfehérjét annak a Km kazettát is tartalmazó mutánsnak a fikobiliszómája, melyben a 33 és a 30-as kötőfehérje is jelen volt, mint amelyikben csak a 33-as kötőfehérje volt jelen azt bizonyította, hogy a kis rúdkötőfehérjének nagyobb az affinitása a 30 mint a 33 kDa-os kötőfehérjét tartalmazó fikocianin hexamerekhez. A kis rúdkötőfehérje hiányos mutáns nem mutatott különbséget a vadtípushoz képest. Ezért túltermeltettük a kis rúdkötőfehérjét, hogy meghatározzuk a szerepét. A mutánsok melyekben a kis rúdkötőfehérjét a *psbAII* promóter kontrolja alá helyeztük azt mutatták, hogy a transz visszahelyezett gén terméke gyorsan lebomlik. Ismert, hogy a kötőfehérjék érzékenyek a proteolízisre amíg nem kapcsolódnak a fikobiliproteinekhez.

A kötőfehérjék mennyisége meghatározza a fikobiliszómába beépülő fikobiliproteinek mennyiségét és ezáltal a fotoszintetikus apparátushoz történő energiatovábbítás hatékonyságát. Szabad, a fikobiliszómához nem kapcsolódó, fikocianinok jelenléte a különböző rúdkötőfehérje mutánsokban azt bizonyította, hogy ezeknek a kötőfehérjéknek a hiánya nem befolyásolja a fikocianin bioszintézist.

A mutánsaink szelektáláshoz Km és Ω kazettát használtunk. A mutánsaink fikobiliszómája a Km kazetta beépítésekor kisebb mennyiségben tartalmazta az inaktivált gén után kódolt fehérjéket, ami az adott kötőfehérje hiányának, vagy a beépített Km kazetta hatásának a következménye lehetett. A Km kazettát széles körben használják, de nem vizsgálták miként hat a beépítése az inaktivált gén környezetében elhelyezkedő gének átírására. A *cpc* operonról átíródó mRNS-ek méretének és mennyiségének Northern-blot analízisével kimutattuk, hogy a kanamicin rezisztencia kazetta genomba történő beépítése orientációjától függetlenül hatással lehet más, a beépítés által közvetlenül nem érintett gén expressziójára. A *cpc* operonról három mRNS íródik át. Legnagyobb mennyiségben az 1,6 kb-os, a *cpcB* és *cpcA* gént tartalmazó mRNS íródik át. A két hosszabb mRNS közül az egyik a fikocianin alegységeit kódoló gének mellett a 33 és a 30 kDa-os kötőfehérjék szekvenciáit, míg a másik mindezeken felül még a 10 kDa-os kötőfehérje kódoló szekvenciáját is tartalmazza. Ennek az utóbbi két mRNS-nek a mérete és a mennyisége is változott a rúdkötőfehérje mutánsokban. A Km kazetta a rúdkötőfehérjéket tartalmazó transzkriptumok stabilitását csökkentette. Km kazetta specifikus próbával az *aphI* promoterétől kiinduló és a kazettán túlnyúló transzkriptumokat mutattunk ki. Így amennyiben a Km kazetttát az átírással ellentétes irányban helyezzük antiszensz mRNS hatással is számolnunk kell. Vagyis az ellentétes irányban átíródó mRNS hozzákötődhet az eredetileg átíródó mRNS-hez, ezáltal akadályozva a fehérjeátírást és így az inaktivált gén előtt elhelyezkedő gének által kódolt fehérjék mennyiségét is lecsökkentheti. Két kis rúdkötőfehérje hiányos mutánst hoztunk létre, az egyikben közvetlenül a kis rúdkötőfehérjét kódoló génbe építettük be az Ω kazettát, míg a másikban az Ω kazettát a kódoló gén elé építettük be elrontva ezzel az egyik *cpc* operonról átíródó mRNS 3' stabilizáló szerkezetét. Ez utóbbi mutáns fikobiliszómája kevesebb fikocianint tartalmazott mint a vadtípus és a másik kis rúdkötőfehérje mutáns. Ennek oka az érintett mRNS csökkent stabilitása lehetett, ezért arra a következtetésre jutottunk, hogy az Ω kazettának nincsen 3' stabilizáló hatása.

RT-PCR-al és Northern-blot analízissel bizonyítottuk, hogy a vadtípusú sejtekben mindkét rúd-mag kötőfehérjét kódoló *cpcG1* és *cpcG2* génről íródik át mRNS. A fikobiliszóma szerkezetének kialakításában azonban csak a *cpcG1* által kódolt fehérjének van szerepe, hiszen amikor ezt a gént inaktiváltuk a rudak nem kapcsolódtak a fikobiliszóma mag részéhez. Ugyanakkor a *cpcG2* gén inaktiválása nem befolyásolta a fikobiliszóma szerkezetét.

Az FNR 34,3 kDa-os formájáról általánosan elfogadott, hogy a 46,3 kDa-os forma lebomlásával keletkezik. Az FNR-t kódoló *petH* gént megvizsgálva azonban két olyan aminosav kódot találtunk az első metionin után melyek lehetnek fehérje átírásának kezdő kódjai: a valin 102 melyet GTG kódol és a metionin 113 melyet ATG kódol. A V mutánsban a valin 102 kódját kicseréltük szintén valint kódoló GTC kódra, mely azonban nem fehérje átírást kezdő kód. Az I mutánsban a metionin 113 ATG kódját kicseréltük ATC-re mely nem fehérje átírást kezdő kód és izoleucint kódol. A vadtípus és a mutánsok FNR tartalmát Western-blot analízissel vizsgáltuk. A vadtípus és a V mutáns mindkét FNR formát tartalmazta, a 46,3 kDa-os formát nagyobb és a 34,3 kDa-os formát kisebb mennyiségben. Az I mutáns csak a 46,3 kDa-os formát tartalmazta, mely jelezheti azt, hogy a metionin 113 egy második fehérje átírás kezdő pontja. Amennyiben a metionin 113 a fehérje bontás specifikus helye, akkor a metionin lecserélése izoleucinra megakadályozhatja a fehérjelebontást, ami szintén lehet a magyarázata annak, hogy csak a nagyobb forma van jelen az I mutánsban. Ezért annak érdekében, hogy bizonyítsuk a metionin 113 fehérjeátírást kezdő kód olyan mutánsokat hoztunk létre az eredeti metionin 113 kódjának megváltoztatása nélkül, melyek közül az egyikben egy citozin beépítésével a *petH* génbe, a 110. kód stop kód lesz; illetve a másikban a *petH* gén egy citozinjának eltávolításával a 113. kód lesz a stop kód. Ebben a két mutánsban így az első metionintól induló fehérje átírás leáll a stop kódnál, de amennyiben a metionin 113 fehérje átírás kezdő kódja, akkor tőle kiindulva íródhat át fehérje. Ezekben a mutánsokban detektáltuk a 34,3 kDa-os FNR-t, vagyis a metionin 113-tól kiindulva történik fehérje átírás a *petH* génről. Ezzel bizonyítottuk, hogy minden korábbi feltételezéssel ellentétben a 34,3 kDa-os formája az FNR-nak *Synechocystis* PCC6803 cianobaktériumban nem a 46,3 kDa-os formájának a lebomlásával keletkezik, hanem egy a *petH* génről történő második fehérjeátírás terméke.

Az FNR ugyanolyan mennyiségben volt megtalálható a különböző fikobiliszóma rúd mutánsokból tisztított fikobiliszóma mintákban, mint a vadtípusúban, de nem volt jelen a csak fikobiliszóma mag-komplexet tartalmazó mintákban. Ez azt bizonyította, hogy az FNR nem képes közvetlenül a maghoz kapcsolódni, ugyanakkor nem is a kis rúdkötőfehérjével van versenyben ugyanazon kötőhelyért, hanem feltehetően a rudak maghoz közelebbi részén kötődik a rudakhoz.

Vizsgálataink során tehát több korábban nyitott kérdést sikerült megválaszolnunk, ugyanakkor további vizsgálatok szükségesek a kis rúdkötőfehérje szerepének meghatározásához, melyben a kis rúdkötőfehérje a *cpc* operon közelében történő

túltermeltetése segíthet. A különböző körülmények között nevelt túltermeltetett, illetve a hiányos mutáns és a vadtípus fikobiliszómájának vizsgálata adhat információt, valamint elektron mikroszkópos felvételek bizonyíthatják, hogy a kis rúdkötőfehérje valóban felelős az egységes rúdhosszakért.

Továbbra is nyitott kérdés vajon miért nem játszik szerepet a *cpcG2* gén által kódolt rúd-mag kötőfehérje a fikobiliszóma felépítésében annak ellenére, hogy RNS átírás történik a génről. A *cpcG2* gén előtt nem található Shine-Dalgarno szekvencia, melynek hiánya megakadályozhatta a fehérjeátírást. A *cpcG2* gén transzlációs összekapcsolása a *psbAII* gén promóterével igazolhatja ezt a feltevést. A mutáns létrehozása folyamatban van. Érdekes, hogy amint azt az eredményeink bizonyították, *Synechocystis* PCC6803 fikobiliszómájának szerkezetében csak a *cpcG1* gén által kódolt rúd-mag kötőfehérje vesz részt, ugyanakkor a *Synechococcus* WH8102 cianobaktérium fikobiliszómájában mind a két rúd-mag kötőfehérjét kódoló gén terméke megtalálható. Érdemes lenne megvizsgálni, hogy vajon ennek az utóbbi cianobaktériumnak a fikobiliszómájában milyen szerepet játszik a két különböző gén által kódolt rúd-mag kötőfehérje.

Azt bebizonyítottuk, hogy *Synechocystis* PCC6803 cianobaktériumban az FNR-t kódoló *petH* génről két fehérje íródik át, kérdés azonban az, hogy mi a szerepe az FNR két formájának. Vajon különböző szerepet töltenek-e be, mint ahogy a növények leveleiben illetve a gyökereiben található FNR formák. A különböző FNR mutánsaink jó vizsgálati hátteret nyújtanak ennek tanulmányozásához, hiszen rendelkezésünkre áll olyan mutáns melyben csak a 34,3 kDa-os forma, vagy csak a 46,3 kDa-os forma van jelen. Ezekben a mutánsokban megvizsgálhatjuk, hogy milyen folyamatokra van hatással az egyes formák hiánya. Illetve a vadtípusban vizsgálható, hogy különböző körülmények között melyik forma szintetizálódik nagyobb mennyisében, vagyis melyikre van nagyobb szükség. Érdekes lenne izolálni a PC-hexamerhez kapcsolódó 46,3 kDa-os és a szabad 34,3 kDa-os formát, hogy megvizsgálhassuk *in vitro* az enzimaktivitásukat. A vizsgálatok eredményei megvilágíthatják számunkra, hogy mi a két FNR forma szerepe a cianobaktériumokban.

L' assamblage des phycobilisomes chez la cyanobactérie *Synechocystis* PCC6803

Les cyanobactéries sont des procaryotes qui réalisent la photosynthèse oxygénique. Il est maintenant admis que les cyanobactéries sont les ancêtres des chloroplastes, organites qui dans les algues et les plantes assurent la photosynthèse. Dans les cyanobactéries et les algues rouges des complexes macromoléculaires appelé phycobilisomes (PBS) collectent l'énergie lumineuse et la transmettent aux centres réactionnels ou elle est transformée en l'énergie chimique (NADPH et ATP). Les PBS sont composés de deux éléments structuraux le coeur et les battonets. Ces deux éléments sont principalement composés de protéines chromophorylées appelées phycobiliprotéines et, en plus petites quantités, de protéines non chromophorylées appelées linkers. Les phycobiliprootéines s'assemblent en trimères ou en hexamère qui constituent les éléments de base de l'architecture du PBS. Deux questions se posent au regard de cette structure supramoléculaire : comment ce complexe s'assemble et comment assure-t-il aussi efficacement son rôle. Les linkers jouent un rôle primordiale mais nous disposons de très peu d'informations les concernant. Ces derniers induisent l'assemblage des phycobiliprotéines et modulent leurs propriétés spectrales de façon à optimiser le transfert d'énergie vers le centre réactionnel. En revanche, on ne dispose d'aucune information structurale concernant les linkers, alors que les structures tridimensionnelles des phycobiliproteines sont très bien connus.

Le PBS de la cyanobactérie *Synechocystis* PCC6803, objet de ce travaille, consiste en un coeur tricylindrique duquel six bâtonnets rayonnent. Chaque bâtonnet est formé par l'empilement de trois hexamères de phycocyanine. Le linker LRC (qui relie le coeur aux bâtonnets) est codé par deux gènes indépendants (*cpcG1* et *cpcG2*). La raison de cette duplication est inconnue. Les autres sous unités des bâtonnets sont codés dans l'opéron *cpc*. Cet opéron contient cinq gènes : *cpcB* et *cpcA* (codant respectivement les sous unités α et β de la phycocyanine) et *cpcC2*, *cpcC1* et *cpcD* (codant respectivement les linkers LR 30, 33 et 10). Le rôle des LR n'avait pas été étudié dans *Synechocystis* PCC6803 mais des informations contradictoires existent concernant ceux de *Synechococcus* PCC7942.

Dans ce travail, le rôle de chaque linker du rod du PBS a été étudié par mutagenèse des gènes codants ces linkers chez *Synechocystis* PCC6803. Les spectres d'absorption et la composition des PBSs issus de mutants déficients et de souches complementées en trans nous ont ainsi révélé l'épistasie de *cpcC2* sur *cpcC1*. La caractérisation des mutants par des méthodes biochimique et biophysique nous a ainsi permis de déterminer l'ordre de

l'assemblage séquentiel des héxamères de phycocyanine dans les rods. Par ailleurs nous avons utilisé l'effet polaire produit par l'insertion d'interposons dans l'opéron *cpc* dans trois mutants allèliques de *cpcC1* pour proposer un mode de régulation transcriptionel de l'abondance relative des linkers 30 et 33. Cette partie du travail à été publié en 2004 Ughy et Ajlani, Microbiology, 150, 4147-4156.

Le LRC, qui lie les rods au core du PBS, étant codé par deux gènes indépendants (*cpcG1* et *cpcG2*) nous nous sommes intéressé à leurs rôles respectives. Tout d'abord nous avons montré que ces deux gènes étaient transcrit puis en créant des inactivation de l'un ou de l'autre, nous avons trouvé, fait très peu documenté, que *cpcG2* était un pseudogène transcrit et que seul *cpcG1* avait une fonction. Cette partie du travail est en cours de rédaction.

La Férredoxine-NADP(H) oxidoréductase (FNR), enzyme qui catalyse la production du pouvoir réducteur (NADPH) lors de la dernière étape de la photosynthèse oxygénique, se trouve attaché au phycobilisomes des cyanobactéries. En effet, le domaine N-terminal de la FNR cyanobacterienne contient une séquence similaire au LR10. La localisation exacte de la FNR au niveau des rods du PBS fait l'objet de publications contradictoires.

Aussi bien dans les cyanobactéries que dans les plantes supérieures, la FNR peut catalyser l'oxydation du NADPH afin de fournir des électrons a certaines voies du métabolisme. Deux isoformes de cette enzyme sont détecté (immunodétection sur des extraits cellulaires totaux) dans *Synechocystis* PCC6803, l'une, de 46 kDa, est associé au PBS et l'autre, de 34 kDa, est supposé être un produit de dégradation de la première. Nous avons émis l'hypothèse que la 34 kDa serait produite par une initiation alternative de la traduction du gène *petH* unique codant la FNR. Une méthionine en position 113 (M113) pouvant être le second site d'initiation a été remplacée par une isoleucine dans la FNR de *Synechocystis* PCC6803, le mutant qui porte cette substitution ne produit pas l'isoforme de 34 kDa ce qui renforça notre hypothèse mais n'exclu pas l'hypothèse de protéolyse. En revanche, des mutants de *petH* portants des décalage de cadre de lecture en amont de M113 résultant en un arrêt de la traduction initiée par M1 produisent uniquement l'isoforme de 34 kDa. Ces résultats nous ont permis d'exclure la protéolyse comme source de l'isoforme de 34 kDa et d'affirmer que les deux isoformes étaient produites à partir du même gène par des sites d'initiations de traductions différents. Des études physiologiques et biochimiques des mutants FNR visant à déterminer le rôle de chaque isoforme sont en cours.

LIST OF PUBLICATIONS

* **Ughy, B.**, Ajlani, G.
>
> Phycobilisome rod mutants in *Synechocytis* sp. strain PCC6803
> Microbiology 2004. 150: 4147-4156

* Domonkos, I., Malec, P., Sallai, A., Kovács, L., Itoh, K., Shen, G., **Ughy, B.**, Bogos, B., Sakurai, I., Kis, M. Strzalka, K., Wada, H., Itoh, S., Farkas, T., Gombos, Z.
>
> Phosphatidylglycerol is essential for oligomerization of photosystem I reaction center
> Plant Physiology 2004. 134: 1471-1478

* Várkonyi, Zs., Masamoto, K., Debreczeny, M., Zsiros, O., **Ughy, B**., Gombos, Z., Domonkos, I., Farkas, T., Wada, H., Szalontai, B.
>
> Low-temperature-induced accumulation of xanthophylls and its structural consequences in the photosynthetic membranes of the cyanobacterium *Cylindrospermopsis raciborskii*: An FTIR spectroscopic study
> PNAS 2002. 99(4): 2410-2415

Gombos, Z., Kis, M., Zsiros, O., **Ughy, B.,** Várkonyi, Zs., Wada, H., Farkas, T., Nagy, F.
>
> Light induction of lipid desaturation and its role in acclimation to low temperature.
> In: Photosynthesis: Mechanism and Effects Vol. III. (1998) G. Garab (ed.) 1783-1786. Kluwer Academic Publishers , Printed in the Netherlands

Várkonyi, Zs., Zsiros, O., Farkas, T., Garab, G., **Ughy, B.,** Szegletes, Zs., Gombos, Z.
>
> Adaptation mechanism of the photosynthetic apparatus of *Cylindrospermopsis raciborskii* ACT 9502 to different environmental effects.
> In:Photosynthesis: Mechanism and Effects Vol. III. (1998) G. Garab (ed.) 1819-1822. Kluwer Academic Publishers , Printed in the Netherlands

Zsiros, O., Várkonyi, Zs., Mustárdy, L., **Ughy, B.,** Gombos, Z.
>
> Light is necessary in the acclimation process of photosynthetic organism to low-temperature stress
> In: Advances in Plant Lipid Research (1998) Sánchez, J., Cerdá-Olmedo, E., Martinez-Force, E. (eds) 122-125. Printed in Spain, Universidad de Sevilla

Gombos, Z., Kis, M., Zsiros, O., **Ughy, B.,** Várkonyi, Zs., Wada, H., Tasaka, Y., Farkas, T., Murata, N.
>
> Light induction of lipid desaturation and its role in acclimation to low temperature.
> In: Advances in Plant Lipid Research (1998) Sánchez, J., Cerdá-Olmedo, E., Martinez-Force, E. (eds) 118-121. Printed in Spain, Universidad de Sevilla

(* The main publications related to my PhD work).

ACKNOWLEDGEMENTS